The Role of Epoxygenated Fatty Acids in Diabetic Retinopathy

By

Megan E. Capozzi

Dissertation
Submitted to the Faculty of the
Graduate School of Vanderbilt University
in partial fulfillment of the requirements
for the degree of

DOCTOR OF PHILOSOPHY
in

Molecular Physiology and Biophysics
May, 2017
Nashville, Tennessee

Approved:

John S. Penn, Ph.D.

Roger J. Colbran, Ph.D.

Milam A. Brantley Jr., M.D., Ph.D.

Ambra Pozzi, Ph.D.

Ann Richmond, Ph.D.

ACKNOWLEDGEMENTS

This work would not have been possible without the financial support of National Institutes of Health grants R01 EY07533 (JSP), R01 EY023639 (JSP), P30 EY008126 (Core Grant in Vision Research), P30 DK020593 (Core Grant for Vanderbilt Diabetes Research Center); an Unrestricted Grant from Research to Prevent Blindness, Inc.; and the Carl Marshall Reeves & Mildred Almen Reeves Foundation, Inc.

First, I would like to thank the members of my committee for their expert guidance in helping to develop my project. I would also like to thank several members of the lab, whom it has been my pleasure to work and collaborate with over the course of the last decade. These include several lab members who have become great friends: Sandra Hammer, Meredith Giblin, Jaime Dickerson, Taylor Smith, Stephanie Evans, Annie Daorai, Rong Yang, Dolly Ann Padovani-Claudio, and Yueli Zhang. I would like to especially thank Gary McCollum, who I have had the pleasure to work with for my full tenure in the lab. He has always challenged me scientifically, helped me develop my writing skills, and provided endless amounts of entertainment and positivity. Lastly, I am so thankful for my mentor, John Penn, who has been patient and supportive while dedicating so much time to my scientific and professional development. He has shaped me as both a scientist and person, and I will always be grateful for his commitment to my progress. I can’t imagine having a better mentor and role model.

I am grateful for the endless support of my family. I would like to thank my parents, Robin and John, and my brother, Mike, who have always provided encouragement and love. Their confidence in me has been a source of comfort and

encouraged me to always push forward. Lastly, I would like to thank my husband, David. He has been an incredible support system and source of encouragement. He's been there for late nights and weekends in the lab as well as the fun times outside of the lab, and I am so thankful for the happiness he has brought into my life.

TABLE OF CONTENTS

LIST OF TABLES

LIST OF FIGURES

CHAPTER I

INTRODUCTION

Diabetic retinopathy background

Diabetes mellitus is a chronic, systemic disease characterized by several metabolic changes including abnormal insulin signaling, altered blood lipid levels, and elevated blood glucose. Diabetes mellitus occurs in two primary types. Type 1, or insulin-dependent, diabetes is an auto-immune disease that specifically targets the insulin-producing β-cell of the pancreatic islet. Type 2 diabetes, often referred to as adult-onset or non-insulin-dependent diabetes, is most commonly associated with obesity and is characterized by peripheral resistance to insulin. Type 2 diabetes accounts for about 90% of all diabetes cases. As of 2012, an estimated 29.1 million Americans have diabetes, costing an estimated 245 billion dollars in medical expenses.[1]

Secondary to diabetes, various microvascular complications are prevalent, including diabetic nephropathy, diabetic neuropathy, and diabetic retinopathy (DR). Diabetic retinopathy is the leading cause of blindness in working aged Americans.[2] Of the estimated 285 million diabetics worldwide, one third show signs of DR.[3] The pathology of DR presents in two clinically distinct forms referred to as non-proliferative (NPDR), the early stage characterized by fundus abnormalities including microaneurysms, hemorrhages and vasoregression, and proliferative (PDR), the later stage characterized by pre-retinal neovascularization. Additionally, diabetic macular edema (DME), characterized by fluid accumulation in extravascular parenchyma, is the

leading cause of vision loss associated with diabetes, largely due to its high prevalence in patients with type 2 diabetes.[3,4]

Various risk factors are associated with DR. Of all identified risk factors, the time from diagnosis is the most highly correlated with retinopathy progression.[5] For example, in The Wisconsin Epidemiologic Study of Diabetic Retinopathy (WESDR), which used a type 1 diabetes patient population, prevalence of any retinopathy was 25% at 5 years and 80% at 15 years; PDR prevalence was 0% at 3 years and 25% by 15 years with diabetes.[5,6] Several additional clinical studies worldwide have supported time from diagnosis as the most prominent risk factor for DR.[7-10] Furthermore, the mean age of initial diagnosis, particularly of type 2 diabetes, continues to decrease.[11] Thus, the rates of vision-threatening pathology from DR can be expected to increase.

Another prominent risk factor for DR pathogenesis is control of blood glucose. In the Diabetes Control and Complications Trial (DCCT) and United Kingdom Prospective Diabetes Study (UKPDS), intensive blood glucose control, which is defined as 3 or more daily injections of insulin, was associated with a slowed progression of DR.[12,13] A meta-analysis of worldwide diabetic retinopathy studies confirmed elevated HbA_{1c} as a major risk factor for DR progression.[3] These studies concluded that early and tight blood glucose control is important for limiting DR progression and the need for ophthalmic treatment. Despite the benefits of tight blood glucose control, intensive treatment strategies carry the risk of potentially fatal hypoglycemia.[14]

Dyslipidemia, defined by elevation of either serum cholesterol or triglycerides, has more recently been accepted as a DR risk factor. The Early Treatment Diabetic Retinopathy Study (ETDRS) initially identified a positive correlation between diabetic

retinopathy pathology and serum lipid levels,[15] and meta-analysis from 35 clinical studies established a relationship between high serum cholesterol and prevalence of DME.[7] Supporting these correlations, lipid-lowering therapeutic strategies have been observed to slow the progression of DR. In the Fenofibrate Intervention and Event Lowering in Diabetes (FIELD) and the Action to Control Cardiovascular Risk in Diabetes (ACCORD) studies, the lipid-lowering drug, fenofibrate, delayed retinopathy progression and the need for laser treatment, a common therapeutic strategy for DR.[16,17] Notably, these effects were observed independent of glycemic control.

Currently, there are two major therapeutic strategies for treatment of diabetic retinopathy. The first therapeutic strategy, developed in 1985, is laser photocoagulation for the treatment of DME or PDR.[18] Laser photocoagulation is applied either focally to cauterize leaky vessels or in a panretinal grid to ablate oxygen utilizing cells, thus increasing oxygenation in the perfused portions of the retina and reducing growth factor production.[19] The goal of laser application is to protect high acuity central vision by delaying disease advancement, but this comes at the expense of the peripheral retina. Consequently, this treatment is successful at slowing the progression of neovascularization and preserving vision in the late stages of the disease, but it also kills the post-mitotic neuronal cells of the retina. Thus, patients lose peripheral and night vision, and in some cases, photocoagulation causes eventual worsening of macular edema.[20]

Despite the efficacy of laser photocoagulation, the invasive nature and negative side effects of laser treatments provides a strong impetus to develop additional therapies for DR. Anti-vascular endothelial growth factor (anti-VEGF) is an additional

therapeutic strategy that was more recently been approved for DME and, in some cases, PDR. VEGF is a potent angiogenic and permeability factor that is elevated in the vitreous of patients with DR.[21,22] Anti-VEGF therapy was quickly approved for clinical use in DR patients because it was already used as a therapy for age-related macular degeneration to treat choroidal neovascularization. Several products in the clinic prevent or limit VEGF signaling. These include targeted antibodies against VEGF, such as ranibizumab (Lucentis) and bevacizumab (Avastin), the RNA aptamer pegaptanib (Macugen), which binds the VEGF-A165 isomer, and the soluble VEGF receptor aptamer, aflibercept (Eylea). These anti-VEGF therapies are all delivered intravitreally, thereby maximizing retinal efficacy and limiting systemic effects. While these therapies are predominantly used in diabetics for the treatment of DME, they have more recently been used for treatment of PDR in conjunction with panretinal photocoagulation, which remains the proven standard of care.

These VEGF-directed therapies have demonstrated great promise in the clinic. For instance, 61.4% of DR patients treated with bevacizumab had complete regression of neovascularization.[23] While the observed efficacy is promising, there are a number of problems associated with anti-VEGF therapies. First, they require repeat injections every few months, which makes patient compliance a challenge. Additionally, these repeated intravitreal injections increase the likelihood of endophthalmitis, an inflammatory and potentially blinding infection to the eye that can occur following globe puncture during injection.[24] The incidence of endophthalmitis in response to anti-VEGF, is low, ranging from 0.009-1.9%,[25,26] however, intravitreal injections are repeatedly administered, increasing the likelihood of infection. Lastly, VEGF receptors are

expressed in retinal neuronal and glial cells, and VEGF activation of these receptors is involved in their survival.[27,28] Hence, while anti-VEGF therapies are successful in limiting DME, they may cause long-term neuronal problems when administered chronically for many years.[29,30] It is important to note that anti-VEGF therapies are not efficacious in all patients.[30] Therefore, there remains a need to develop novel therapeutic strategies that are less invasive, more sustainable, and carry fewer complications. Moreover, anti-VEGF and laser photocoagulation are directed at late stages of the disease when substantial retinal abnormalities are detected by retinal fundus imaging. Strategies to target early stages may be more efficacious, because they can prevent the onset of the severe and irreversible consequences.

Diabetic retinopathy pathogenesis

Despite DR being characterized clinically by vascular changes, many retinal cell types are affected before any detectable retinopathy is diagnosed. Neural cells, including photoreceptors, bipolar cells, and ganglion cells; vascular cells, including endothelial cells and pericytes; and glial cells, including macroglia (Müller cells and astrocytes) and microglia are all altered by diabetes (**Figure 1**). The causes of retinal cell dysfunction are interrelated, because each cell type has been demonstrated to produce both autocrine and paracrine factors that potentiate disease progression. Ultimately, retinal changes, including retinal neuron and pericyte death, glial and endothelial cell activation, and breakdown of endothelial cell junctions, are thought to increase in severity, eventually leading to overt signs of DR.

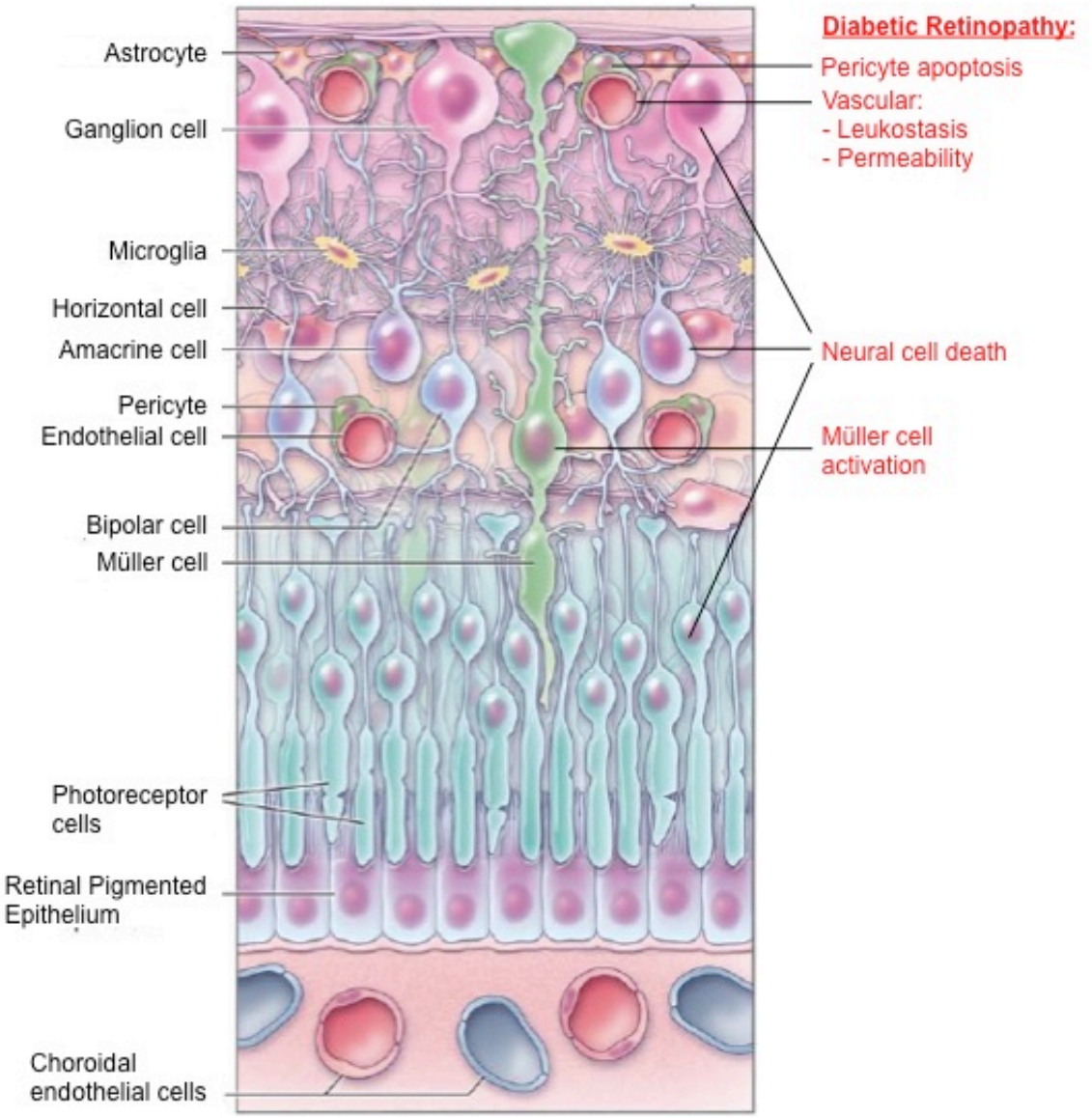

Figure 1. Retinal cells and their alterations in diabetic retinopathy. Adapted from Antonetti et al. (2012).[31] This diagram depicts the laminar distribution of cells and relative localization in the retina. For orientation, vitreous is at the top of the image and sclera is at the bottom. In red on the right of the diagram, the alterations observed during diabetic retinopathy and discussed in the introduction are emphasized.

Retinal neurons are among the most metabolically active cells in the body.[32] Thus, retinal neural cells are highly sensitive to diabetes-related retinal dyshomeostasis. Retinal neuronal death is an early component of diabetes, leading DR to be, at least in part, considered a neurodegenerative disease.[33,34] Barber and colleagues observed

elevated neuronal cell death by TUNEL-positive staining in experimental diabetes models and patients with diabetes,[35] validating earlier studies identifying neural cell death.[36,37] These changes manifest clinically via multiple functional deficits. In patients with diabetes but without observable fundus changes, alterations were detected in diagnostic tests for retinal electrical activity (measured by electroretinograms (ERGs)), visual field, and contrast sensitivity – all are associated with neural dysfunction or cell death.[38-46]

In response to diabetes, glial cells become reactive. There are two major subsets of glia in the retina, microglia and macroglia (astrocytes and Müller cells). While all glial cell types are responsive to diabetes, Müller glial cell reactivity is the focus of this dissertation and only their alterations are summarized. In experimental models of diabetes and in retinas from patients with DR, glial fibrillary activated protein (GFAP), a factor associated with glial activation, is elevated in Müller cells.[47] Concomitant with increased GFAP levels, elevations in inflammatory factors are also observed.[48] These inflammatory factors and their effects will be further discussed in the next section. Water handling by Müller cells is also changed by diabetes. Aquaporin (AQP) channels AQP1 and AQP4 are predominantly found in macroglial cells in the retina. In models of DR, Müller cell AQP1 and AQP4 exhibit altered expression and localization, and these changes are thought to contribute to the increased liquid retention associated with diabetic macular edema.[49,50] Müller cells are also the major handler of glutamate in the retina. Müller cells uptake extracellular glutamate that is used for neuronal transmission, thereby modulating the gain for synaptic signaling.[51] In experimental models of DR, Müller cells have decreased glutamate uptake activity, suggesting that this dysfunction

may lead to glutamate cytotoxicity and neuronal cell death.[51-53] Taken together, Müller cell changes are directly linked to various retinal functional deficits observed in DR, and thus limiting their activation may be an ideal target for treatment of early DR.

Diabetic retinopathy is clinically determined by alterations to the vasculature, and these changes are derived, in part, from endothelial cell dysfunction. Diabetes-induced vascular alterations include immune activation, loss of barrier function, and pericyte dropout; all of which can lead to vision-threatening pathology. The role of immune activation in diabetes-induced retinal pathology will be the focus of the next section. Yet, vascular inflammation, as well as hyperglycemia and elevated growth factors, contributes to blood-retina barrier (BRB) breakdown, and thus vascular permeability.[54] These diabetic stimuli are prominent in diabetes and interfere with endothelial tight junctions, leading to increased vascular permeability,[55-59] a hallmark of DR. Vaso-regression also contributes to loss of barrier function and is largely attributed to pericyte dropout. Pericytes are mural cells that associate closely with the endothelium, and pericyte-endothelial cell communication is necessary to maintain stable tight junctions.[60] For example, pericyte loss by genetic deletion of platelet-derived growth factor (PDGF) recapitulated vascular damage associated with STZ-induced DR.[61] In retinal pericyte cell cultures, death can be initiated by both elevated glucose and fatty acids.[62,63] Additionally, pericyte death is observed in animal models of DR and retinas from diabetic patients.[64,65]

Several animal models are used to recapitulate the disease outcomes for DR, and a summary of these models are listed in **Table 1**. The most commonly used and well-characterized model for DR is the streptozotocin- (STZ-) induced diabetes model,

which mimics complications associated with type 1 diabetes. In this model, the STZ alkylating agent is injected into rodents and taken up by GLUT2 receptors, which are highly expressed in the insulin-producing beta cells.[66] This leads to DNA damage and consequent cell death specifically in pancreatic beta cells and thus the loss of insulin production. In this model, early events such as glial reactivity, vascular leakage, neural cell death, and inflammation occur around 8 weeks post-diabetes induction in mice.[67-71] Mouse models that mimic type 2 diabetes, such as the db/db (leptin-receptor deficient) or diet-induced obesity models, also develop retinal pathology similar to the STZ-treated animals,[72-74] however, this pathology takes longer to develop due to the more gradual onset of insulin resistance and subsequent diabetes.

DR Models	DR Pathology	Pros	Cons
STZ-induced diabetes mouse model (Type 1 model)	-Up-regulation of inflammatory cytokines -Leukostasis -Vascular leakage -Neural cell death -Pericyte loss -Basement membrane thickening	-Recapitulates early disease stages -Relevance to metabolic condition in humans -Control of hyperglycemia onset	-No severe pathology (i.e. no NV) -Relatively slow onset of pathology (4+ weeks)
db/db mouse model (Type 2 model)	-Vascular leakage -Pericyte loss -Basement membrane thickening	-Recapitulates early disease stages -Relevance to metabolic condition in humans	-No severe pathology (i.e. no NV) -Least characterized model of DR, compared to other options listed -Slow onset of pathology (8+ weeks)
TNFα intravitreal injection	-Leukostasis -Vascular leakage	-Fast induction of pathology (<24hrs) -Recapitulates early disease stages -Allows for controlled drug delivery regimen	-No metabolic/systemic similarities to diabetes -Pathology is resolved -No severe pathology (i.e. no NV)
Oxygen-induced retinopathy mouse model	-Development of pre-retinal NV -Up-regulation of inflammatory cytokines -Vascular leakage	-Fast induction of pathology (3 weeks) -Only model to develop pre-retinal NV	-No metabolic/systemic similarities to diabetes -Spontaneous resolution of pathology

Table 1. Summary of *in vivo* mouse DR models.

To recapitulate specific steps observed in the chronic disease models, acute models are often used. One short-term model is the ischemia/reperfusion (IR) model, in which a temporary high intraocular pressure is exerted for about 120 minutes to create ischemia, followed by removal of the pressure source and reperfusion. This model recapitulates a variety of diabetes-relevant endpoints and allows for controlled dosing of therapeutic test agents. For instance, neuronal cell death, capillary dropout, vascular permeability, cell adhesion molecule expression, leukostasis, and cytokine up-regulation are all observed within 7 days from IR.[75] Another way to model early disease pathogenesis is to inject either inflammatory cytokines, like TNFα, or growth factors, like VEGF, directly into the vitreous cavity. These factors rapidly induce a number of early-stage disease processes, on the scale of hours, including leukostasis and vascular permeability.[56,76,77] **Chapter IV** of this dissertation will describe experiments using intravitreal injection of TNFα as a means to develop proof of several concepts involving retinal inflammation.

Lastly, the oxygen-induced retinopathy (OIR) model is used to model PDR because no diabetic animal models have demonstrated retinal neovascularization similar to what is observed clinically in PDR. OIR animals do not have systemic diabetes and instead more accurately model retinopathy of prematurity (ROP), a disease that occurs in prematurely born infants. In the mouse OIR model developed by Lois Smith and colleagues,[78] retinal vasculature develops in room air conditions (20.9% O_2) for 7 days, followed by a hyperoxic exposure (75% O_2) for 5 days, during which the central vasculature regresses. Animals are then returned to room air, and in the next 5-day

period pre-retinal pathologic neovascularization occurs in response to the central ischemic area in the retina, mimicking abnormal vascular growth observed in PDR.[79] The vascular regression from hyperoxia more closely mimics ROP progression that was first observed in the 1950s and currently occurs in many developing countries.[80] However, premature infants with very low birth weights (<2500g) have delayed vascular development as opposed to regressed vasculature, and this is more accurately modeled in the rat model of OIR developed by John Penn and colleagues.[81,82] In this model, immediately upon birth when retinal vasculature has not yet developed, rats are exposed to a daily alternating oxygen concentration (50%/10% O_2) for 14 days. At removal from alternating oxygen to room air, retinal vascular development has been delayed and a large avascular area is observed in the periphery, consistent with human ROP.[83] The peripheral ischemic area drives hypoxia and up-regulates hypoxia-derived growth factors such as VEGF, which then promotes pathological neovascularization.[84] Both models exhibit elevated inflammatory mediators as well as angiogenic factors that are observed in DR.[79,85] While the mouse OIR model is used more frequently due to the advantage of genetic manipulation, the studies of angiogenesis in **Chapter V** of this dissertation will utilize the rat OIR model due to its greater physiologic relevance to human disease and our use of pharmacologic, rather than genetic, manipulations of the pertinent pathways.

Inflammation in diabetic retinopathy

Inflammation is the body's response to injury or pathogens and is critical for healing. This process is mediated by the interaction of leukocytes with endothelium upon activation by pro-inflammatory cytokines (e.g., TNFα or interleukins), chemokines,

or local chemo-attractants. These inflammatory factors are involved in drawing immune cells to injured or diseased tissues and activating endothelium to express cell adhesion molecules (e.g., VCAM-1, ICAM-1, selectins) that are involved in the rolling and tethering of leukocytes to the endothelial cell wall. When activated acutely, inflammation plays a beneficial role, such as in wound healing or infection resolution. However, when inflammation is chronically activated, such as in diabetes, rheumatoid arthritis, or atherosclerosis, tissue damage can occur.

Retinal inflammation is a result of both circulating inflammatory factors and local inflammatory activation. In patients with DR, levels of inflammatory mediators in serum and vitreous are elevated. For example, Doganay and colleagues demonstrated a correlation of serum interleukin-8 (IL-8) and tumor necrosis factor-alpha (TNFα) with the stage of DR. Patients with diabetes, but without DR, showed basal serum levels of IL-8 and TNFα, while PDR patients had about double the serum levels of non-DR patients, and NPDR patients showed an intermediate amount of these inflammatory factors.[86] Furthermore, elevated cytokines (e.g., TNFα, IL-1β, IL-6, IL-8) are observed in the vitreous humor of patients with DR.[22,87-91] These inflammatory factors have also been confirmed to be elevated in the retina of DR animal models.[87,88,92]

Several cell types, including retinal glia and endothelial cells, secrete soluble cytokines in response to diabetes-relevant culture conditions.[93-95] Müller cells are particularly responsive to diabetic conditions. In both diabetic models and human DR retinal tissue, Müller cell GFAP is elevated, representing an activated state of this glial population.[47,52,96] Activated Müller cells are known to elaborate several inflammatory and angiogenic mediators. For instance, in response to hypoxia, a stimulus that is

perhaps related to the late stages of DR, Müller cells were observed to be the major producers of VEGF compared to retinal astrocytes, microvascular endothelial cells, and retinal pigment epithelial cells.[97] Furthermore, Müller-cell derived VEGF was found to be sufficient for induction of leukostasis and vascular permeability in the STZ-induced diabetes model and for pre-retinal neovascularization in an ischemia-induced retinopathy model.[69,98] In Müller cells isolated from STZ-induced diabetic animals, several acute-phase inflammatory transcripts were significantly elevated, and this corresponded to elevated retinal IL-1β protein levels.[48] There is precedence for IL-1β to amplify the inflammatory response by both paracrine and autocrine effects on the Müller cells.[93,99,100] It is hypothesized that auto-amplification of these soluble cytokines may partially explain the delayed nature of DR pathology, because accumulation of inflammatory mediators may need to reach a threshold before retinal dysfunction is observed. This suggests that anti-inflammatory therapies administered early in the disease process would be highly efficacious because they would interrupt the cycle of chronic inflammatory cytokine elevation.[101] While inflammatory mediator amplification can be assessed *in vitro*, culture conditions for inflammatory mediator induction have not been developed, and thus this is the goal of the studies reported in **Chapter III** of this dissertation.

In response to the elevated inflammatory mediators, endothelial cells become activated, leading to the development of sight-threatening DR pathology as highlighted in **Figure 2**. The up-regulated inflammatory cytokines observed in DR patients (TNFα, IL-1β, IL-6, IL-8) are experimentally linked to leukostasis. In vascular cells, pro-inflammatory cytokines induce expression of the adhesion proteins VCAM-1,[102-104]

ICAM-1[102,104] and E-selectin,[105,106] leading to leukocyte adhesion to the vessel wall.[107-109] The adhered leukocytes elaborate cytotoxic stimuli,[110-112] which may promote pericyte and endothelial cell death.[113,114] These events have been associated with retinal capillary occlusion and capillary dropout,[115-117] leading to retinal ischemia and ultimately retinal hypoxia. In the later stages of disease progression, elevated retinal levels of hypoxia-inducible factors, such as VEGF, promote both hyperpermeability and neovascularization, the hallmark of PDR.

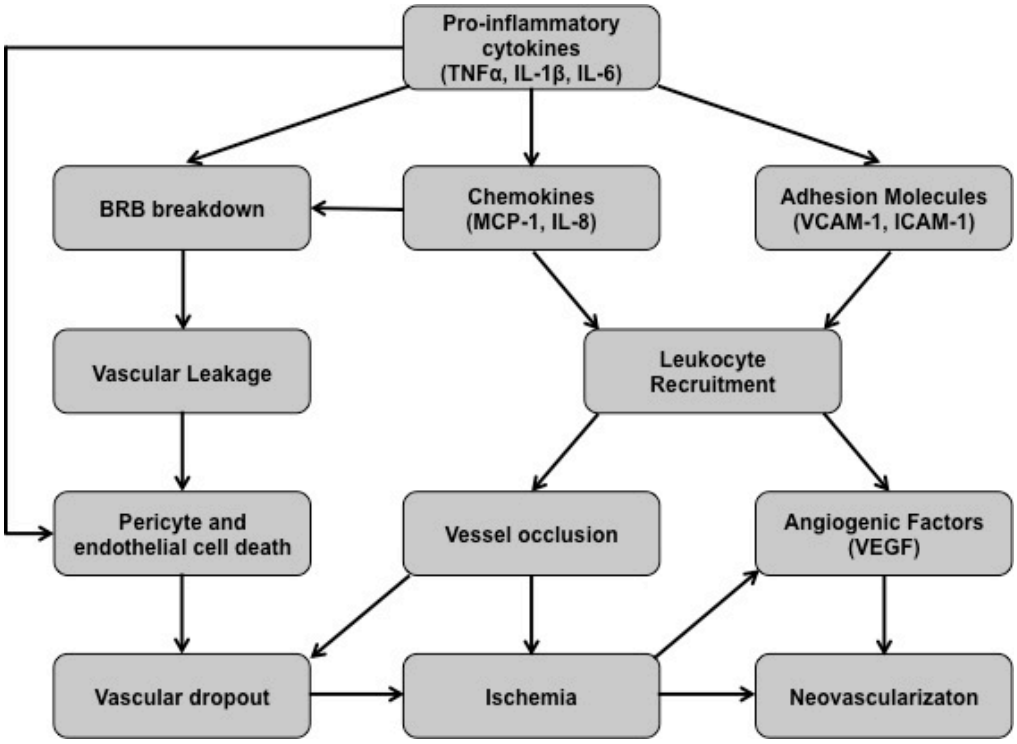

Figure 2. The role of inflammation in diabetic retinopathy pathogenesis. Adapted from Zhang et al. 2011 (ref 88). This model demonstrates the close association of inflammation with the development of vision-threatening pathology in late stage DR.

Experiments in DR models have elucidated chronic retinal inflammation as a viable therapeutic target for early stage DR. For example, TNFα neutralization using the soluble TNFα receptor, Etanercept, reduced retinal inflammation and blood-retina-

barrier (BRB) breakdown in a rat model of diabetes.[118,119] Furthermore, blockade of ICAM-1 inhibited both VEGF- and diabetes-induced retinal inflammation and vascular leakage,[117,120,121] thus suggesting a causative role of inflammation in vascular permeability. Pharmacologic anti-inflammatory strategies have also been studied for their potential efficacy in DR. COX-2 inhibition demonstrated efficacy in both rodent and dog models of diabetes by reducing leukostasis and vessel degeneration.[118,122-124] Conversely, in patients, aspirin has not exhibited substantial benefits in the clinic.[101,125,126] Anti-inflammatory steroids, such as dexamethasone, have been shown to reduce ICAM-1, leukostasis, and vascular leakage, yielding positive outcomes for DR.[101,127] However steroids carry the increased risk of glaucoma and cataract. Taken together, these findings suggest that inflammation is a viable therapeutic target, and there is a strong impetus to develop novel anti-inflammatory agents for treatment of DR.

Epoxygenated fatty acids background

Tissues metabolize fatty acids to biologically active lipid mediators through the cyclooxygenase (COX), lipoxygenase (LOX) or cytochrome P450 epoxygenase (CYP) pathways. There are 57 human genes that encode functional cytochrome P450 proteins and these enzymes are involved in metabolizing a wide variety of both endogenous and exogenous compounds.[128] A subset of these enzymes has the ability to metabolize polyunsaturated fatty acids; enzymes of the CYP4 family possess hydroxylase activity and enzymes of the CYP2 family possess epoxygenase activity. CYP epoxygenase enzymes of the CYP2C and CYP2J families are the most highly characterized, however several CYPs in different families have been found to have epoxygenase activity.[129]

Epoxide products are derived from arachidonic acid (epoxyeicosatrienoic acid; EET), linoleic acid (epoxyoctadecaenoic acid; EpOME), eicosapentaenoic acid (epoxyeicosatetraenoic acid; EpETE), and docosahexaenoic acid (epoxydocosapentaenoic acid; EDP).[130] This dissertation will focus on the enzymatic products of arachidonic acid (AA) and docosahexaenoic acid (DHA) because they have high relative mole percents compared to other polyunsaturated fatty acids in relevant retinal cells.[131] CYP enzymatic activity yields four EET regioisomers from AA (5,6-EET, 8,9-EET, 11,12-EET, and 14,15-EET) and five EDP regioisomers from DHA (7,8-EDP, 10,11-EDP, 13,14-EDP, 16,17-EDP, and 19,20-EDP) via epoxide addition to any of the olefin bonds. These epoxides induce a variety of biological activities, including vaso-dilatory, angiogenic, pro-survival, and anti-inflammatory actions.

The tissue levels of these epoxides are primarily limited by the soluble epoxide hydrolase (sEH) enzyme, which hydrolyzes the epoxide group to yield diol products, the dihydoxyeicosatrienoic acids (DHETs) or dihydroxydocosapentaenoic acids (DHDPs). The diols are generally biologically inactive, and in some cases have opposing effects to their epoxide substrates.[132,133] EETs and EDPs can also undergo chain elongation, β-oxidation, or are incorporated into cell membranes, particularly when sEH is inhibited.[134,135] The sEH enzyme is encoded by the *EPHX2* gene, and functionally occurs as a homodimer of two 62-kDa monomers in the cytosol. The C-terminal domain of the enzyme possesses epoxide hydrolysis activity while the N-terminal domain has phosphatase activity; the functional relevance of this phosphatase activity in mammals remains unclear.[136] sEH metabolizes epoxide regioisomers at different rates, based on

the proximity of the epoxide group to the carboxylic acid.[137] Notably, DHA-derived epoxides are better substrates for sEH, with the exception of 19,20-EDP.[138]

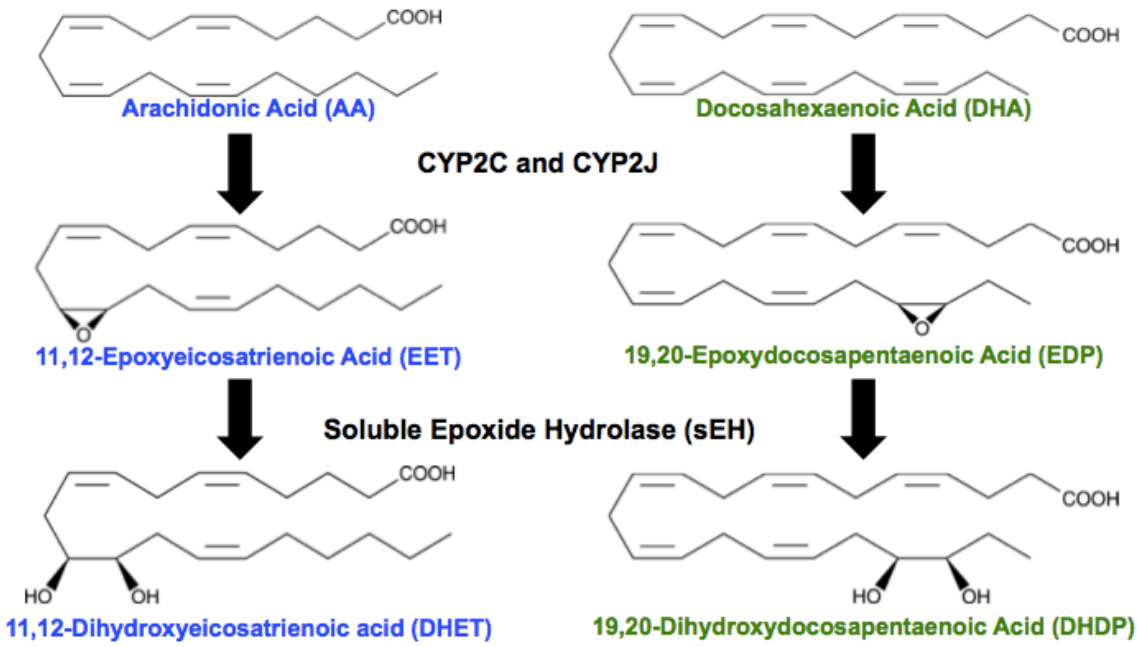

Figure 3. Structures of CYP substrates (AA and DHA), CYP products (EET and EDP), and sEH products (DHET and DHDP).

Activities of epoxygenated fatty acids

While no specific EET or EDP receptor has been identified, epoxides have been shown to exert their activities through a number of signaling pathways (**Figure 4**). EET signaling has been studied more than EDP, and thus most of what is known about epoxide signaling is from EET studies. Evidence suggests that EETs may activate intracellular signaling cascades through the activation of GPCRs. Treatment of cells with exogenous EETs increases adenosine 3'5'-cyclic monophosphate (cAMP) and protein kinase A (PKA), and this may be mediated through $G\alpha_s$.[135,139,140] Generation of cAMP may be, in part, attributable to EET activation of prostaglandin receptors.[141] More recently, EET has been shown to exert its mitogenic effects through the lipid-binding

GPCR, GPR40.[142] Peroxisome proliferator-activated receptors (PPARs), a family of transcription factors that bind a variety of ligands to exert functions predominantly related to lipid metabolism and cell differentiation, have also been shown to mediate EET biological activities.[143-145] Additional intracellular signaling cascades are activated in response to EET stimulation, including MAPK and PI3K/Akt as well as inhibition of IKK.[146-149] Due to the wide range of cellular influences, EETs may serve as ligands to a variety of receptors, and not necessarily a single, unidentified EET-specific receptor.

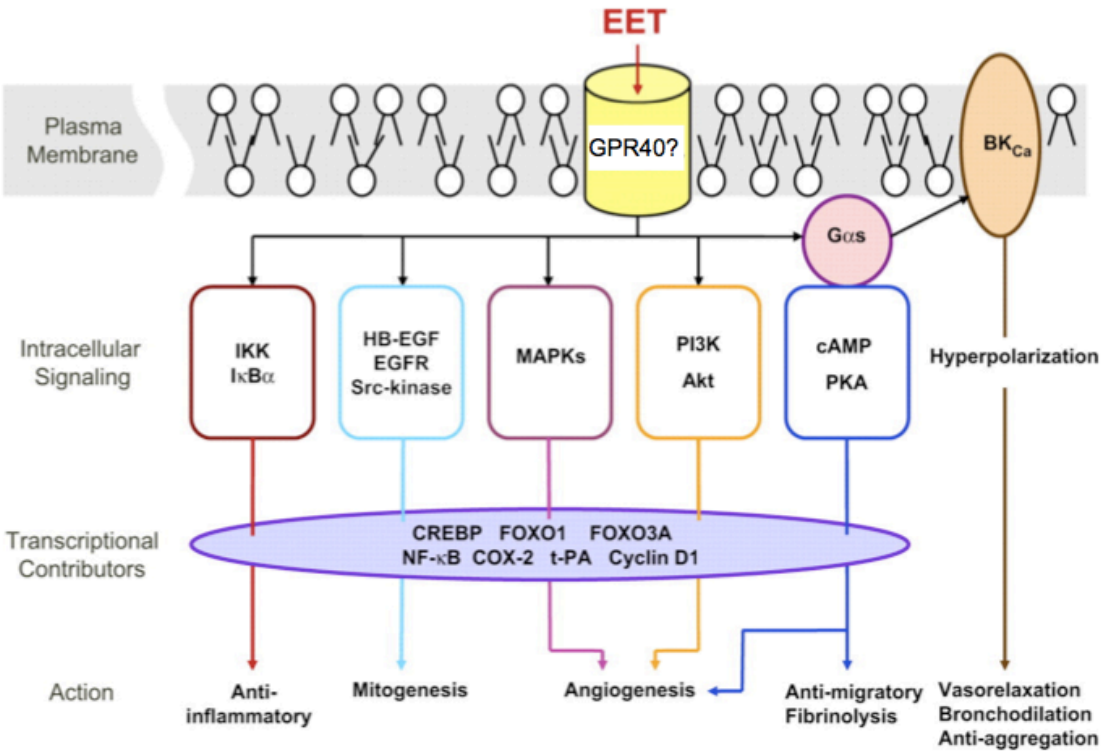

Figure 4. Signaling pathways and activities regulated by EET. EDP-induced behaviors were not included because they have not been thoroughly studied. Figure adapted from Spector & Norris 2007 (ref 135).

The effects of EETs have been most thoroughly studied in regards to endothelial cell behaviors. Interest in AA-derived epoxides stemmed from their identification as endothelial-derived hyperpolarizing factors (EDHFs) due to their NO- and PGI_2-

independent vaso-relaxation via K_{Ca} activation in bovine coronary arteries.[150,151] EDPs also demonstrated similar vaso-activity, and in certain vascular beds they were more potent vaso-dilatory agents.[152,153] Several studies verified the effects of EETs and EDPs on vaso-relaxation, making it the most studied behavior induced by CYP-derived epoxides. Due to potent vaso-dilatory effects of the epoxides, sEH inhibition was assessed in clinical trials for treatment of moderate hypertension (NCT00847899). Though the inhibitor AR9281, developed by Arete Therapeutics, did not result in any adverse events, sEH inhibition was not efficacious for hypertension in phase II clinical trials.[137,154]

EETs also possess potent pro-angiogenic activities, and these activities have been most widely studied in the field of cancer.[155] CYP-derived EET production has been shown to play a significant role in promoting endothelial cell proliferation and mitogenesis.[156,157] Particularly relevant to retinal vaso-proliferative disease, some CYPs are regulated by hypoxia. Although *CYP2J2* was down-regulated in hypoxia, *CYP2C8/9* enzymes were hypoxia-inducible in human umbilical vein endothelial cells (HUVEC) and bovine retinal microvascular endothelial cells (BRMEC).[158,159] The hypoxia-induced EET products are downstream signaling intermediates in the VEGF signaling pathway;[149,160] accordingly, CYP inhibitors reduced EC proliferation and overexpression of *CYP2C8* promoted EC proliferation *in vitro.*[161] A number of *in vivo* studies also support a role for EETs in angiogenesis. For example, administration of exogenous EETs induced vascularization in the Matrigel plug assay, and overexpression of rat *CYP2C11* increased muscle capillary density in an ischemic rat hind limb model.[148,162] Furthermore, increased EET production promoted tumor growth and metastases in a

number of *in vivo* cancer models.[153,155,163] Conversely, EDPs appear to be anti-angiogenic. In matrigel plug and tube formation assays, 19,20-EDP dose-dependently inhibited VEGF-induced angiogenesis.[164] Additionally, Kip Connor's group observed a significant reduction of choroidal angiogenesis with systemic 19,20-EDP administration in the laser-induced choroidal neovascularization model.[165] Contrary evidence has been suggested by Lois Smith's group, in which they postulate that endothelial cell-specific CYP overexpression promotes retinal neovascularization in the OIR mouse model when mice were fed an ω-3 rich diet.[166] However, Hu et al. showed that physiologic angiogenesis was driven by the diol product of 19,20-EDP, 19,20-DHDP,[132] suggesting that the elevated angiogenesis observed with CYP overexpression may be attributed to sEH products. Further work is necessary to understand the role of DHA-derived epoxides in pathological retinal angiogenesis.

In 1999, Node and colleagues first demonstrated the anti-inflammatory effects of EETs. In bovine aortic endothelial cells, TNFα induced the translocation of a pro-inflammatory transcription factor, NFκB; 11,12-EET inhibited TNFα-induced NFκB translocation via inhibition of IκBα degradation, thus reducing the transcription of VCAM-1, a well-characterized NFκB target gene.[146] Subsequent studies have validated this response in a variety of contexts, and these studies will be elaborated in the next section.

A limited amount of information is known regarding EETs and EDPs in retinal tissue. *CYP2C8* exhibited the highest expression among the CYP epoxygenases examined in post-mortem human retinal tissue with no ocular disease.[167] Its murine functional homolog, *Cyp2c44*, was also shown to be highly expressed in the retina,

localizing primarily to capillary pericytes and glia.[168] In the developing mouse retina 19,20-DHDP mediated developmental angiogenesis; thus, sEH deletion slowed the developing vascular network.[132] Interestingly, deletion of Müller cell-specific *Ephx2* (the gene coding sEH) recapitulated the vascular development phenotype of the whole body *Ephx2* KO,[169] suggesting that Müller cells may be the primary source of epoxide hydrolysis in the retina. The 11,12-EET regioisomer and the 19,20-EDP regioisomer were found to be the most abundant in the retina,[151,169] and thus are the primary EET and EDP regioisomers used in the experimental work of this dissertation.

Epoxygenated fatty acids in inflammation

Several *in vitro* studies using various inflammatory stimuli have identified an anti-inflammatory role for EETs. Limited mechanistic studies have been performed using EDPs, however overexpression of CYPs or genetic/pharmacologic reduction of sEH activity likely elevates EETs and EDPs similarly. As described above, the anti-inflammatory capacity of EETs was first identified in bovine aortic endothelial cells; CYP2J2 overexpression and 11,12-EET treatment inhibited TNFα-, IL-1β-, and LPS-induced VCAM-1 expression by preventing activation of NFκB.[146] EET anti-inflammatory activity via NFκB inhibition has been validated in other macrovascular endothelial cells and monocytes.[103,170-174] Anti-inflammatory activities have also been attributed to EET activation of PPARα and PPARγ.[143-145,175] The gene targets of these signaling pathways include cell adhesion molecules and chemokines. Thus, pulmonary EC derived from mice overexpressing human CYP2J2 or -2C8 exhibited reduced levels of LPS-induced

adhesion molecule and chemokine expression, and the CYP inhibitor MS-PPOH and a putative EET antagonist 14,15-EEZE nullified these anti-inflammatory effects.[176]

Evidence from *in vivo* studies also supports the anti-inflammatory effects of EET and EDP. Rats injected with TNFα showed elevated plasma levels of cytokines and soluble forms of adhesion molecules, and decreased levels of the anti-inflammatory cytokine IL-10; normal levels were recovered by systemic overexpression of human CYP2J2.[177] In a model of cerebral ischemia, EC-specific human CYP2J2 or -2C8 reduced infarct size while also reducing levels of TNFα and IL-1β transcripts.[178] Similarly, *Ephx2*$^{-/-}$ mice and mice overexpressing EC-specific human CYP2J2 or -2C8 all showed reduced levels of inflammatory gene expression and neutrophil recruitment in the lung following LPS injection.[176] These effects might also be mediated by alterations in monocyte behavior. In a model of sterile resolving peritonitis, EETs were involved in resolution of inflammation by clearance of pro-inflammatory monocytes; pro-inflammatory monocyte accumulation was increased by CYP inhibition using SKF-525A and was reduced by sEH deletion.[179] Pharmacologic manipulation of sEH produces similar anti-inflammatory responses. For example, in a mouse model of acute inflammation induced by systemic LPS, pharmacologic inhibition of sEH reduced plasma TNFα and IL-6 levels compared to vehicle treatment.[180] Likewise, sEH inhibition mitigated high fat diet-induced hepatic IL-1β up-regulation, and increased IL-10 in DHA-enriched fat-1 animals, suggesting an influence by EDP.[181] Together, these data confirm a role for EET/EDP in inhibition of vascular cytokine production and leukostasis. Furthermore, the inflammatory mediators that are the focus of this dissertation, TNFα, IL-1β, IL-6, and IL-8, all have proven to be regulated by CYP-derived epoxides.[181-185]

Though epoxides demonstrate potent anti-inflammatory activities, in inflamed tissues their beneficial effects are limited by alterations in the normal balance of CYP/sEH enzyme levels. For example, in mice receiving intraperitoneal LPS injections CYP epoxygenase expression and EET product formation were reduced in the liver, kidney, and lungs.[186] Furthermore, distinct cytokines have differential effects on hepatic CYP expression.[187] Conversely, sEH expression is elevated in various models of inflammation. For example, in macrophages from diabetic animals, LPS stimulation increased sEH expression, and this induction was even greater than in macrophages from control mice.[188] Additionally, sEH levels were elevated at the graft-vein junction in a porcine model of arteriovenous grafts, and this elevation was confirmed in cultured monocytes.[189] Taken together, these data suggest that CYP and sEH dysregulation contributes to a cycle of chronic inflammation initiated by cytokine elevation; cytokines attenuate CYP levels and elevate sEH levels, thereby decreasing anti-inflammatory epoxides. The decreased epoxide levels consequently create a permissive environment for persistent inflammation.

Epoxygenated fatty acids in diabetes and obesity

In a wide range of diabetes-relevant culture conditions, CYP-derived epoxides exert anti-iflammatory effects. For example, homocysteine, which is elevated in diabetic retinopathy and associated with atherosclerosis,[190,191] induces NFκB activity in mouse aortic endothelial cells and CYP2J2 overexpression reduced this activation.[173] Palmitic acid, which is elevated in the serum and tissues of diabetic patients and animal models,[192-194] induced TNFα, IL-1β and IL-6 up-regulation in HepG2 cells, while CYP2J2

overexpression and 14,15-EET inhibited this induction.[195,196] EETs are also able to modulate the activity of immune cells and macrophages in culture. For example, peripheral blood mononuclear cells (PBMC) isolated from $Ldlr^{-/-}$ mice, which have elevated serum cholesterol, show increased adherence when rolled over P-selectin-coated plates or TNFα-treated endothelial cell monolayers; treatment with soluble epoxide hydrolase inhibitors plus 14,15-EET or co-deletion of sEH decreased PBMC adhesion.[197] Thus, epoxide anti-inflammatory activities have been observed in several diabetes-relevant culture conditions using cells derived from a variety of tissue beds.

CYP and sEH enzymes have been investigated in diabetic animals and patients, and in the related contexts of hypertension and metabolic syndrome. The overwhelming majority of evidence supports a protective role of EET and EDP, and points to altered CYP and sEH levels and compromised EET/EDP production under diabetic conditions. STZ-treated diabetic mice that underwent experimental occlusion of the middle cerebral artery exhibited increased sEH in cerebral vessels and decreased EET levels in brain, relative to non-diabetics.[198] The diabetic mice sustained larger brain infarct than controls, and pretreatment with an sEH inhibitor eliminated this difference and normalized EET concentrations, without altering glycemia.[198] In the *db/db* mouse model of diabetes, systemic CYP2J2 overexpression reduced activation of the NFκB signaling pathway in liver, leading to decreased production of TNFα, IL-1β and IL-6.[196] sEH inhibition also decreased *ICAM-1, VCAM-1* and *IL-6* expression and macrophage infiltration in aortic vessels of $ApoE^{-/-}$ mice treated with angiotensin II.[199] Furthermore, sEH deletion or inhibition attenuated STZ-induced diabetic nephropathy and reduced renal phospho-IKK to total IKK ratios, indicating less activation of NFκB.[200] Taken

together, these data provide the basis for epoxide therapies as a potential anti-inflammatory therapy for early DR.

In a variety of *in vitro* and *in vivo* experimental settings, diabetes-relevant conditions consistently perturb CYP and sEH expression, reducing EET/EDP levels.[201-206] The results of these studies are summarized in **Table 2**. In porcine aortic endothelial cells (EC) treated with high glucose, CYP expression and activity were significantly decreased within 24 hours, resulting in reduced EET production.[204] Homocysteine induced sEH expression in endothelial cells, and consequently sEH inhibition mitigated homocysteine-induced VCAM-1 expression.[207] Additionally, sEH was up-regulated in HepG2 cells treated with PA, leading to increased endoplasmic reticulum (ER) stress.[206] In the Zucker obese rat model, expression of the rat homologs of human CYP2C enzymes, CYP2C11 and CYP2C23, were decreased in renal and mesenteric arteries, while sEH expression was increased.[201,205] Studies in diet-induced hypertensive or obese Zucker rats, models of type 2-related pre-diabetes, demonstrated that protein levels of CYP2C11 and -2C23 were significantly decreased in kidney vasculature, correlating with endothelial dysfunction, microalbuminuria and hypertension.[208-211] Additionally, in the rat STZ diabetes model, hepatic CYP2C11 was almost completely absent by 4 weeks post-diabetes induction.[212] Lastly, and of particular relevance to the hypothesis of my project, 11,12-EET and 14,15-EET are significantly reduced in the vitreous of patients with DR compared to non-diabetic controls.[89] Taken together, these findings suggest that during diabetes CYP and sEH expression are altered in a way that reduces EETs and EDPs, causing a permissive environment for inflammation in diabetic retinopathy.

Cell or tissue	Diabetes-relevant stimulus or model	Effect of diabetes-relevant stimulus on CYPs, epoxides, or sEH	Ref
Porcine aortic endothelial cell	High glucose	Lower CYP expression and activity, lower EET production	204
Human umbilical vein endothelial cells	Homocysteine	Elevated sEH expression	207
HepG2 cells	Palmitic acid	Elevated sEH protein levels	206
Rat renal arteries	Obese Zucker rat	Lower CYP protein levels	201
Rat mesenteric arteries	Obese Zucker rat	Lower CYP expression, elevated sEH expression	205
Rat renal arteries	Diet-induced obesity	Lower CYP protein levels	208
Liver	STZ-induced diabetes	Lower CYP protein levels	212
Vitreous	Diabetic retinopathy patients	Lower EET levels	89

Table 2. Summary of studies observing alterations to enzyme and/or epoxide levels.

Apart from their expected effects on inflammation, EET/EDP-elevating strategies have other beneficial features. For example, STZ-treated *Ephx2*$^{-/-}$ mice or WT mice treated with sEH inhibitors exhibited increased glucose tolerance, and *Ephx2*$^{-/-}$ mice maintained on high fat diets showed decreased insulin resistance.[213,214] Similarly, CYP2J3 overexpression in db/db mice and fructose-fed rats resulted in decreased peripheral insulin resistance.[215] Also, obese *Ephx2*$^{-/-}$ mice exhibited elevated kidney EET levels, accompanied by improved vascular function in the kidney compared to obese control mice.[216] In activity-restricted primates, decreased capillary blood volume is associated with an increased ratio of vaso-constrictor HETEs to vaso-dilatory EETs, and this correlated with insulin resistance.[217] A recent study further suggests that EETs have a direct role in hepatic insulin sensitivity because EET treatment increased Akt activity without affecting insulin receptor or insulin receptor substrate-1 levels.[218] These outcomes suggest added benefits of therapeutic epoxide manipulation in diabetes and

its complications.

Several clinical studies have verified the results of these *in vitro* and *in vivo* studies. For instance, plasma EET levels are decreased in patients with metabolic syndrome.[219] Furthermore, a G50T polymorphism in CYP2J2, resulting in decreased expression and activity, was significantly associated with early type 2 diabetes onset.[220] A close association has also been identified between a G860A polymorphism in the *EPHX2* gene and elevated insulin resistance in type 2 diabetics.[221] These findings point to an important role for sEH regulation of epoxide levels in diabetes and demonstrate the safety of therapeutic sEH inhibition. Further supporting this concept, sEH inhibitors have been used clinically for impaired glucose tolerance and hypertension.[222-226]

Based on the role of EETs and EDPs in inflammation, and their decreased levels in various tissue beds affected by diabetes, I hypothesized *that endogenous EET/EDP levels would be decreased in response to diabetes-relevant conditions, and thus their experimental elevation would be efficacious in treating early stages of DR*. In order to test this hypothesis, I have employed several pharmacologic manipulations to alter the enzyme activities and/or epoxide levels involved in the pathway. The relevant metabolic pathways, as well as these experimental manipulations, are outlined in **Figure 5**.

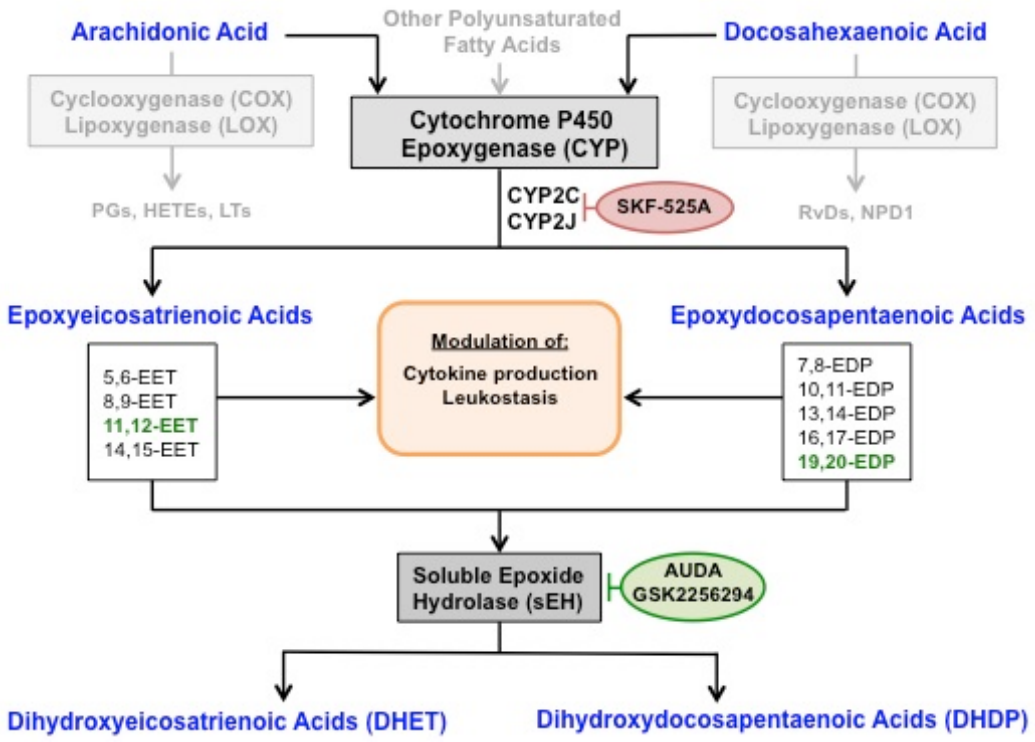

Figure 5. Overview of the CYP/sEH pathway and experimental manipulations used in this dissertation. Tools used to limit EET/EDP production are shown in red (SKF-525A) and tools used to increase EET/EDP levels are shown in green (11,12-EET, 19,20-EDP, AUDA, and GSK2256294).

In the following chapters, I sought to address this hypothesis by analyzing the effect of epoxides in disease-relevant *in vitro* and *in vivo* models of retinal inflammation and angiogenesis. In **Chapter III**, I established diabetes-relevant *in vitro* models for Müller cells that can be used to determine the effect of EETs and EDPs on initiation and amplification of inflammatory factors. Next, in **Chapter IV**, I examined the paracrine effects of inflammatory mediators on endothelial cells and determined the role of EET and EDP manipulation on retinal vascular inflammation. A visual model demonstrating my hypothesis regarding EET/EDP in retinal inflammation during DR is shown in **Figure 6**. Lastly, I demonstrated in **Chapter V** that retinal angiogenesis is promoted by EETs, suggesting that pharmacologic strategies developed to elevate their levels may be

contraindicated for late-stage diabetic retinopathy. The results of these studies provide a basis for understanding and further exploring the role of epoxides in the pathogenesis of DR.

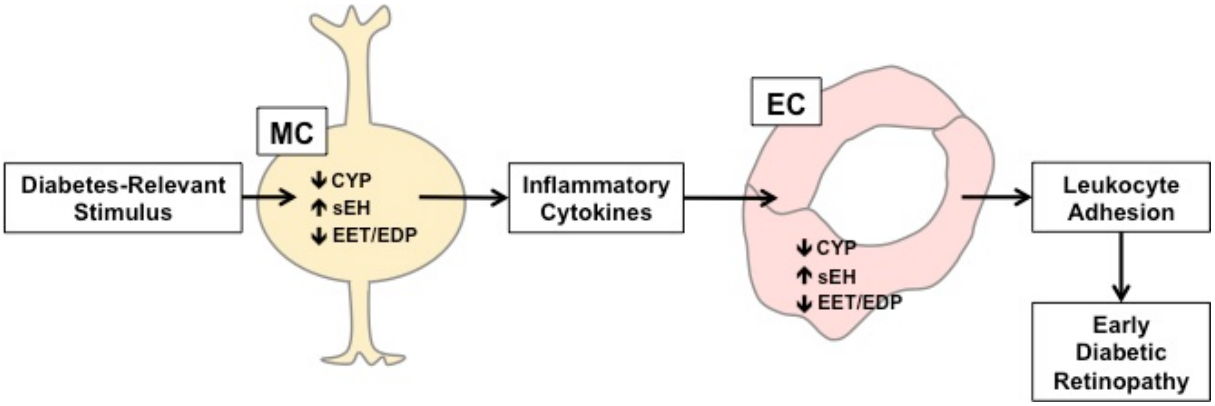

Figure 6. Hypothetical model of the role of epoxides in early diabetic retinopathy.

CHAPTER II

METHODS

Human Retinal Cell Culture

Human Müller cell isolation, culture and treatment

Primary human retinal Müller Cells were isolated from human donor tissue (NDRI) within 24hrs post-mortem, using a modified protocol developed by Hicks and Courtois.[227] The retina was dissected from the eye cup and dissociated in Dulbecco's Modified Eagle Medium (DMEM; Life Technologies) containing trypsin and collagenase. Following incubation in dissociation medium, cells were cultured in DMEM containing 10% fetal bovine serum (FBS) and 1x antibiotic/antimycotic solution. Passages 4 through 6 were used for all experiments.

In **Chapter III**, Müller cells were cultured in 6-well dishes and at 70% confluence, Müller cells were cultured in serum-reduced conditions (2% FBS) for 12 hours before treatment. Cells were then treated in serum-reduced medium containing either elevated D-glucose (30.5mM) or L-glucose (osmotic control; 5.5mM D-glucose plus 25mM L-glucose) for 24 hours. Next, medium was removed and replaced with the same D-glucose or L-glucose treatment in the presence of either BSA-bound palmitic acid (PA; 250μM) or fatty acid-free BSA control (100mg/ml in PBS). PA was prepared at 200mM in EtOH. Once dissolved, PA in EtOH was incubated with 100mg/ml BSA in PBS at 5mM for 90 minutes at 37°C before added to media. The treatment groups in **Chapter III** are therefore referred to as the following: LG/BSA (L-glucose 24 hours, L-glucose + BSA 24 hours), LG/PA (L-glucose 24 hours, L-glucose + PA 24 hours), DG/BSA (D-

glucose 24 hours, D-glucose + BSA 24 hours), or DG/PA (D-glucose, D-glucose + PA 24 hours).

For cytokine stimulation of Müller cells, cells were cultured in 6-well plates, and at 80% confluence, cells were placed in serum-reduced conditions for 12 hours. Cells were then treated for either 2, 4, 8, 12, or 24 hours with 1ng/ml of the following human recombinant proteins: TNFα (Millipore), IL-1β (R&D Systems), IL-6 (R&D Systems), or IL-8 (R&D Systems).

In **Chapter V**, Müller cells were seeded in 6-well plates at $2x10^5$ cells/well and maintained under standard culture conditions, as described above. At 90% confluency, cells were exposed to either normoxia (20.9% O_2) or hypoxia (0.1% O_2) for 24 hours. Oxygen levels were maintained at 0.1% using the ProOx 110 (BioSpherix).

Human retinal microvascular endothelial cell culture and treatment

Primary human retinal microvascular endothelial cells (HRMEC; Cell Systems) were validated by assessing cytoplasmic VWF and uptake of Di-I-Ac-LDL. Cells were cultured in phenol red-free endothelial basal medium (EBM; Lonza) containing 10% FBS with SingleQuots (Lonza) and grown on attachment factor- (Cell Signaling) coated culture dishes. Cultures were incubated at 37°C, 5% CO_2, and 20.9% O_2 and 95% relative humidity. Passages 6 to 10 were used for all experiments.

In **Chapter IV**, endothelial cells were treated in 100cm^2 plates (for epoxide quantification), 6-well plates (for qRT-PCR), 10cm^2 dishes (for immunoblots), glass microscope slides (for PPFC), or 96-well plates (for NFκB activity assay). Unless otherwise specified, cells were placed in serum-reduced media (2% FBS), which

contained 1x antibiotic/antimotic instead of Singlequots, for 12 hours. Cells were then treated with vehicle (0.3% EtOH and 0.1% DMSO), TNFα (1ng/ml) plus vehicle, or TNFα plus 11,12-EET (0.5μM), 19,20-EDP, 12-(3-adamantane-1-yl-ureido)-dodecanoic acid (AUDA; 10μM), 11,12-DHET (0.5μM), 19,20-DHDP (0.5μM), or combinations of 11,12-EET or 19,20-EDP and AUDA.

In **Chapter V**, human retinal microvascular endothelial cells were seeded in 6-well plates at $2x10^5$ cells/well and maintained under standard culture conditions, as described above. For hypoxia experiments, at 90% confluency, cells were exposed to either normoxia (20.9% O_2) or hypoxia (0.1% O_2) for 24 hours. Oxygen levels were maintained at 0.1% using the ProOx 110 (BioSpherix).

Human retinal astrocyte cell culture and treatment

Primary cultures of human retinal astrocytes (Sciencell) were plated in tissue culture flasks coated with poly-L-lysine (Sciencell). Astrocytes were cultured in Astrocyte Growth Medium (Sciencell), containing 2% fetal bovine serum (FBS), astrocyte growth supplement, and a penicillin/streptomycin solution. Cultures were incubated at 37°C, 5% CO_2, 20.9% O_2, and 95% relative humidity. Passages 4 to 6 were used. In **Chapter V**, human retinal astrocytes were seeded in 6-well plates at $2x10^5$ cells/well and maintained under standard culture conditions, as described above. At 90% confluency, cells were exposed to either normoxia (20.9% O_2) or hypoxia (0.1% O_2) for 24 hours. Oxygen levels were maintained at 0.1% using the ProOx 110 (BioSpherix).

RNA isolation, RNAseq, and analysis

Treated cells were lysed and RNA purified using the RNeasy mini kit (Qiagen) according to the manufacturer's protocol. Total RNA was isolated and submitted to the Vanderbilt Technologies for Advanced Genomics (VANTAGE) core for RNAseq analysis. RNA sample quality was confirmed using the 2100 Bioanalyzer (Agilent Technologies; Santa Clara, CA). All RNA samples had an RNA integrity number > 8.0. Samples were prepared for sequencing using the TruSeq RNA Sample Prep Kit (Illumina; San Diego, CA) to enrich for mRNA and prepare cDNA libraries. Library quality was assessed using the 2100 Bioanalyzer. Sequencing was performed using a single read, 75 bp protocol on the Illumina HiSeq 3000 (Illumina). This method was used in **Chapter III**.

Alignment and differential expression

The Vanderbilt Technologies for Advanced Genomic Analysis and Research Design (VANGARD) core performed sequence alignment and differential expression analyses. Alignment and gene mapping was performed using QC3.[228] Differential expression was assessed using MultiRankSeq, which uses the results of three statistical algorithms (DESeq, edgeR, and baySeq) to more rigorously determine significantly altered gene transcripts.[229] Briefly, each algorithm generates a rank of differentially expressed genes based on statistical significance of differential read counts. These ranks are summed, generating a list of transcripts with the greatest differential expression by all three algorithms. For analysis, only transcripts with an adjusted p-value <0.05 determined by any two (L-glucose vs. D-glucose and L-

glucose/PA vs. D-Glucose/PA) or all three (BSA vs. PA and vehicle vs. cytokines) algorithms were used for analysis. This method was used in **Chapter III**.

Pathway analysis

Pathway enrichment analysis was performed using the Database for Annotation, Visualization and Integrated Discovery (DAVID; v6.7). Lists of significantly up-regulated genes were submitted to the DAVID website and compared to a human reference gene background. The Kyoto Encyclopedia of Genes and Genomes (KEGG) Pathway annotation and Biocarta annotation (only PA-treated Müller cells) was used for pathway enrichment analysis. Pathways were considered significantly enriched with $p<0.05$. This method was used in **Chapter III**.

Quantitative real time RT-PCR

After treatment, cells were washed twice with cold PBS and total RNA was collected using the RNeasy Mini kit (Qiagen). Total RNA isolated from the culture wells was reverse transcribed using the High-Capacity cDNA Archive Kit (Applied Biosystems). Quantitative RT-PCR was performed in duplicate by co-amplification of cDNA vs. a normalization control (either *18S* or *ACTB*), using gene-specific TaqMan Gene Expression Assays (**Table 3**; Applied Biosystems). The delta Ct method was used to determine relative expression of the targeted mRNA normalized to the selected normalization control. All commercial assays were performed according to the manufacturer's protocol. This method was used in **Chapters III-V**.

Target	Primer	Species	Chapter
IL8	Hs00174103_m1	Human	3
MMP1	Hs00899658_m1	Human	3
PTGS2	Hs00153133_m1	Human	3
PTGIS	Hs00919949_m1	Human	3
18S	Hs99999901_s1	Human	3,4
TNFA	Hs01113624_g1	Human	3
IL1B	Hs01555410_m1	Human	3
IL6	Hs00985639_m1	Human	3
VCAM1	Hs01003372_m1	Human	4
ICAM1	Hs00164932_m1	Human	4
CYP2C8	Hs02383390_s1	Human	5
CYP2C9	Hs02383631_s1	Human	5
CYP2C11	Rn01502203_m1	Rat	5
CYP2C23	Rn00582954_m1	Rat	5
ACTB	Rn00667869_m1	Rat	5
ACTB	Hs01060665_g1	Human	5

Table 3. Gene expression assays used in studies.

Immunocytochemical analysis

After treatment, cells were fixed with 4% paraformaldehyde in PBS for 30 minutes. Cells were then washed three times in PBS containing 0.1% Triton-X 100 in PBS (PBST) for 15 minutes each, followed by blocking in 4% BSA in 0.3% PBST for 1 hour at room temperature. Cells were then incubated in primary antibodies for glial fibrillary acidic protein (GFAP; 1:2000; Agilent Technologies) or glutamine synthase (GS; 1:250; Millipore) in blocking buffer overnight at 4^{o}C. Cells that were incubated without primary served as a negative control. After incubation in primary, cells were washed and then were incubated with secondary antibody (1:1000; Thermo Fisher

Scientific) for 1 hour at room temperature. After washing in PBST, cells were mounted in Vectashield Hardset with DAPI mounting media (Vector Laboratories) and images were captured with an AX70 upright microscope (Olympus) and DP71 digital camera (Olympus) at 20x magnification. This method was used in **Chapter III**.

Epoxygenated fatty acid quantification

Human Müller cells (**Appendix C**) or HRMEC (**Chapter IV**) were treated for 21 hours or 9 hours, respectively, followed by treatment with EET and EDP substrate (10μM AA and 10μM DHA; Sigma-Aldrich) for 3 hours. Media was collected, triphenylphosphine (TPP; Sigma-Aldrich) was added, and samples were evacuated with argon. After adding synthetic [$^2H_{11}$]-labeled 8,9-DHET, 11,12-DHET, 14,15-DHET, 16,17-DHDP, and 19,20-DHDP (5ng each) as internal standards, the EET/EDPs and DHET/DHDPs were extracted with acidified $CHCl_3$/CH_3OH (2:1) and purified by silica solid phase extraction, separating EET/EDPs and DHET/DHDPs. The EET/EDPs were converted to the corresponding DHET/DHDPs by treatment with acetic acid overnight. The samples were quantified by LC/MS/MS using an Acquity BEH C18 columns (1.0 × 100mm; 1.7μm) connected to a TSQ-Quantum Vantage triple quadrupole spectrometer (Thermo Fisher Scientific). DHET/DHDP positional isomers were resolved using a linear solvent gradient that went from 70% 15mM aqueous ammonium acetate (pH 8.5), 30% acetonitrile to 40% 15mM aqueous ammonium acetate (pH 8.5), 60% acetonitrile in 6 minutes and at a flow of 0.18ml/min. For analysis, we utilized collision-induced fragmentation of the DHET/DHDPs at m/z 337 and the [$^2H_{11}$]-DHET/DHDP internal standards at m/z 448. These same product ions were also used for the deuterated

internal standards. Quantifications were done using the ratio of the area of the DHET/DHDP peaks compared to the area of the corresponding deuterated DHET/DHDP peaks. Cell lysates were collected, total protein was measured using a Pierce bicinchoninic acid assay (BCA; Thermo Fisher Scientific), and EET and EDP levels were normalized to the total protein. This method was used in **Chapter IV**.

Immunoblot analysis

After treatment, cells were washed twice in cold PBS and lysed using radio-immunoprecipitation assay (RIPA) buffer (Qiagen) with protease inhibitors (Roche). Samples were equilibrated for total protein concentration using a BCA assay (Pierce), and prepared in 4x Laemmli Buffer (Bio-Rad) containing 355mM β-mercaptoethanol (Bio-Rad) and then heated for 10min at 96°C. Fifteen µg of protein were loaded onto a 10% SDS gel (Bio-Rad) and the gels were run for 1 hour and 45 minutes. Samples were then transferred to nitrocellulose membranes using the iBlot system (Thermo Fisher Scientific). Membranes were blocked and probed in 5% BSA for CD54/ICAM-1 (1:1000; Cell Signaling) and β-Actin (1:4000; Thermo Fisher Scientific) or 5% milk for VCAM-1 (1:1000; Abcam) Blots were then labeled with horseradish peroxidase-conjugated secondary antibodies (1:2000). β-Actin was used as a loading control. Membranes were incubated in Pierce ECL Western blotting substrate and developed with a ChemiDoc MP (Bio-Rad). Blots were then quantified using ImageJ software. This method was used in **Chapter IV**.

Parallel plate flow chamber

HRMEC were plated on glass slides coated with attachment factor. Once confluent monolayers formed, cells were placed in serum-reduced culture medium for 12 hours and then treated as stated for 4 hours. After treatment, slides were placed in a parallel plate flow chamber (GlycoTech), as described previously.[76] PBMC (Sanguine Biosciences) were resuspended in Hank's Buffered Salt Solution (HBSS) at a concentration of 5 x 10^5 cells/ml. Cells were then flowed over treated monolayers at a shear stress of 1dyn/cm^2 for 7 minutes, and non-adherent cells were then removed with HBSS at 2dyn/cm^2 for 2 minutes. Eight fields were randomly captured and adhered leukocytes were counted by a masked observer. Data are shown as the average of the eight captured fields for one slide and reported as adherent cells per mm^2. This method was used in **Chapter IV**.

NFkB activity assay

HRMEC were seeded on 96-well black-walled, clear bottom plates. Each well was transfected with NFkB-responsive luciferase constructs, negative control constructs, or positive control constructs from the Cignal NFkB Reporter Assay (Qiagen). For transfection, 75µL of fresh 10% media was added to each well 30 minutes prior to treatment. Each well was then transfected with 200ng of each construct, 1.8µL of Targafect solution A (Targetingsystems), and 3.6µL Virofect (Targetingsystems) in 50µL of Optimem (Life Technologies). The transfection mix was prepared in a separate tube, and 15 inversions were performed between the additions of each reagent. After preparation, the transfection mix was incubated at 37°C for 25 minutes. Twelve hours

after initiation of transfection, cells were washed and treated with fresh 10% medium for 12 hours. Twenty-four hours post-transfection, cells were treated with vehicle or TNFα (1ng/ml) in the presence or absence of 11,12-EET (0.5μM) or 19,20-EDP (0.5μM) with AUDA (10μM) for 24hrs after initiating transfection. Luciferase was quantified using the Dual-Glo Luciferase Assay System (Promega), according to the manufacturer's protocol. Data are reported as the relative ratio of firefly-to-Renilla luciferase. This method was used in **Chapter IV**.

Intravitreal injection

All experiments were approved by the Vanderbilt University Institutional Animal Care and Use Committee and were performed in accordance with the ARVO Statement for the Use of Animals in Ophthalmic and Vision Research. Rodents were anesthetized by isoflurane (Butler Animal Health Supply) inhalation. Before intravitreal injection, 0.5% proparacaine (Allergan) was topically applied to the cornea. The globe was penetrated approximately 0.5mm posterior to the ora serrata, using a 30-gauge needle with a 19° bevel and a 10μL syringe (Hamilton Co.). The needle was advanced to the posterior vitreous at a steep angle to avoid contact with the lens. The injection bolus was delivered near the trunk of the hyaloid artery proximal to the posterior pole of the retina. After injection, a topical antibiotic suspension (Vigamox; Alcon) was applied. In **Chapter IV**, 6 week-old C57BL/6J mice (Charles Rivers) were injected intravitreally with 2μl of vehicle (0.1% DMSO and 0.3% EtOH), TNFα (50ng/ml), TNFα with 11,12-EET (0.5 μM) plus AUDA (10μM), or TNFα with 19,20-EDP (0.5μM) plus AUDA (10μM). In **Chapter V**, at 14(0) and 14(3) Sprague-Dawley rat pups received intravitreal injections (5μL) of

vehicle (0.1% ethanol in PBS) or increasing concentrations of SKF-525A (0.5μM – 5.0μM). This method was used in **Chapter IV** and **V**.

Retinal leukostasis

Six hours after treatment, mice were anesthetized with ketamine (100mg/kg) and xylazine (10mg/kg) and perfused with 0.9% saline for 1min, followed by FITC-conjugated concanavalin-A (40μg/ml in 2.5ml PBS; Vector Laboratories) at a rate of 6.5ml/min. Mice were then perfused with saline for 5mins to remove any non-adherent leukocytes. Retinas were immediately dissected into 4% paraformaldehyde, flat-mounted, and images were captured with an AX70 upright microscope (Olympus) and DP71 digital camera (Olympus) at 4x magnification. Adherent leukocytes in the vasculature were counted using ImageJ and divided by the total retinal vascular area quantified using Adobe Photoshop. Normality of the dataset was confirmed with a D'Agostino & Pearson normality test with an alpha=0.05. This method was used in **Chapter IV**.

VEGF enzyme-linked immunosorbent assay (ELISA)

Human retinal astrocytes and human Müller cells were seeded in 6-well plates. At 70% confluency, cells were treated with vehicle (0.1% EtOH) or 5.0μM SKF-525A. Plates were either maintained in standard culture conditions (37°C, 5% CO_2, 20.9% O_2) or transferred to hypoxic conditions (37°C, 5% CO_2, 0.1% O_2). Cells were treated for 24 hours, conditioned media were collected, and frozen at -80°C until use. Cells were collected using TrypLE (Invitrogen) and then lysed in 50μL RIPA buffer with protease

inhibitors. VEGF was measured with a VEGF colorimetric sandwich ELISA kit (R&D systems) and the normalized to total protein using a BCA assay (Pierce). This method was used in **Chapter V**.

HRMEC proliferation

HRMEC were seeded at 3 X 10^3 cells/well in a 96-well plate and cultured for 8 hours in 10% FBS medium. Cells were then cultured in serum-reduced (0.5% FBS) medium for 12 hours. Cells were treated with 0.5% FBS medium containing vehicle (0.1% EtOH) or increasing concentrations of 11,12-EET (0.05μM – 0.5μM), recombinant human 25ng/ml VEGF vehicle (0.1% EtOH; Millipore) or VEGF containing increasing concentrations of SKF-525A (0.5μM – 5.0μM; ENZO Life Science). After treatment for 24 hours, cells were labeled with BrdU for 12 hours. BrdU incorporation was quantified using a colormetric BrdU ELISA (Roche), according to the manufacturer's protocol. Absorbance values were normalized to the 0.5% FBS vehicle for relative quantification. This method was used in **Chapter V**.

HRMEC tube formation

Twenty-four well tissue culture plates were coated with 300μL of growth factor reduced Matrigel® (Becton Dickenson). HRMEC were seeded at 2 X 10^4 cells/well on polymerized Matrigel®. Cells were treated with 0.5% FBS medium containing vehicle (0.1% EtOH), increasing concentrations of 11,12-EET (0.05μM – 0.5μM), 50ng/mL VEGF containing vehicle (0.1% EtOH), or increasing concentrations of SKF-525A (0.5μM – 5.0μM). After 8 hours of treatment, tubes were observed with an inverted

widefield fluorescence microscope (Nikon Eclipse Ti-E) and captured at 2x magnification. Capillary-like structures were measured to determine the mean tube length per field using ImageJ software (NIH), and these values were normalized to the 0.5% FBS vehicle treatment group. The relative tube length per field of each treatment group is reported. This method was used in **Chapter V**.

Rat model of oxygen-induced retinopathy (OIR)

All animal procedures used in this study were approved by the Vanderbilt University Institutional Animal Care and Use Committee and were performed in accordance with the ARVO Statement for the Use of Animals in Ophthalmic and Vision Research. Within 8 hours after birth, litters of at least 14 Sprague-Dawley rat pups and their mothers (Charles Rivers Laboratories) were transferred to oxygen exposure chambers (BioSpherix), in which they were subjected to alternating 24 hour periods of 50% and 10% oxygen for 14 days. On postnatal day 14, referred to as 14(0), the oxygen-exposed rats were returned to room air. They remained in room air for an additional six days, hereafter described as 14(1) through 14(6). Age-matched rat litters were also maintained in room air (RA) to serve as controls. This method was used in **Chapter V**.

Retinal RNA isolation

Retinas from 14(2) and room air day-matched controls (P16) were harvested by winkling directly into 150μL RNA*later*® Solution (Ambion) and frozen at -20°C until use. Total RNA was isolated from tissue using RNA lysis buffer supplemented with β-

mercaptoethanol using an RNeasy kit (Qiagen). A 5mm stainless steel bead (Qiagen) was added to each sample then samples were lysed using the TissueLyser LT (Qiagen) at 50Hz for 3 minutes. RNA isolation and quantification was performed as described above. This method was used in **Chapter V**.

Quantification of retinal vascular area and neovascular area

On 14(6), rats were sacrificed, their eyes enucleated and their retinas dissected in 4% paraformaldehyde. The retinal vasculature was stained for adenosine diphosphatase (ADPase; Sigma) activity.[81] To accomplish this, isolated retinas were washed with tris buffer three times and once in tris buffer containing 0.1% Tween® 20 (Sigma). Retinas were then incubated in ADPase at 37°C for 15-25 minutes, until retinas were white in color. Retinas were washed 3 times in tris buffer and then developed using ammonium sulfide. Retinas were washed 3 more times in tris buffer and then flatmounted. Images of ADPase-stained retinas were digitized, captured, and displayed at 20x magnification. For each retinal image, total retinal area, total vascular area, and pre-retinal vessel tuft area were outlined with an irregular polygon using Adobe photoshop. The pixels within the polygon were counted, and the total number of pixels from each polygon in a retina were pooled and converted to square millimeters. The vascular area measurements are shown as a percentage of the total retinal area. This method was used in **Chapter V**.

Retinal VEGF quantification

OIR-exposed rats received intravitreal injections of vehicle (0.1% EtOH in PBS) or SKF-525A (5.0μM) on 14(1). Room air age-matched animals (P15) were injected with vehicle as a control. Retinas were collected on day 14(2), the peak day of retinal VEGF following oxygen exposure,[84] sonicated in lysis buffer, and assayed for VEGF protein concentration with a colorimetric sandwich ELISA kit (R&D systems). The amount of VEGF (pg/mL) in retinas was normalized to total protein concentration (mg/mL) of retinal lysates using a BCA assay (Pierce). This method was used in **Chapter V**.

Statistical analysis

For **Chapters III** and **IV**, data were analyzed with the Prism software (GraphPad) using analysis of variance (ANOVA) with Fisher's LSD post hoc analysis. Values of $p<0.05$ were considered statistically significant.

For **Chapter V**, data were analyzed with commercial software (JMP; SAS Institute) using ANOVA with Student's post hoc analysis. $p<0.05$ was considered statistically significant.

CHAPTER III

MÜLLER CELL STIMULATION BY PALMITIC ACID AND ELEVATED GLUCOSE

From: Capozzi M.E., Penn J.S. Palmitic Acid Induces Müller Cell Inflammation and is Potentiated by Co-treatment with Glucose. *In review*.

Overview

Based on the results of several clinical trials demonstrating that tight glycemic control slows the progression of DR, including the DCCT and UKPDS, hyperglycemia has been considered the driving cause of DR pathology. Owing to the long recognized reputation for glucose in DR, basic research has focused on elevated glucose in cell culture models to recapitulate mechanisms of DR. Yet, results from several clinical studies suggest glucose may not be the primary driver of DR, because overt hyperglycemia is not necessary for the development of pathology. For example, multiple case studies observed diabetic retinopathy pathology in patients with relatively normal glucose tolerance.[230-232] Additional evidence comes from case studies of patients with bariatric surgery, in which there have been instances when retinopathy progressed, despite lowering of HbA1c.[233] This provides the impetus to develop an understanding of non-glucose driven pathology in both *in vitro* and *in vivo* disease models for mechanistic understanding of DR pathogenesis.

Recent studies have demonstrated a strong association between dyslipidemia and DR. In the Fenofibrate Intervention and Event Lowering in Diabetes (FIELD) and The Action to Control Cardiovascular Risk in Diabetes (ACCORD) studies, the lipid

lowering drug, fenofibrate, delayed retinopathy progression, independent of glycemic control.[16] In humans and animal models, diabetes increases fatty acid concentrations in systemic circulation and tissues, leading to inflammation, insulin resistance, and disease progression.[234,235] Mounting evidence supports the use of fatty acids as a diabetes-relevant stimulus in non-ocular experimental contexts, but their use in the context of DR remains limited.[95,102,193] Serum and tissue profiles from diabetic patients and experimental models of diabetes demonstrate that one saturated fatty acid, palmitic acid (PA), is elevated above others.[192-194] Increased retinal levels of PA, as well as the unsaturated fatty acids, oleic acid (OA) and linoleic acid (LA), have been observed early in rodent models of diabetes.[193,236] Furthermore, there is evidence of these fatty acids evoking inflammatory responses in retinal microvascular endothelial cells.[95,237] These data suggest that elevated fatty acids may be causally linked to retinal inflammation occurring early in the pathogenesis of DR.

An initial study in our lab (**Appendix A**) compared the effects of oleic acid and linoleic acid to those of elevated D-glucose to determine the relative consequences of these stimuli on the production of three DR-relevant inflammatory and angiogenic mediators; VEGF, IL-6, and IL-8. We used these stimuli to determine their effect on four human retinal cell types, three of which were primary (human Müller cells, human microvascular endothelial cells, and human retinal astrocytes), and the other of which was a transformed line of retinal pigmented epithelium (ARPE-19). From this study we identified that fatty acids serve as more potent stimulators of inflammatory mediator and growth factor production, and that this induction was specific to Müller cells. This observation served as the basis for the present study.

In the following experiments designed to determine the effect of CYP-derived epoxides in disease-relevant Müller cell cultures, we chose to use PA as the pathogenic stimulus for several reasons. First, PA treatment increased sEH protein levels in hepatocyte and adipocyte cultures.[206] PA also induced TNFα, IL-1β and IL-6 up-regulation in HepG2 cells, while CYP2J2 overexpression and 14,15-EET inhibited this induction.[195,196] These examples demonstrate that PA is both diabetes-relevant and pro-inflammatory, and suggest that its inflammatory properties are mitigated by EET/EDP treatment. Additionally, because it is saturated, our use of PA offers a distinct advantage over pro-inflammatory unsaturated fatty acids because it is not epoxygenated by CYPs,[238] thus our epoxide measurements would not be confounded by contributions from metabolism of the stimulus.

It is important to note that dyslipidemia occurs in the absence of diabetes, and hyperlipidemic patients do not have the same retinal pathology as that observed in DR. Thus there is potential for glucose to affect retinal cells, despite the limited effects on human primary cells that are unrelated to osmolarity (**Appendix A**). These considerations suggest that culture conditions using combinations of DR-relevant stimuli may be more relevant models to understand pathology in controlled *in vitro* experiments. Therefore, the first goal of these experiments was to compare PA- and D-glucose treated primary human Müller cell cultures and to determine whether combination treatment further promoted DR-relevant pathways using whole transcriptome analysis for differential gene expression.

Being that Müller cells are implicated as the main producers of inflammatory mediators, we next wanted to determine the effects of these inflammatory mediators on

their autocrine production, termed “auto-amplification.” Therefore, while the purpose of using D-glucose and PA in our initial studies is to recapitulate mechanisms involved in inflammatory initiation, in the next step of the study we used cytokines as stimuli to demonstrate their effects on amplification of inflammation in primary human Müller cells. We used the four inflammatory stimuli that are consistently elevated in the vitreous of patients with diabetic retinopathy; TNFα, IL-1β, IL-6, and IL-8. To assess their relative effects, we treated human Müller cells with each cytokine and used whole transcriptome analysis of differential expression to understand their comparative potencies as well as the full complement of activated factors. Thus, the overall goal of this chapter is to define relevant Müller cell conditions that are representative of both the initiation of inflammation as well as the amplification of inflammation by Müller cells in the diabetic retina. This platform will provide a basis for both mechanistic studies as well as assessment of therapeutic strategies in *in vitro* culture models.

Results

RNAseq Quality and Alignment

In order to determine the effects of PA, D-glucose, and their combination on transcriptional changes in Müller cells, RNAseq was performed. The four experimental groups (2 samples of each) were treated as follows: LG/BSA (24 hours of L-glucose, followed by 24 hours of L-glucose plus BSA); LG/PA (24 hours of L-glucose, followed by 24 hours of L-glucose plus PA); DG/BSA (24 hours of D-glucose, followed by 24 hours of D-glucose plus BSA); DG/PA (24 hours of D-glucose, followed by 24 hours of D-glucose plus PA). The average read count was 11318908.38 reads per sample,

mapping on average 93.88% of the human genome (**Table 4**). The read counts were not statistically different between treatment groups using an ANOVA (p=0.2387).

Sample	Total Reads	Mapped (%)
LG/BSA1	11058763	93.38
LG/BSA2	10249362	93.83
LG/PA1	11245915	93.79
LG/PA2	12642057	93.71
DG/BSA1	11138539	94.01
DG/BSA2	10804232	93.25
DG/PA1	11808323	94.78
DG/PA1	11604076	94.31
Average	11318908.38	93.88

Table 4. Summary of reads mapping to the human genome using QC3.

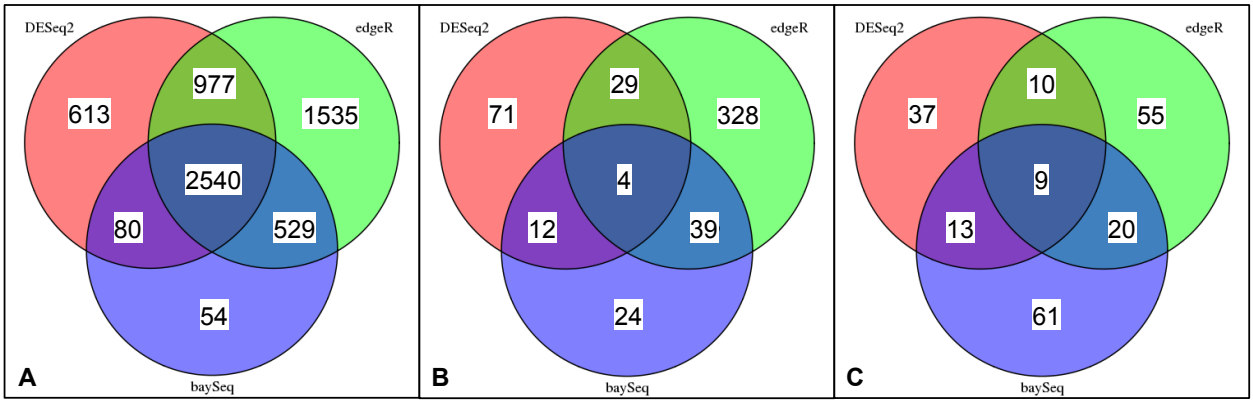

Figure 7. Transcripts with adjusted p-value<0.05 for A) LG/BSA vs. LG/PA, B) LG/BSA vs. DG/BSA, C) LG/PA vs. DG/PA.

The Effect of PA Treatment on Human Müller Cell Gene Expression

As shown in **Figure 7A**, 2540 hits were significantly changed as demonstrated by all three statistical tests (DESeq2, edgeR, and baySeq) between the LG/BSA and

LG/PA groups. Of these, 740 were down-regulated while 1800 were up-regulated. The protein-coding genes with the largest log2fold changes are reported in **Table 5.**

We then performed pathway analysis using only the significantly up-regulated genes to determine which biological pathways were enriched in our data set. Of these genes, 582 were identified in the KEGG database (**Figure 8**) and 173 were identified in the Biocarta database (**Figure 9**). Twenty-four pathways were significantly enriched by KEGG analysis and 11 pathways were significantly enriched by Biocarta analysis. Many interesting and relevant pathways were enriched, including inflammatory pathways linked to “NOD-like receptor signaling pathway” (19 hits) “RIG-I-like receptor signaling” (12 hits) and “Toll-like receptor signaling pathway” (15 hits). Additionally, in Biocarta pathway analysis, the “NFκB Signaling Pathway” (8 hits) and several associated NFκB pathway terms were enriched, in addition to “Signal transduction through IL1R” (8 hits). Additional DR-relevant pathways in the KEGG analysis include “Amino sugar and nucleotide sugar metabolism” (15 hits) “Neurotrophin signaling pathway” (22 hits), “MAPK signaling pathway” (36 hits), “PPAR signaling pathway” (13 hits), and “Apoptosis” (7 hits). MAPK signaling was also significantly enriched in Biocarta analysis.

Ensembl Gene ID	Gene Target	Log2fold change	Adj p value
ENSG00000081041	CXCL2	5.131169228	3.48E-121
ENSG00000180535	BHLHA15	4.970842312	2.06E-107
ENSG00000167861	HID1	4.556667723	4.04E-110
ENSG00000078081	LAMP3	4.125085146	3.52E-55
ENSG00000173110	HSPA6	4.097445282	6.88E-64
ENSG00000167772	ANGPTL4	3.943015061	0
ENSG00000004799	PDK4	3.804721573	1.73E-73
ENSG00000163734	CXCL3	3.763486125	9.79E-57
ENSG00000130487	KLHDC7B	3.660859835	4.54E-51
ENSG00000162772	ATF3	3.640394145	0
ENSG00000169429	CXCL8	3.546291509	4.45E-97
ENSG00000147872	PLIN2	3.366381211	7.28E-273
ENSG00000137491	SLCO2B1	3.359650884	1.19E-23
ENSG00000099958	DERL3	2.985336774	9.33E-42
ENSG00000133134	BEX2	2.952925525	4.57E-46
ENSG00000180660	MAB21L1	-1.477045754	5.61E-19
ENSG00000186847	KRT14	-1.497222046	7.37E-102
ENSG00000167244	IGF2	-1.501273659	7.04E-114
ENSG00000131095	GFAP	-1.525215644	2.41E-13
ENSG00000205221	VIT	-1.564053796	1.28E-28
ENSG00000105989	WNT2	-1.597706963	3.55E-46
ENSG00000130592	LSP1	-1.628532041	4.50E-10
ENSG00000137672	TRPC6	-1.629488495	3.81E-45
ENSG00000179772	FOXS1	-1.669083989	1.64E-13
ENSG00000163909	HEYL	-1.703173713	3.48E-08
ENSG00000104415	WISP1	-1.752999127	9.97E-21
ENSG00000185585	OLFML2A	-1.826404845	7.21E-51
ENSG00000078401	EDN1	-1.96860795	5.77E-41
ENSG00000163815	CLEC3B	-2.078011452	3.05E-43
ENSG00000106511	MEOX2	-2.333794203	2.36E-23

Table 5. List of top 15 up-regulated genes (green) and down-regulated (red) genes in comparison of LG/BSA vs. LG/PA samples. Log2fold change is the average from all statistical tests. Adjusted p-value is reported from EdgeR analysis.

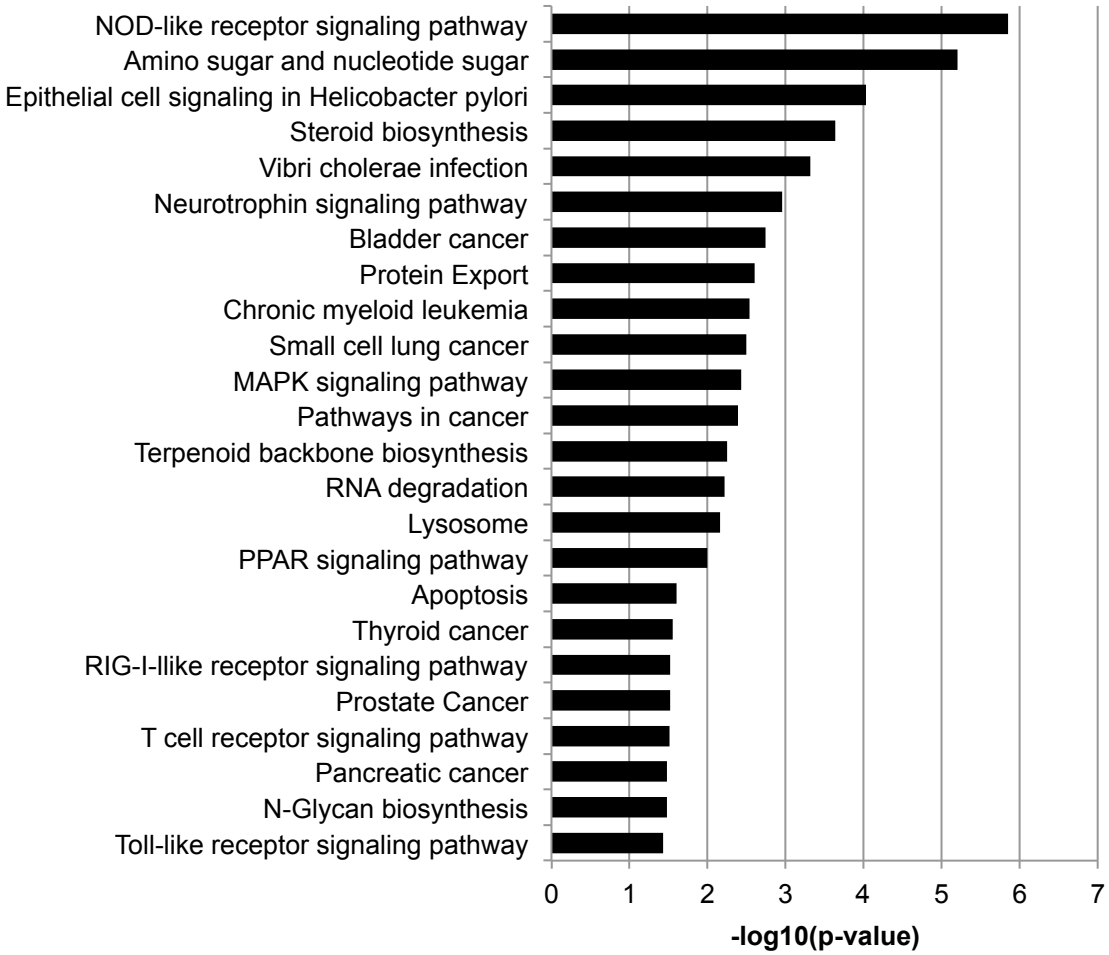

Figure 8. KEGG pathways enriched by PA-treatment alone. Pathway enrichment was determined using DAVID v6.7 with a $p<0.05$.

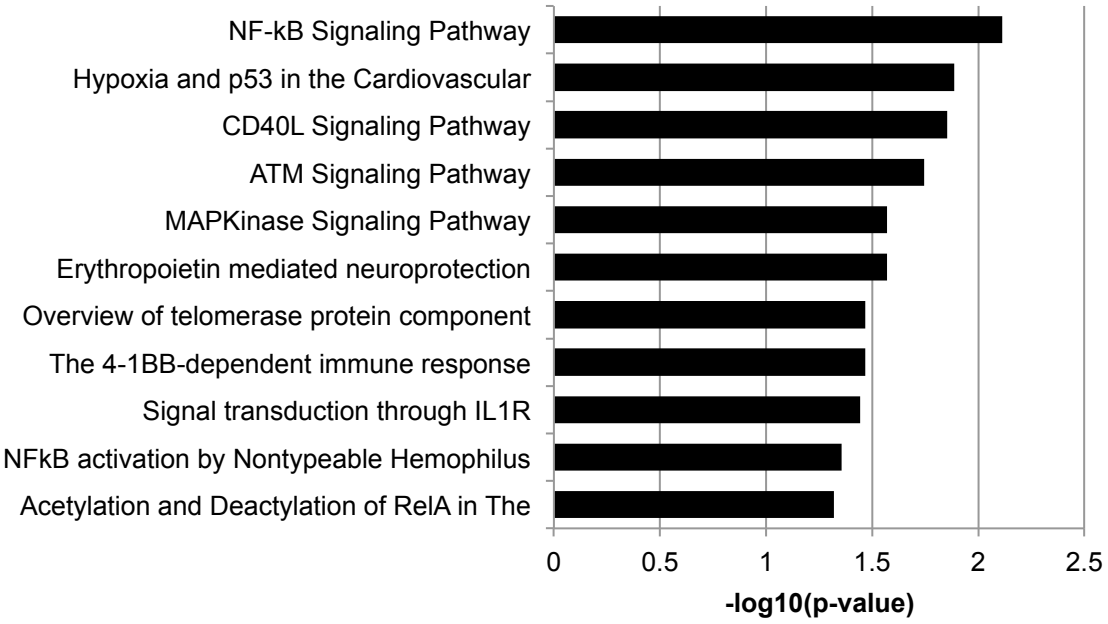

Figure 9. Biocarta pathways enriched by PA-treatment alone. Pathway enrichment was determined using DAVID v6.7 with a $p<0.05$.

The Effect of D-glucose Treatment on Müller Cell Gene Expression

As shown in **Figure 7B**, using the stringency of all three statistical tests, only four genes were significantly altered between the LG/BSA and DG/BSA groups. Therefore, the 74 genes that were significant by any two statistical tests were used in pathway analysis in order to have a large enough population of hits. The top ten up-regulated and down-regulated hits from this group are reported in **Table 6**. Using this gene list, only the “Splicesome” pathway was significantly altered (6 hits; p=4.2E-5).

Ensembl Gene ID	Gene Target	Log2fold change	Adj p value
ENSG00000134321	RSAD2	4.923508774	4.09E-08
ENSG00000269483	AC006272.1	2.919487587	0.019466295
ENSG00000164344	KLKB1	2.548189429	0.00071155
ENSG00000111335	OAS2	2.17216683	7.02E-05
ENSG00000089127	OAS1	2.168790961	4.62E-06
ENSG00000183486	MX2	2.010356923	0.000545912
ENSG00000137959	IFI44L	1.925914084	6.37E-08
ENSG00000185885	IFITM1	1.304828318	0.003807034
ENSG00000137965	IFI44	1.292143094	6.64E-10
ENSG00000115267	IFIH1	1.147805314	0.001221134
ENSG00000126458	RRAS	-0.222524777	0.035308923
ENSG00000175274	TP53I11	-0.228925103	0.038692229
ENSG00000168159	RNF187	-0.235492533	0.044616825
ENSG00000167244	IGF2	-0.247562395	0.026513466
ENSG00000182809	CRIP2	-0.249868373	0.010900659
ENSG00000183087	GA56	-0.268869012	0.007495434
ENSG00000163017	ACTG2	-0.332161513	0.029633892
ENSG00000070404	FSTL3	-0.344548454	0.005595595
ENSG00000049540	ELN	-0.359844309	0.021121557
ENSG00000130176	CNN1	-0.410923384	0.007865768

Table 6. List of top 10 up-regulated genes (green) and down-regulated (red) genes in comparison of LG/BSA vs. DG/BSA samples. Log2fold change is the average from all statistical tests. Adjusted p-value is reported from EdgeR analysis.

The Effect of PA and D-glucose Combination Treatment on Müller Cell Gene Expression

We next compared the effect of PA on Müller cells after pre-treatment with D-glucose (DG/BSA vs. DG/PA). While only 9 genes were significantly altered according to all three statistical tests, we used the 51 genes that were altered by any two statistical tests (**Figure 7C**) for analysis. In **Table 7**, the top 10 up-regulated and down-regulated genes are listed. Seventeen genes were up-regulated, and six of those were recognized

by KEGG analysis. The only significantly enriched pathway was “Pathways in cancer” (5 hits; p=8.1E-5) and within this pathway, genes specifically related to proliferation and angiogenesis were enriched. These included genes that encode: Cyclin D1, COX-2, MMP1, IL-8, and c-Jun. Because of their known relationships to diabetes pathology, we focused our validation on *CXCL8* (*IL8*) and *PTGS2*. In **Figure 10**, we demonstrate PA induction of these targets, as well as a greater induction by pre-treatment with D-glucose. PA treatment (LG/BSA vs. LG/PA) induced *IL8* expression by 11.5-fold ($p<0.0001$) and *PTGS2* expression by 3.5-fold ($p<0.0001$). Compared to PA-treated human Müller cells (LG/PA), D-glucose pre-treated cells (DG/PA) further induced *IL8* expression by 52.6% ($p<0.0001$) and *PTGS2* expression by 24.2% ($p=0.0440$). The comparison of relative expression determined from qRT-PCR analysis to RNAseq analysis is shown in **Appendix B**.

Ensembl Gene ID	Gene Target	Log2fold change	Adj p value
ENSG00000039600	SOX30	2.205032696	0.008276689
ENSG00000159167	STC1	0.776414785	8.46E-07
ENSG00000196611	***MMP1***	***0.702045263***	***0.00040217***
ENSG00000169429	***CXCL8***	***0.592836812***	***3.57E-07***
ENSG00000073756	***PTGS2***	***0.528668486***	***1.66E-06***
ENSG00000122861	***PLAU***	***0.421038355***	***0.004849631***
ENSG00000162772	***ATF3***	***0.227905481***	***0.000343642***
ENSG00000128590	***DNAJB9***	***0.226338735***	***0.000903843***
ENSG00000100934	SEC23A	0.221898127	0.046332084
ENSG00000137831	UACA	0.195567228	0.000562227
ENSG00000135480	***KRT7***	***-0.386967885***	***0.033509088***
ENSG00000128510	***CPA4***	***-0.418677262***	***6.12E-05***
ENSG00000171992	***SYNPO***	***-0.427503511***	***0.000329537***
ENSG00000130176	***CNN1***	***-0.455594004***	***5.73E-05***
ENSG00000049540	***ELN***	***-0.460297597***	***0.000196689***
ENSG00000163431	***LMOD1***	***-0.462317808***	***4.04E-07***
ENSG00000137124	***ALDH1B1***	***-0.464431223***	***8.43E-07***
ENSG00000163017	***ACTG2***	***-0.481167848***	***5.73E-05***
ENSG00000107796	***ACTA2***	***-0.558187261***	***0.013391793***
ENSG00000149596	***JPH2***	***-0.618904013***	***0.007443867***

Table 7. List of top 10 up-regulated genes (green) and down-regulated (red) genes in comparison of LG/PA vs. DG/PA samples. Bold/italicized genes indicate that these transcripts were also significantly altered in LG/BSA vs. LG/PA sample comparison. Log2fold change is the average from all statistical tests. Adjusted p-value is reported from EdgeR analysis.

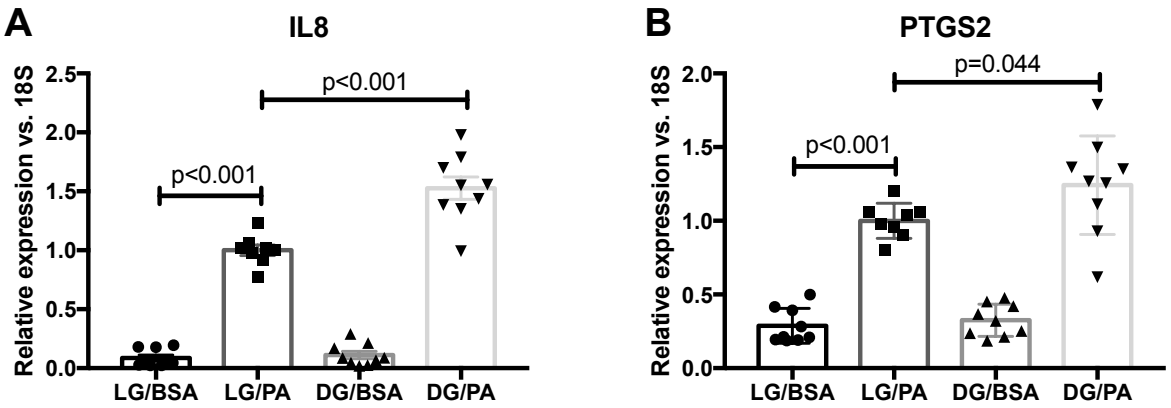

Figure 10. Validation of targets amplified in the DG/PA treatment group. Cells were acquired from 3 different donors, and treated the same as reported for the RNAseq analysis. (A) *IL8* and (B) *PTGS2* were induced by PA, and further amplified with pre-treatment of D-glucose. Data is reported as mean ± SEM (n=9).

Validation of Müller Cell Phenotype

As shown in **Table 4**, GFAP was one of the most highly down-regulated genes in response to PA treatment. This suggested that the treatment conditions may be causing the treated Müller cell cultures to de-differentiate. Thus, we verified that Müller cells did not de-differentiate in any of our culture conditions by assessing two common markers of Müller cell identity, GFAP and glutamine synthase (GS). As shown in **Figure 11**, Müller cell levels of GFAP and glutamine synthase (GS), as well as Müller cell morphology, remained constant in all treatment groups.

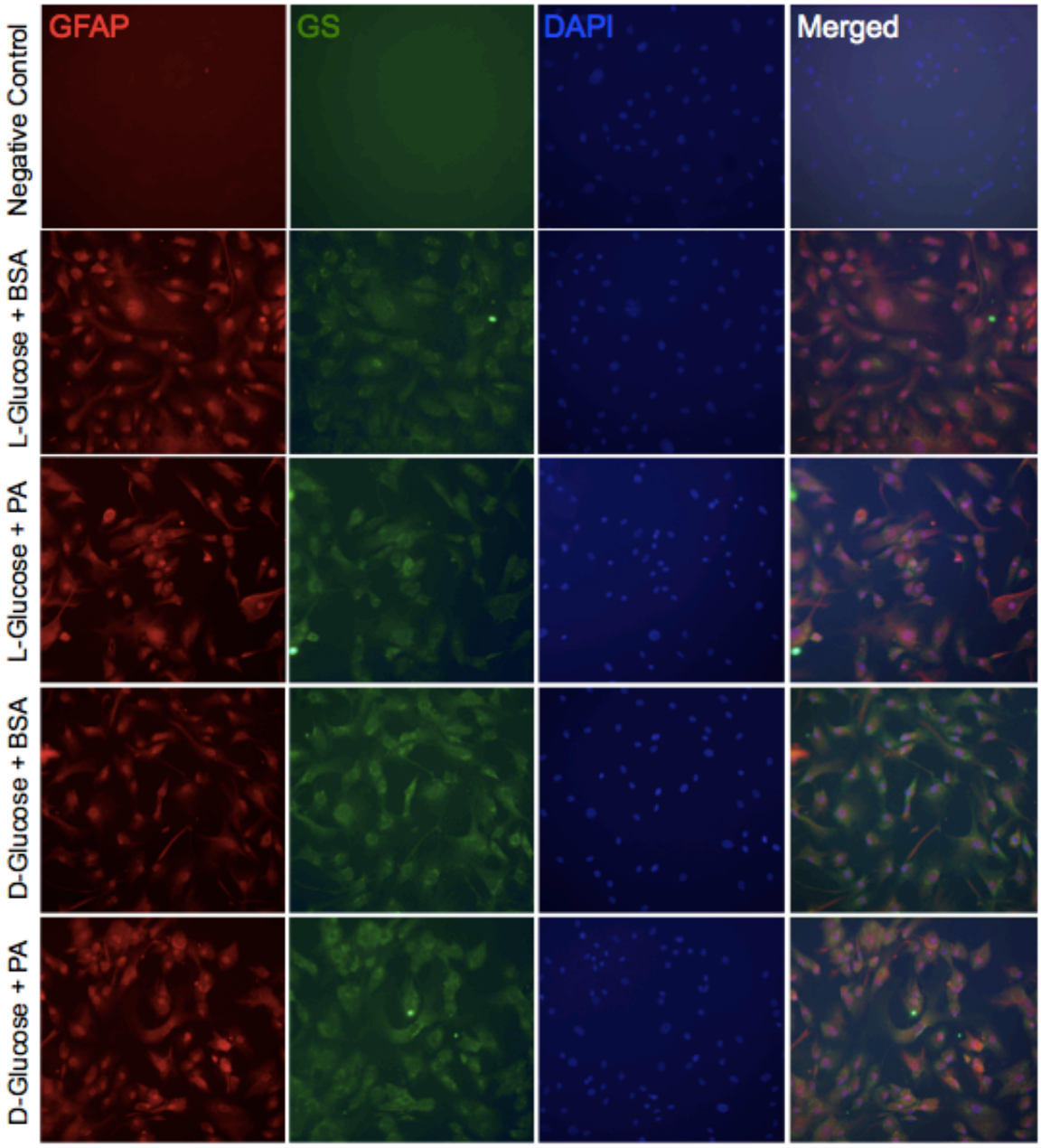

Figure 11. Validation of Müller cell phenotype across treatment groups. Mullller cells were treated as described for RNAseq analysis. GFAP (glial fibrallary activated protein) and GS glutamine synthase) were used for validation of Müller cell phenotype. DAPI was used to identify cell nuclei. All images were taken at 20x magnification.

Cytokine Auto-amplification by Müller Cells

We next sought to determine the effects of cytokine-stimulated Müller cells on the production of these same cytokines, termed auto-amplification. In **Figure 12**, we

performed a time course using inflammatory mediators that are consistently elevated in the vitreous of patients with diabetic retinopathy: TNFα, IL-1β, IL-6, and IL-8. All treatments were administered at 1ng/ml. IL-1β was the most potent stimulus, inducing TNFα, IL-1β, and IL-6 significantly more than the other mediators at all time points assessed (**Figure 12A-C**). TNFα demonstrated similar potency to IL-1β for the induction of IL-8 (**Figure 12D**).

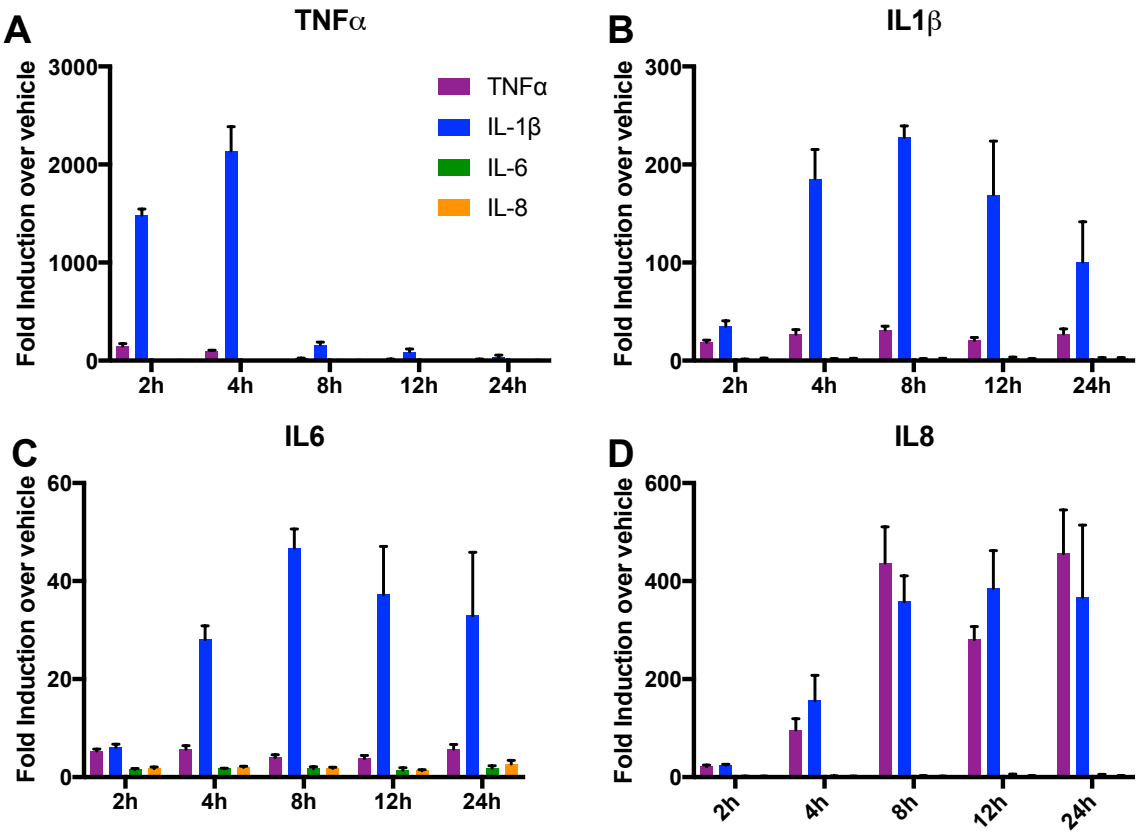

Figure 12. Time course of inflammatory mediator effect on auto-amplification. Müller cells were treated with 1ng/ml of each inflammatory mediator (see graph key). Expression of (A) *TNFα*, (B) *IL1β*, (C) *IL6*, and (D) *IL8* were compared to *18S* expression as a control, and data are reported as the fold induction over the vehicle. Bars represent mean ± SD (n=3).

RNAseq Analysis of Cytokine-stimulated Müller cells

RNAseq was performed using two samples from each treatment group, which were treated for 8 hours with 1ng/ml of the following human recombinant proteins: TNFα, IL-1β, IL-6, or IL-8. As shown in **Figure 13**, only TNFα and IL-1β induced significant alterations in Müller cell gene expression, as determined by using all three statistical tests (DESeq2, EdgeR, and baySeq). IL-1β had a larger effect than TNFα, because it differentially expressed 1477 gene targets while TNFα altered 212 gene targets. The top up-regulated and down-regulated genes are shown in **Table 8** for TNFα and **Table 9** for IL-1β. Interestingly, the list of most up-regulated genes are similar (*CCL20*, *CSF2*, *CXCL8*, and *CXCL10*) for TNFα and IL-1β, yet the size of the inflammatory response is greater in IL-1β treated cells. This is demonstrated by KEGG pathway analysis in **Figure 14** and **Figure 15**; "Cytokine-cytokine receptor interaction" is the most significant pathway up-regulated by both TNFα and IL-1β, but the number of hits and significance in IL-1β-stimulated cells (42 hits; p=1.9E-20) is much greater than that for TNFα-stimulated cells (13 hits; p=2.4E-8). All pathways enriched by TNFα treatment (**Figure 14**) were also enriched by IL-1β (**Figure 15**).

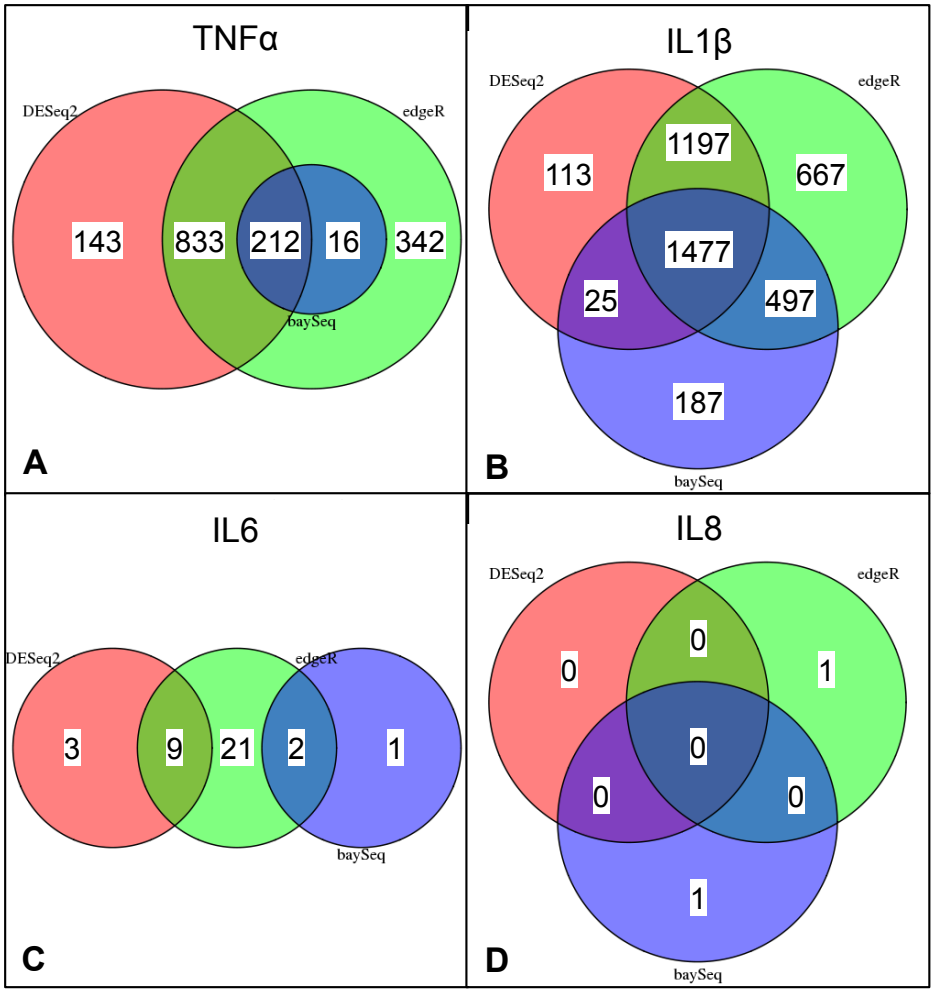

Figure 13. Transcripts with adjusted p-value<0.05 for (A) TNFα-treated, (B) IL-1β-treated, (C) IL-6-treated, or (D) IL-8-treated Müller cells.

Ensembl Gene ID	Gene Target	Log2fold change	Adj p value
ENSG00000169245	CXCL10	8.026759425	0.0107210
ENSG00000134321	RSAD2	5.595108551	0.0018596
ENSG00000023445	BIRC3	5.53166577	0.0000267
ENSG00000164400	CSF2	5.524018514	0.0165729
ENSG00000169429	CXCL8	8.026759425	0.0181992
ENSG00000204880	KRTAP4-8	5.595108551	0.0210578
ENSG00000090339	ICAM1	5.53166577	0.0004370
ENSG00000151572	ANO4	5.524018514	0.0055333
ENSG00000183486	MX2	8.026759425	0.0047475
ENSG00000115009	CCL20	5.595108551	0.0017661
ENSG00000145681	HAPLN1	-4.442665891	0.0003414
ENSG00000168079	SCARA5	-4.473338093	0.0038751
ENSG00000131471	AOC3	-4.559672004	0.0053784
ENSG00000174600	CMKLR1	-4.599861157	0.0000071
ENSG00000149451	ADAM33	-4.626852708	0.0040869
ENSG00000124920	MYRF	-4.629950113	0.0001252
ENSG00000162595	DIRAS3	-4.792761404	0.0000533
ENSG00000091972	CD200	-4.913172953	0.0002284
ENSG00000132622	HSPA12B	-5.179285136	0.0025991
ENSG00000034971	MYOC	-7.660169261	0.0000376

Table 8. List of top 10 up-regulated genes (green) and down-regulated (red) genes in comparison of vehicle vs. TNFα-treated samples. Log2fold change is the average from all statistical tests. Adjusted p-value is reported from EdgeR analysis.

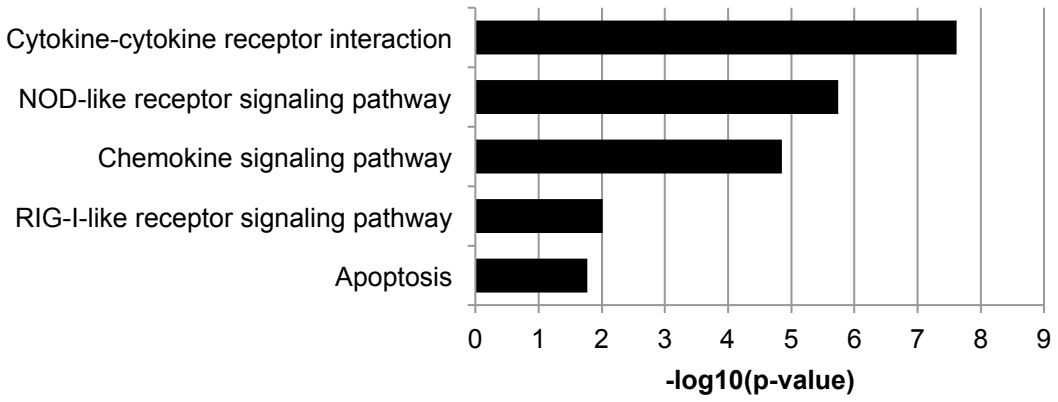

Figure 14. KEGG pathways enriched by TNFα treatment. Pathway enrichment was determined using DAVID with a p<0.05.

Ensembl Gene ID	Gene Target	Log2fold change	Adj p value
ENSG00000108342	CSF3	10.4153456	0
ENSG00000007908	SELE	9.50836945	9.29E-285
ENSG00000163734	CXCL3	8.970547385	0
ENSG00000163739	CXCL1	8.756812978	0
ENSG00000081041	CXCL2	8.557509753	0
ENSG00000115009	CCL20	8.322086144	0
ENSG00000169429	CXCL8	8.055145731	6.47E-212
ENSG00000164400	CSF2	7.767223895	6.87E-230
ENSG00000125538	IL1B	7.113063114	0
ENSG00000169245	CXCL10	6.877020604	2.35E-68
ENSG00000143850	PLEKHA6	-2.347383947	0
ENSG00000111087	GLI1	-2.387906314	0.00481442
ENSG00000143631	FLG	-2.438031045	0
ENSG00000168497	SDPR	-2.471388158	0
ENSG00000144229	THSD7B	-2.525244528	0.002870717
ENSG00000196196	HRCT1	-2.527825526	6.75E-14
ENSG00000162630	B3GALT2	-2.55306345	9.83E-06
ENSG00000125378	BMP4	-2.773861711	0
ENSG00000181072	CHRM2	-2.783228974	0
ENSG00000134215	VAV3	-3.351086987	3.15E-09

Table 9. List of top 10 up-regulated genes (green) and down-regulated (red) genes in comparison of vehicle vs. IL-1β-treated samples. Log2fold change is the average from all statistical tests. Adjusted p-value is reported from EdgeR analysis.

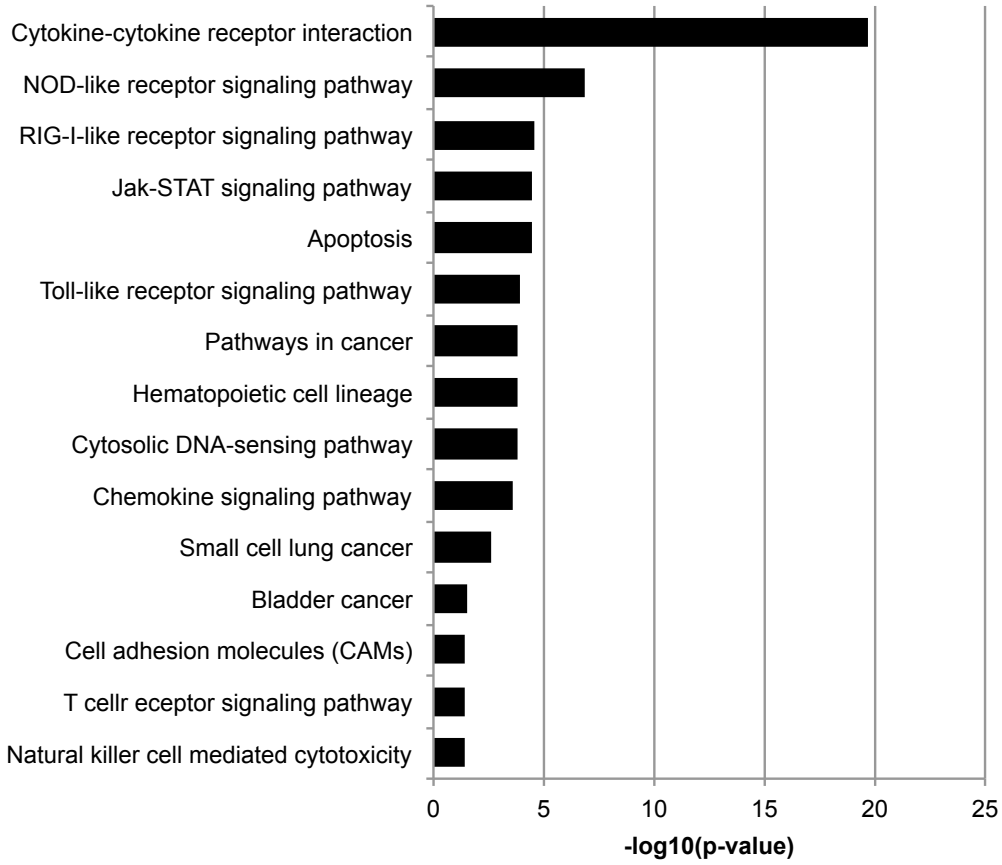

Figure 15. KEGG pathways enriched by IL-1β treatment. Pathway enrichment was determined using DAVID with a $p<0.05$.

Conclusions

Pathways Regulated by PA and DG/PA

The most important finding from this study is that elevated glucose, interacting with the saturated fatty acid, PA, generates a more robust induction of diabetes-relevant gene expression than either stimulus alone. A particularly important finding was that glucose alone had little to no effect on Müller cells, despite it being the most commonly used stimulus for DR basic research. These results are important for the interpretation of several clinical studies. First, our findings support the results of the FIELD and ACCORD studies, which demonstrated that modulation of dyslipidemia, independent of

glucose control, reduced the need for laser treatment of DR.[16,17] Furthermore, our results suggest that the interpretation of the findings in the DCCT and UKPDS trials, in which glycemic control was significantly associated with DR progression,[12,13] be considered in a broader context because several metabolic changes are associated with glycemic control. Yet, many *in vitro* studies in the DR field use glucose as a diabetes-relevant stimulus due to the results of these clinical studies. Intensive glycemic control is achieved by insulin treatment, and several metabolic changes occur with insulin therapy in diabetics. Thus, the data in the present study, in which conventional elevated glucose conditions yielded no response from Müller cells, demonstrate the need for a more careful consideration of metabolic changes in DR basic research, beyond glucose alone.

Several disease relevant targets were identified after treatment of human Müller cells with PA alone, while no notable targets were detected with D-glucose treatment alone. Of the most highly expressed genes stimulated by PA, three are from the C-X-C family of chemokines (CXCL2, CXCL3, and CXCL8). These chemokines all signal through the CXCR2 receptor, while CXCL8 also signals through the CXCR1 receptor. These ligands have been implicated in neutrophil migration and chemotaxis.[239] While virtually nothing is known regarding CXCL2 and CXCL3 in diabetic retinopathy, CXCL8 (also called IL-8) has been found to be elevated in the vitreous of diabetic retinopathy patients.[240-242] Other interesting targets on this list include PLIN2 and ANGPTL4, which are well-characterized targets of PPARβ/δ signaling. This signaling pathway was also significantly enriched with PA treatment (**Figure 8**). Our lab has demonstrated that PPARβ/δ signaling is involved in several pathological steps of DR, including TNFα-

induced retinal vascular leukostasis (Capozzi et al. *in review*), VEGF-induced vascular permeability,[243] and retinal angiogenesis.[244] Furthermore, ANGPTL4 has recently been demonstrated to be an important factor in diabetes-induced angiogenesis in PDR.[245,246] These data further demonstrate that PA is a useful stimulus for understanding elements of DR pathogenesis in retinal cell culture, because PA-stimulated cultures faithfully recapitulate important pathogenic endpoints observed in the diabetic retina.

In PA treated cells, we also observed significant enrichment of the neurotrophin pathway. Of the identified targets, nerve growth factor (NGF) was the only ligand up-regulated in this pathway. Notably, NGF is increased in the diabetic rat retina and in tears of diabetic patients.[247-249] While NGF is predominantly involved in neuronal cell survival, it is expressed as proNGF and requires cleavage to exert its pro-survival activity.[248] ProNGF signals through a separate receptor, $p75^{NTR}$, which has been found to cause neuronal cell death and vascular permeability in the retina.[250] In diabetic retinopathy, the ratio of proNGF/NGF is increased, suggesting a greater pro-inflammatory and pro-apoptotic activity.[248] While further work should be directed at understanding the relative amount of proNGF and NGF in PA-treated Müller cell cultures, our data recapitulates the up-regulation of NGF transcription that is observed in DR models and patients.

The most exciting results from this study is that D-glucose pre-treatment of human Müller cells amplifies the response to PA, while exerting few effects alone. Compared to PA treatment, PA co-treatment with D-glucose further stimulated a limited subset of targets, predominantly involved in inflammation and angiogenesis. Two of these targets, *IL8* (or *CXCL8*) and *PTGS2*, were verified to be induced by PA and

further amplified by co-treatment with D-glucose (**Figure 10**). COX-2 (*PTGS2* product) is an inducible enzyme involved in prostaglandin synthesis, and is a target of non-steroidal anti-inflammatory drugs (NSAIDs). NSAIDs and COX-2 inhibitors have been shown to reduce retinal leukostasis and vascular permeability in diabetic rodents, independent of VEGF levels.[118] COX-2 is also involved in the late stages of disease, and its inhibition prevents the development of ischemia-induced neovascularization.[251,252] Additionally, PGE_2, a downstream product of COX-2 metabolism, is up-regulated in the vitreous of diabetic patients with PDR.[253] Our lab has previously shown that PGE_2 can signal via the EP4 receptor to stimulate retinal angiogenesis.[254] Therefore, our data further validated COX-2 as a potential drug target. More importantly, our data demonstrated the utility of combination treatment of PA and D-glucose for understanding DR pathology in Müller cells.

Interestingly, we identified several angiogenic factors up-regulated by PA and/or DG/PA treatment, including but not limited to: CXCL8, ANGPTL4, COX-2, and VEGF. Notably, these have all been shown to be hypoxia-inducible factors, and in fact, "hypoxia and p53 in the cardiovascular system" was an enriched pathway by Biocarta analysis (**Figure 9**). Yet, we observed their induction in the absence of hypoxia. This suggests that metabolic changes independent of hypoxia-induced growth factor induction may mediate the progression from early to late angiogenic stages of DR. This finding is supported by a recent study, which demonstrated that altered lipid and glucose usage in $Vldlr^{-/-}$ animals drives retinal Vegfa expression and subsequent neovascularization in the absence of hypoxia.[255] This VEGF up-regulation was observed in photoreceptors exposed to conditions of abundant fatty acids, such as

excess palmitic acid in culture.[255] The present study suggests that excessive fatty acids may also affect other highly metabolic cell types in the retina, such as the Müller cells.

Our results from DG/PA-treated human primary Müller cells may have greater mechanistic relevance to early glial changes associated with DR for several reasons. First, our use of human-derived cells allowed for analysis of targets relevant to the human disease. For example, one of the targets that was most highly amplified in LG/PA and was more amplified in DG/PA was IL-8. IL-8 is well characterized for its role in leukostasis, and it is found in high levels in the vitreous of diabetic patients.[240,241] However, it is not expressed in mice. Thus, its importance to the disease process is largely undefined because of its lack of identification in studies using rodent-derived cells or rodent models of diabetes. This supports our practice of using human-derived cells. Another important aspect of the study is the inclusion of an appropriate osmotic control. As shown in **Appendix A**, VEGF was induced similarly when Müller cells were treated with either L-glucose or D-glucose, suggesting that osmotic stress, and not signaling mechanisms, is the main inducer of VEGF in these cells. Yet, many researchers claim that elevated glucose stimulates VEGF in various Müller cell lines without using this critical osmotic control. Therefore, while our results are consistent with the literature that shows D-glucose stimulation of VEGF production, it is likely that these changes are a result of osmotic stress alone. A recent study clearly demonstrated the role of osmotic stress in microvascular endothelial cell induction of COX-2.[256] The potential role of osmotic induction of COX-2 was controlled for in our study because an osmotic stress was applied in all treatment groups. Lastly, the use of human primary Müller cells may be more relevant to understanding mechanisms of DR pathogenesis.

Virtually all studies assessing glucose-induced behaviors in the literature use either transformed cell lines (rMC-1 or MIO-MI) or rodent-derived Müller cells.[257-262] In preliminary studies, our lab has demonstrated that constitutive VEGF expression levels in the human transformed cell line, MIO-MI, are similar to hypoxia-induced VEGF expression levels in primary human Müller cells, suggesting that these cells are not appropriate for experiments of this type. Taken together, due to the technical limitations of many other studies, we believe the results of this study highlight more relevant targets and induction profiles for the human disease.

Pathways Regulated by Inflammatory Cytokines

In this study, only TNFα and IL-1β were able to stimulate inflammation in human retinal Müller cells. IL-1β was the more potent stimulus compared to TNFα, because it altered more transcripts (1477 vs. 212; **Figure 13**), it significantly enriched more pathways (15 vs. 5; **Figures 14 and 15**) and the significance of enrichment for pathways altered by both treatment groups was greater for IL-1β (**Figures 14 and 15**). This suggests that IL-1β is a more potent regulator of Müller cell behavior, and thus its neutralization or inhibition of its downstream signaling may be more important to disease progression than other inflammatory mediators that are elevated in DR.

Notably, of the 10 most up-regulated targets for each treatment, four were the same for both TNFα and IL-1β (*CCL20*, *CSF2*, *CXCL8*, and *CXCL10*; **Table 8** and **9**). All of these targets encode chemokines that are involved in leukocyte recruitment and are altered in the retina of experimental diabetes models and/or vitreous of patients with diabetic retinopathy.[240-242,263] Interestingly, one of the most significantly altered genes by

IL-1β treatment is the gene that encodes IL-1β. This “auto-amplification” has been hypothesized in the diabetic retina, and is suggested as an initial cause as well as propagator of Müller cell and retinal endothelial cell activation.[93] Our data supports the hypothesis that IL-1β auto-stimulation contributes to the chronic neuroinflammation observed in DR. Thus, inhibition of IL-1β induction could prevent a cycle of amplified cytokine production by Müller glia.

We were surprised to find that IL-8 treatment did not yield any significant alterations of gene expression in primary human Müller cells. Rabbit retinal Müller cells and the transformed cell line MIO-MI have previously been shown to have immunoreactivity for the IL-8 receptors, CXCR1 and CXCR2.[264] Further work is necessary to verify receptor expression in primary human Müller cells. However, CXCR2 is highly expressed in circulating leukocytes, and thus it is more likely that Müller cell production of IL-8, which was on the list of most highly expressed genes in several RNAseq datasets in this Chapter (**Tables 5**, **7**, **8**, and **9**), is of greater functional significance for its recruitment of circulating cells to the retina than for the direct propagation of Müller cell inflammation.

One caveat to this study is that all cytokines were used in equal doses to assess potency, however these doses do not necessarily reflect the physiologic ratios *in situ*. For instance, in response to PA, IL-6 and IL-8 levels are more significantly up-regulated than IL-1β or TNFα. Therefore, fold differences between these inflammatory mediators in relevant culture or *in vivo* conditions may be different, and thus direct comparison of potency may be irrelevant. However, the expression levels of *TNFα, IL1β, IL6, or IL8* will vastly differ based on cell type, culture conditions, levels from different disease models,

or other conditions used for study. Thus, we think this direct comparison of potencies, evidenced by using all mediators at the same concentrations, is advantageous for determining appropriate culture conditions to study mechanisms of DR pathology and potential therapeutics. Future studies should be designed to compare the relevant concentrations of these inflammatory mediators from conditioned medium or soluble fractions of vitreous to learn more about their roles in disease pathology.

Implications of Transcriptome-wide Analysis for Study of Epoxides in Müller Cell Inflammation

After querying the lists of differentially expressed genes, only one CYP epoxygenase was significantly altered (adjusted $p<0.05$ in all three statistical tests) in any of the datasets; CYP2S1 was down-regulated by 86.2% after TNFα treatment for 8 hours. Soluble epoxide hydrolase (*Ephx2*) was not significantly changed in any of the datasets. Though these data must be confirmed via assessment of enzyme activity, the results of our RNAseq suggest that epoxide therapy may be most efficacious against TNFα-induced inflammation in Müller cells. Consistent with the lack of CYP/sEH changes observed in PA-treated Müller cell cultures, PA did not alter the levels of epoxides in culture media in preliminary studies (**Appendix C**). Future work should focus on validating the effects of these diabetes-relevant culture conditions on the CYP and sEH enzyme levels and their activities.

Despite the relative lack of changes to the epoxide-regulating enzymes, the RNAseq datasets still suggest that EET/EDP therapy may be beneficial for any of the treatment conditions described. Based on our pathway analysis, several enriched

pathways are modulated by epoxides, including the PPAR pathway, NFκB-related signaling pathways, cytokine signaling, and apoptosis. Thus, future studies in the lab should be focused on how exogenous addition of EET, EDP, and/or sEH inhibition can modulate the induction of these targets by PA-, DG/PA-, IL-1β-, or TNFα-treated Müller cells.

CHAPTER IV

EFFECT OF EPOXIDES ON TNFα-INDUCED RETINAL VASCULAR INFLAMMATION

From: Capozzi M.E., Hammer, S.S., McCollum, G.W., Penn J.S. (2016) Epoxygenated Fatty Acids Inhibit Retinal Vascular Inflammation. Sci. Rep. 6, 39211.

Overview

Several pro-inflammatory cytokines are elevated in the vitreous of diabetic patients, and these cytokines drive the early stages of disease. Of the primary cytokines selected from the previous chapter (TNFα, IL-1β, IL-6, and IL-8), TNFα is the most potent inducer of endothelial cell adhesion molecules and leukocyte adhesion to endothelial cell monolayers (**Appendix D**). There is ample evidence supporting TNFα as a diabetes-relevant stimulator of retinal inflammation. For example, elevated TNFα levels in the serum and vitreous of DR patients correlate with disease progression and morbidity.[86,89,91,265] Furthermore, deletion of TNFα inhibited diabetes-induced leukostasis and retinal vascular leakage in mice.[266] TNFα induces the expression of the leukocyte adhesion proteins vascular cell adhesion molecule-1 (*VCAM1*) and intercellular adhesion molecule-1 (*ICAM1*) in human retinal endothelial cells.[76,267] Both function in the firm adherence of leukocytes facilitating their immobilization; a process referred to as leukostasis. The pathologic implications of retinal leukostasis were discussed in **Chapter I**. Briefly, when leukocytes adhere to the luminal surface of the retinal capillary endothelium, they are believed to cause the formation of vaso-occlusive thrombi that can obstruct blood flow, causing oxygen starvation and subsequent

capillary death. The death of retinal capillaries is a pivotal point in DR pathogenesis because it results in the formation of focal areas of retinal ischemia that become hypoxic. In response to hypoxia, the retina elaborates vascular endothelial cell grow factor (VEGF) and other growth factors that promote the onset of PDR along with its associated vision-threatening morbidities. Adherent leukocytes also secrete noxious stimuli, such as reactive oxygen species and inflammatory cytokines, which further contribute to inflammation, blood-retina barrier breakdown, retinal vaso-regression, and edema; all hallmarks of DR.[121,268-270] Interestingly, studies have shown that genetic deletion or antibody blockade of ICAM-1 has beneficial effects on multiple pathogenic outcomes in experimental DR, including leukostasis and vascular permeability.[117,121]

Diabetes is known to alter multiple pathways involved in endogenous fatty acid metabolism. Tissues can metabolize fatty acids to biologically active lipid mediators through the cyclooxygenase (COX), lipoxygenase (LOX) or cytochrome P450 epoxygenase (CYP) pathways. While COX, LOX, and their products have received considerable attention in the diabetic retina,[118,123,271-277] relatively little is known about the role of retinal CYP-derived lipid mediators. CYP-derived epoxides, and particularly the EET products, are known to exert a number of potent anti-inflammatory activities in diverse vasculature beds, including reduced *VCAM1* and *ICAM1* expression.[103,143,146,278] Soluble epoxide hydrolase represents a rational and promising therapeutic target to inhibit these adhesion molecules because its inhibition elevates levels of anti-inflammatory epoxides. Thus, sEH inhibition has been the objective of multiple clinical trials in diabetes-related pathology.[222-226] Notably, sEH inhibition has not yet been examined as a treatment for retinal disease.

Reduced levels of EET are observed in the vitreous of patients with NPDR and PDR,[89] and the decreased epoxide levels may be permissive for increased retinal inflammation. Accordingly, therapeutic interventions that raise EET and EDP levels may be expected to ameliorate DR inflammation; however, these approaches have not been assessed. Based on these considerations, in the present study we hypothesized that treatment of primary human retinal microvascular endothelial cells (HRMEC) with a DR-relevant inflammatory cytokine, TNFα, would decrease epoxide production, limiting their anti-inflammatory effects. Conversely, elevation of epoxide levels by their exogenous addition as well as sEH inhibition may block cytokine-induced inflammatory events in HRMEC, providing a basis for a viable therapeutic strategy to inhibit the retinal vascular inflammation that is observed at the onset of diabetic retinopathy.

Results

TNFα Decreases Epoxyeicosatrienoic Acid Levels in HRMEC-Conditioned Medium

TNFα has previously been shown to alter levels of the cytochrome P450 enzymes that produce epoxygenated fatty acids,[186,279] however any effects of TNFα on EET or EDP production by endothelial cells has not been determined. To investigate these effects, HRMEC were treated with TNFα followed by treatment with substrate (AA and DHA; 10μM each), and epoxide levels were measured in the conditioned medium. Although no specific regioisomer was significantly decreased, the sum of all EET regioisomers was significantly lowered by 37.6% ($p<0.001$). While not significant, total EDP was lowered by 26.5% (**Figure 16**).

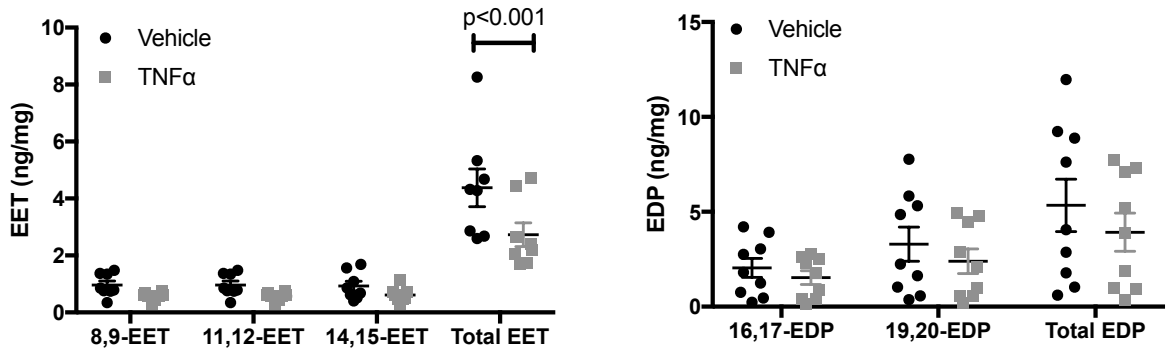

Figure 16. The effect of TNFα on epoxygenated fatty acid levels. HRMEC were treated with vehicle or TNFα (1ng/ml), arachidonic acid and docosahexaenoic acid substrates were provided, and the level of their epoxygenated products was measured in the conditioned media by LC-MS/MS. These data are normalized to the total protein of the cell lysates. Each bar represents the mean ± SEM (n=8 for EET measurements; n=9 for EDP measurements).

11,12-EET or 19,20-EDP in combination with AUDA Inhibit, and 19,20-DHDP Promotes, TNFα-induced VCAM1 and ICAM1 Expression

We investigated the effects of the exogenous addition of epoxides or sEH inhibition on TNFα-induced inflammation in HRMEC cultures. sEH activity was inhibited using 12-(3-adamantane-1-yl-ureido)-dodecanoic acid (AUDA); AUDA stabilizes both exogenous and endogenous EET and EDP by blocking hydrolysis of the epoxides to diols, extending their biological half-lives to presumably potentiate any biological effects. In **Figure 17**, we verified that hydrolysis was reduced in HRMEC cultures following AUDA treatment. We treated HRMEC cultures with exogenous 11,12-EET, 19,20-EDP, AUDA, or the EET and EDP diols, 11,12-DHET and 19,20-DHDP and assessed there effects on TNFα-induced *VCAM1* and *ICAM1* in HRMEC. The concentrations of the epoxides (0.5μM) or the sEH inhibitor AUDA (10μM) were determined from preliminary studies and fall within typical ranges used in the literature.[146,172,280-283] As shown in **Figure 18A**, 11,12-EET significantly reduced (49.6%; p=0.0001) and 19,20-DHDP

increased (84.6%; p=0.001) TNFα-induced *VCAM1* expression, while the other treatments yielded no significant effect on *VCAM1*. None of these treatments had an effect on *ICAM1* expression, with the exception of 19,20-DHDP, which increased TNFα-induced *ICAM1* expression by 54.5% (p=0.0001).

Next, we treated TNFα-stimulated HRMEC with combinations of 11,12-EET or 19,20-EDP and AUDA and assessed any effects on *VCAM1* and *ICAM1* expression. As shown in **Figure 18B**, 11,12-EET plus AUDA inhibited *VCAM1* by 32.5% (p=0.0001) and *ICAM1* by 31.9% (p=0.0001). Similarly, 19,20-EDP plus AUDA inhibited *VCAM1* by 37% (p=0.0001) and *ICAM1* by 20.7% (p=0.0027).

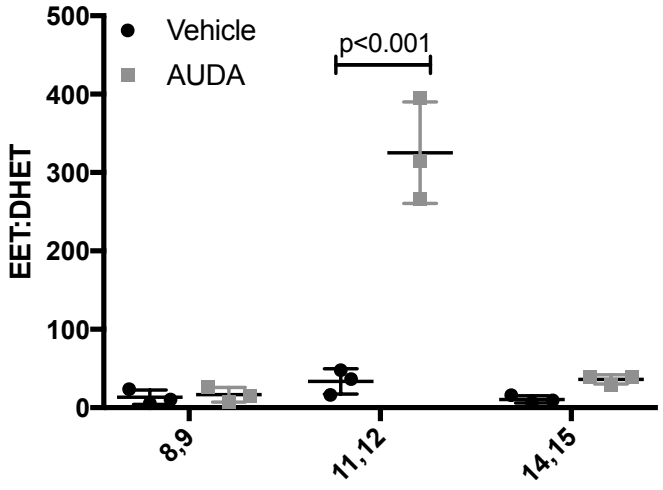

Figure 17. AUDA alters EET-to-DHET ratios. To verify inhibition of epoxide hydrolysis by AUDA, EET:DHET ratio was measured in AUDA-treated HRMEC. EET:DHET for each isomer was increased, but only the ratio of the 11,12 regioisomer was significantly increased. Each bar represents mean ± SD (n=3).

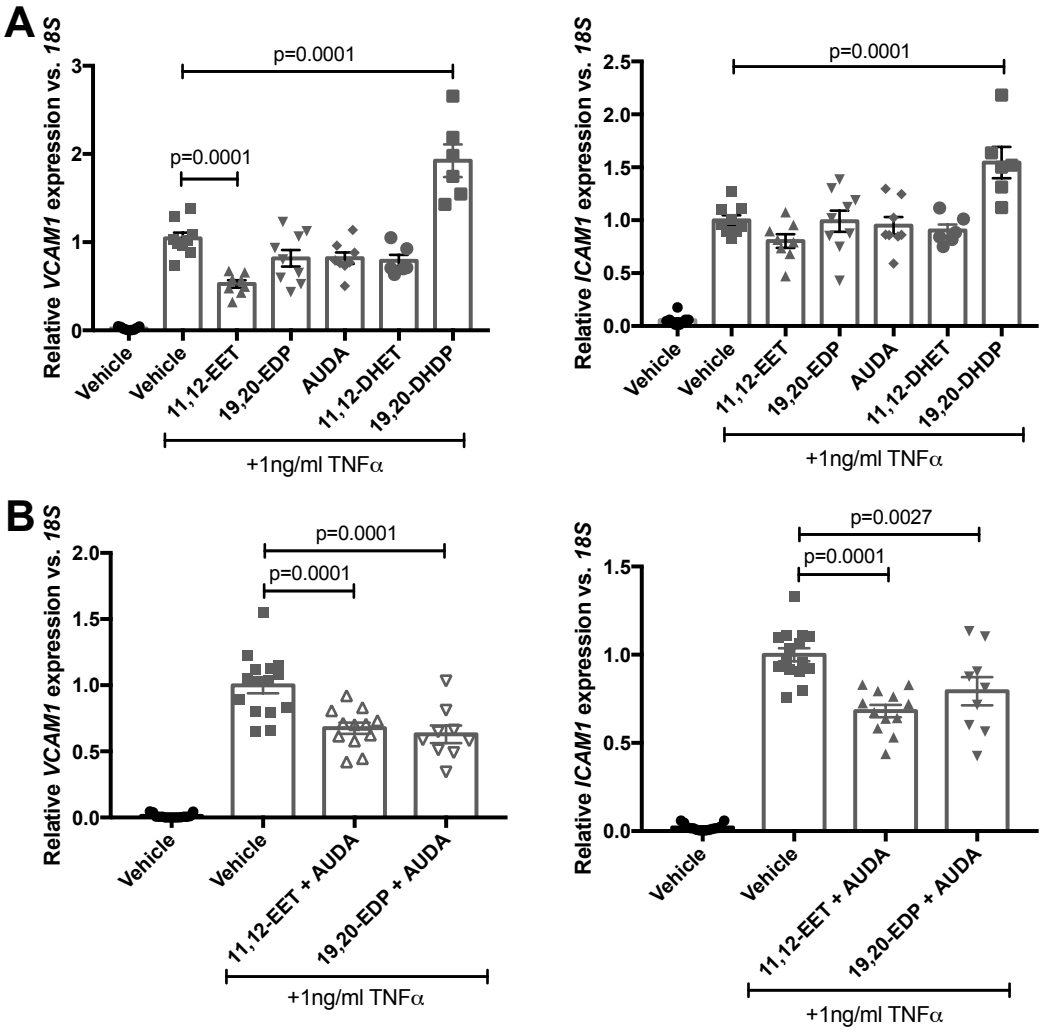

Figure 18. The effect of 11,12-EET, 19,20-EDP, AUDA, or the corresponding diols on TNFα-induced adhesion molecule expression. HRMEC were treated with TNFα in the presence or absence of (A) 11,12-EET (0.5 μM), 19,20-EDP (0.5 μM), AUDA (10 μM), 11,12-DHET (0.5 μM), or 19,20-DHDP (0.5 μM); or (B) combinations of 11,12-EET or 19,20-EDP with AUDA. Expression of *VCAM1* and *ICAM-1* was assessed by qRT-PCR analysis. Each bar represents the mean ± SEM (A: n=6; B: n=12).

11,12-EET or 19,20-EDP with sEH Inhibition Reduces TNFα-stimulated VCAM-1 and ICAM-1 Protein Levels

To further validate the effect of 11,12-EET or 19,20-EDP in combination with AUDA, VCAM-1 and ICAM-1 protein levels were assessed. HRMEC were treated with TNFα in the presence or absence of 11,12-EET or 19,20-EDP plus AUDA for 4 hours;

VCAM-1 and ICAM-1 levels were determined by immunoblot analysis. As shown in **Figure 19**, 11,12-EET plus AUDA inhibited both VCAM-1 and ICAM-1 levels by 27.5% (p=0.0007) and 44.5% (p=0.0004), respectively. 19,20-EDP plus AUDA performed similarly, inhibiting VCAM-1 by 29.2% (p=0.0011) and ICAM-1 by 30.3% (p=0.005).

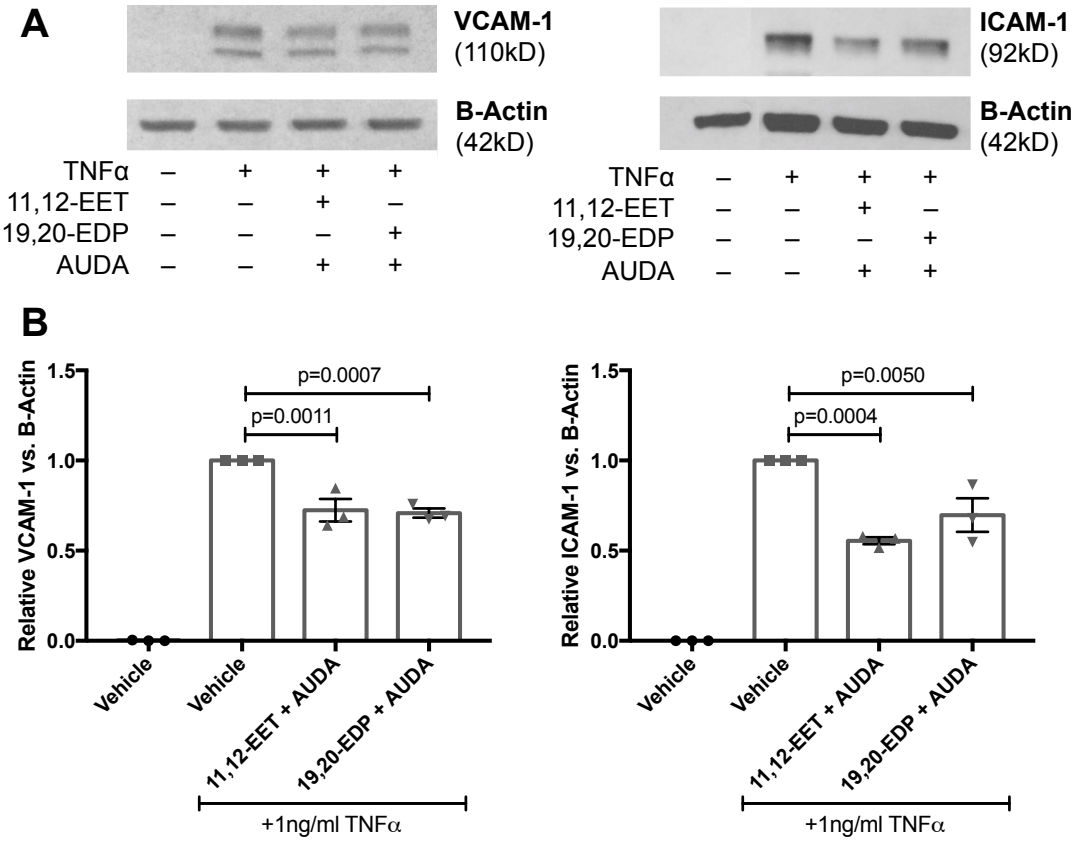

Figure 19. The effect of 11,12-EET or 19,20-EDP plus sEH inhibition on TNFα-induced VCAM-1 and ICAM-1 protein levels. (A) Representative blots from HRMEC treated with TNFα in the presence or absence of 11,12-EET (0.5 μM) or 19,20-EDP (0.5 μM) with AUDA (10 μM); and (B) quantification of 3 individual blots. Each bar represents the mean ± SEM (n=3).

11,12-EET or 19,20-EDP with sEH inhibition Reduces PBMC Adhesion to HRMEC Monolayers

We performed leukocyte adhesion assays to determine how EET- and EDP-dependent VCAM-1 and ICAM-1 expression and protein levels affect TNFα-induced leukocyte adhesion. HRMEC monolayers were cultured in a parallel plate flow chamber and treated with TNFα in the presence or absence of 11,12-EET or 19,20-EDP plus AUDA for 4 hours. Untreated peripheral blood mononuclear cells (PBMC) were flowed over the monolayers and adhesion was measured. As shown in **Figure 20**, TNFα induced PBMC adhesion by 4.3-fold; 11,12-EET or 19,20-EDP plus AUDA inhibited this induction by 47.6% (p=0.0268) and 49.9% (p=0.0436), respectively.

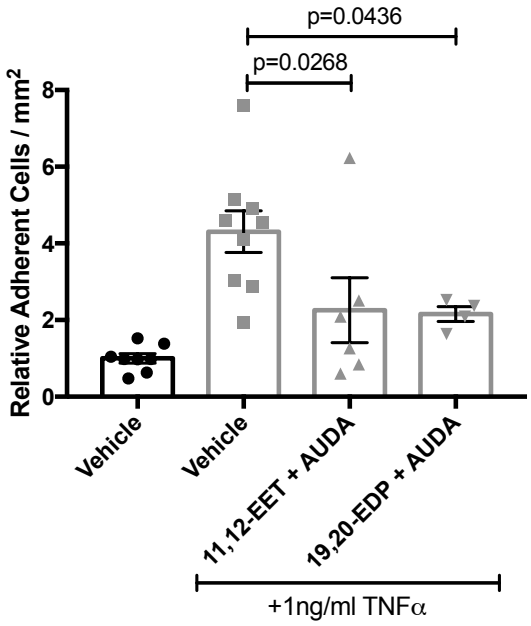

Figure 20. The effect of 11,12-EET or 19,20-EDP plus AUDA on TNFα-induced leukocyte adhesion to HRMEC monolayers. HRMEC monolayers were treated TNFα in the presence or absence of 11,12-EET (0.5 μM) or 19,20-EDP (0.5 μM) with AUDA (10 μM), and PBMC were then flowed over the treated monolayers in a parallel plate flow chamber. Each bar represents the mean ± SEM (vehicle: n=8; TNFα: n=9; 11,12-EET + AUDA: n=6; 19,20-EDP: n=4).

11,12-EET or 19,20-EDP with sEH Inhibition Reduces TNFα-induced NFκB Activity

In various macrovascular endothelial cell types, 11,12-EET exerts its anti-inflammatory effects by preventing IκBα degradation and subsequent NFκB translocation.[146,172,173] To assess whether 11,12-EET and 19,20-EDP are working through this mechanism, NFκB activity was measured using a promoter assay. HRMEC were transfected with a luciferase promoter construct and treated with TNFα in the presence or absence of 11,12-EET or 19,20-EDP plus AUDA. As shown in **Figure 21A**, 11,12-EET or 19,20-EDP plus AUDA inhibited TNFα-induced NFκB activation by 24.6% (p=0.0342) and 28% (p=0.0161), respectively. However, this inhibition was not via a direct effect on IκBα degradation (**Figure 21B**).

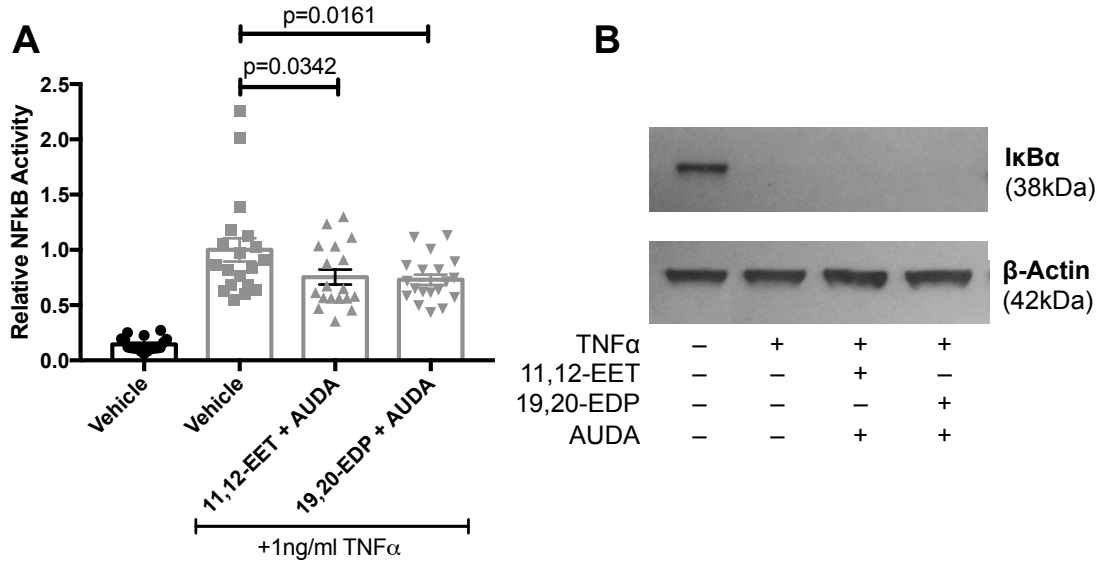

Figure 21. The effect of 11,12-EET or 19,20-EDP plus AUDA on TNFα-induced NFκB activation. (A) HRMEC were transfected with luciferase constructs and treated with TNFα in the presence or absence of 11,12-EET (0.5μM) or 19,20-EDP (0.5μM) with AUDA (10μM). NFκB activity was determined by measuring the ratio of firefly-to-Renilla luciferase. Each bar represents the mean ± SEM (n=20). (B) Representative blot of IκBα, with β-Actin as a loading control. Treatment with 11,12-EET or 19,20-EDP with AUDA inhibition did not prevent TNFα-induced IκBα degradation.

11,12-EET or 19,20-EDP with sEH Inhibition Mitigates TNFα-induced Retinal Leukostasis

For proof of concept *in vivo*, we assessed the effects of elevating EET or EDP levels on an acute mouse model of retinal inflammation. C57BL/6J mice received intravitreal injections of TNFα in the presence or absence of 11,12-EET or 19,20-EDP plus AUDA; adherence of leukocytes to retinal vessels was analyzed six hours post-injection. As shown in **Figure 22**, TNFα induced retinal vascular leukocyte adherence by 87.3% (p=0.0024), similarly to previous reports.[76] Co-treatment with either 11,12-EET or 19,20-EDP plus AUDA completely mitigated the TNFα-induced adherence of leukocytes in retinal vessels (p=0.0241 and p=0.0007, respectively).

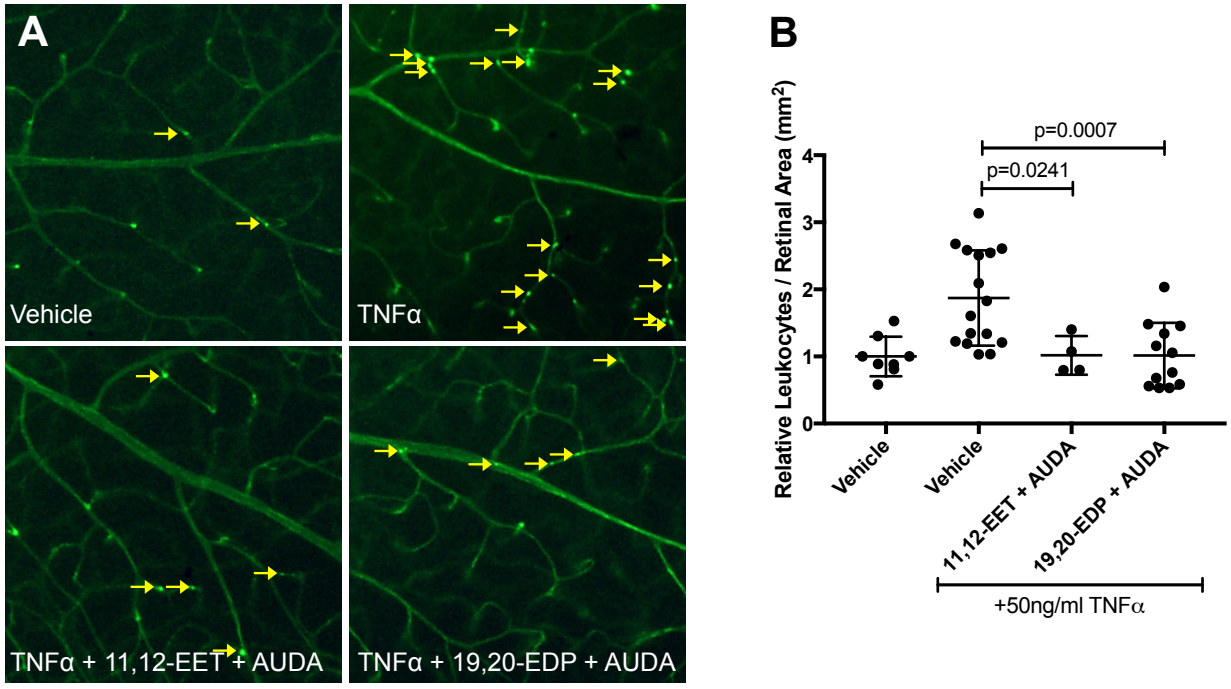

Figure 22. The effect of 11,12-EET or 19,20-EDP plus AUDA on TNFα-induced retinal leukostasis. Mice were injected intravitreally with 50 ng/ml TNFα in the presence or absence of 11,12-EET (0.5μM) or 19,20-EDP (0.5μM) with AUDA (10μM). (A) Representative images of

retinal flatmounts with concanavalin-A perfusion; yellow arrows indicate adhered leukocytes; (B) quantification of adherent leukocytes normalized to retinal area. Bars represent mean ± SD (vehicle: n=8; TNFα: n=16; 11,12-EET + AUDA: n=4; 19,20-EDP + AUDA: n=12).

Conclusions

Our data demonstrated for the first time that 11,12-EET and 19,20-EDP are similarly efficacious against TNFα-induced vascular inflammation. While EET is well established as an anti-inflammatory lipid that inhibits the induction of leukocyte adhesion molecules in various endothelial cell types,[103,146,172,278] these activities have never been demonstrated for EDP. Interestingly, the EET and EDP precursors, AA and DHA respectively, have opposing effects on leukocyte adhesion molecule expression in retinal endothelial cells. AA increases VCAM-1 and ICAM-1 levels,[237] while DHA decreases TNFα-induced VCAM-1 and ICAM-1 levels.[284,285] In the present study, we demonstrated that these opposing roles are no longer observed when using the epoxygenated products, 11,12-EET and 19,20-EDP. It is important to note that the rate of epoxide biosynthesis is limited by substrate availability.[286] Though DHA is abundant in the retina, this is almost exclusively due to enrichment in the retinal photoreceptor outer segment membranes. In the retinal vasculature, AA and DHA are found in equal amounts,[131] suggesting that both substrates, and therefore their products, would likely be found in similar levels at the site of epoxide generation in the vasculature. Thus, both AA- and DHA-derived epoxides may contribute similarly to retinal vascular homeostasis, particularly relating to inflammation.

In this study, we used only one of the four EET regioisomers (11,12-EET) and one of the five EDP regioisomers (19,20-EDP). 11,12-EET was used due to its high relative abundance in retinal endothelial cell cultures (**Figure 16**) and retinal tissue,[132]

as well as its proven anti-inflammatory capacity compared to other regioisomers.[146,171] These data suggest that changes in the levels of 11,12-EET may be highly biologically relevant in the retina. Similarly, 19,20-EDP is the most abundant DHA-derived epoxide product in the retina.[132,138,151] 19,20-EDP is the least efficiently metabolized sEH substrate of the DHA-derived epoxides, suggesting that therapeutic levels may be more easily achieved compared to the other regioisomers.[138]

While diol products are often inactive in the vasculature, in the retina, the 19,20-DHDP has been shown to promote developmental angiogenesis.[132] In the present study, we demonstrate a pro-inflammatory activity for this diol product in retinal endothelial cells. This finding further argues for the use of sEH inhibition as an efficacious therapeutic strategy because it would not only promote elevated levels of anti-inflammatory epoxygenated fatty acids, but also reduce the production of their pro-inflammatory diol products.

The sEH enzyme is highly expressed in the endothelium throughout a variety of tissue beds,[280,287-290] and we demonstrated its activity in HRMEC cultures (**Figure 17**). However, in the developing mouse retina, sEH immunoreactivity did not co-localize with the vascular lectin stain, isolectin GS-IB4 from *Griffonia simplicifolia*.[132] Soluble epoxide hydrolase is constitutively expressed and inducible by systemic factors. In diabetes and obesity, which is associated with a chronic systemic inflammation, sEH levels are elevated, and their levels are responsive to insulin therapy.[205,291] Furthermore, endothelial cell activation with homocysteine, a systemic factor associated with diabetic retinopathy,[190] induced sEH expression and protein levels as well as VCAM-1 expression, while sEH inhibition reduced homocysteine-induced VCAM-1 induction.[207]

Another diabetes-relevant stimulus, angiotensin II, induced sEH levels via c-Jun binding to SP-1 sites in the 5'-flanking region.[289,292] TNFα has been shown to activate c-Jun in endothelial cells,[293] yet its direct effect on sEH expression has not been assessed. Thus, TNFα-induced inflammation may alter EET/EDP levels in our HRMEC cultures via increased sEH expression and activity.

While AUDA potently inhibits sEH activity, as demonstrated in **Figure 17**, it is important to note that it can have off-target effects related to the end points examined in this study. For instance, Fang et al. (2005) demonstrated weak PPARα agonism with AUDA treatment.[294] However, in the present study AUDA does not recapitulate PPARα agonism, because PPARα activation is efficacious against TNFα-induced vascular inflammation,[295] but AUDA alone did not exhibit any effect on these endpoints (**Figure 18 and Appendix E**). Therefore, in the context of this study, we believe that AUDA is functioning by sEH inhibition, because it is only efficacious when paired with exogenous epoxides.

TNFα-induced retinal leukostasis was adapted for use in this study as a model of low-grade chronic inflammation related to DR, as reported previously.[76] We chose to administer a dose of TNFα (50pg) to the vitreous cavity that was based on preliminary dose response profiles within ranges that reflect low-grade retinal inflammation similar to that observed in vitreous from patients with DR.[89,296] Moreover, our reported induction of retinal leukostasis is comparable to that observed in rodent models of diabetes.[266,297,298] The TNFα concentration we chose produced a significant increase in adherent retinal leukocytes with sufficient magnitude to test the addition of exogenous

EET and EDP to achieve statistical significance in this acute model, while at the same time maintaining relevance to the low-grade state of inflammation observed in DR.

In our *in vitro* flow chamber experiments, we observed a partial inhibition of TNFα-induced leukocyte adherence compared to the complete mitigation of TNFα-induced leukostasis we observed in the acute mouse model of retinal inflammation. A number of reasons could explain the differences between these results. First, we narrowed our survey of inflammation-related molecular targets to VCAM-1 and ICAM-1 because they have been shown to mediate TNFα-induced leukostasis,[298-300] and have precedence as EET-dependent targets.[103,143,146,278] However, other targets are likely to contribute to leukocyte adherence in the *in vivo* setting, such as E-selectin or P-selectin, and their levels may also be EET- and/or EDP-dependent. Furthermore, though EET and EDP were locally administered, they may exert additional anti-inflammatory actions on the circulating leukocytes. Our *in vitro* experiments focused on the effects of EET and EDP on the retinal endothelial cells alone. Indeed, evidence from other studies suggests that these epoxides may also exert their effects on macrophages and monocytes.[170-172,179,301,302] Hence, EET- and EDP-dependent effects on circulating cells may represent an important component of the *in vivo* pathogenesis that is absent in our *in vitro* studies. Lastly, our *in vitro* experiments were performed in human-derived microvascular endothelial cells, and our *in vivo* endpoints were performed in mice. The published IC_{50} value for AUDA related to inhibition of mouse sEH (18nM) is lower than that reported for the human variant (69nM).[303] Therefore, AUDA is more potent for the mouse enzyme, and this may contribute to the improved efficacy observed in our mouse model.

This is the first study to directly compare the effects of EET and EDP on molecular and cellular events related to retinal vascular inflammation occurring in DR. While EDP has some bioactivities similar to those of EET, and in some cases demonstrating greater potencies such as in vasodilation,[152] opposite biological outcomes have also been observed. For example, EDP has been reported to be anti-angiogenic whereas EET is likely to be pro-angiogenic depending on the specific experimental context.[148,164,281,283] In the present study we showed a similar potency for EET and EDP to reduce *in vitro* leukocyte adhesion and leukostasis in the mouse. This suggests that the mechanisms by which they exert their anti-inflammatory effects are similar. The mechanistic details of EET and EDP bioactivities remain undetermined. A specific receptor for epoxygenated fatty acids is yet to be identified, although they do signal through a number of pathways, including PPARs and GPCRs.[142,143,304,305] The majority of evidence supporting EET anti-inflammatory activity points to signaling pathways that converge on the transcription factor NFκB. Node et al. originally showed that 11,12-EET exerted anti-inflammatory effects in bovine aortic endothelial cells by inhibiting IKK activity and IκBα degradation, thereby preventing NFκB translocation and initiation of pro-inflammatory mediator transcription.[146] While subsequent studies validated this finding, they were all performed in macrovascular endothelial cell types.[172,173] To our knowledge, this is the first study to show that NFκB activation is inhibited by 11,12-EET or 19,20-EDP in microvascular endothelial cells, but not via IκBα degradation.

Taken together, our data shows for the first time that 11,12-EET and 19,20-EDP, when combined with application of the sEH inhibitor AUDA, are similarly efficacious

against TNFα-induced leukocyte adherence *in vitro* and leukostasis *in vivo*. Both of these epoxides act in part by inhibiting the induction of VCAM-1 and ICAM-1. Based on the results of these studies, the addition of exogenous EET or EDP, along with their stabilization via sEH inhibitors, may represent a viable treatment strategy for DR. We believe that blocking retinal inflammation in the early stages of NPDR with EET and EDP therapy may prevent transition to PDR and its associated morbidities, including blindness.

CHAPTER V

EFFECT OF EPOXIDES ON RETINAL ANGIOGENESIS

From: Capozzi M.E., McCollum G.W., Penn J.S. (2014) The Role of Cytochrome P450 Epoxygenases in Retinal Angiogenesis. Invest Ophthalmol Vis Sci. 10;55(7):4253-60.

Overview

Angiogenesis is the sprouting of new blood vessels from pre-existing vessels and it occurs in both physiologic and pathologic settings. Persistent pathologic angiogenesis contributes to a number of diseases, including cancer and retinopathies. Abnormal retinal angiogenesis, also called neovascularization (NV), results from a vaso-proliferative response to retinal hypoxia and occurs in retinopathy of prematurity (ROP), proliferative diabetic retinopathy (PDR), and age-related macular degeneration (AMD).[306-308] These eye diseases account for the majority of vision loss in developed countries, creating an impetus to investigate the cellular and molecular mechanisms underlying retinal NV and develop effective therapies.

While epoxide therapy for early diabetic retinopathy may be beneficial, as suggested from **Chapter IV**, the pro-angiogenic features of EETs may be contraindicated for late stages of the disease, such as PDR when neovascularization occurs. In fact, inhibition of EET production may be therapeutic for diseases characterized by retinal angiogenesis. Thus, the goal of the present study was to

develop a more complete understanding of EET in diabetic retinopathy by assessing its effect in late stages of the disease, which are characterized by pathologic NV.

Vascular endothelial growth factor (VEGF), a 40kDa dimeric glycoprotein, is the primary mediator of angiogenesis in ocular diseases.[309] Hypoxia is a potent stimulator of retinal VEGF, and ischemia-induced hypoxia is the major source of VEGF in ROP, and perhaps DR. The retinal Müller cells and astrocytes have been shown to produce the highest levels of VEGF of all retinal cell types,[97] and therefore the present study will focus on the production of VEGF by these cells *in vitro*. Endothelial cells are the primary responders to VEGF, and thus will be used for assessment of angiogenic behaviors.

COX, LOX and their products (prostaglandins, thromboxanes, and leukotrienes) have been well characterized in OIR.[252,275,310,311] However, the contribution of AA-derived CYP products to retinal angiogenesis was largely unknown. Therefore, the purpose of this study was to investigate the role of CYP2C epoxygenases and their EET products in retinal angiogenesis. Experimental evidence suggested that CYP2C enzymes are expressed in endothelium, are hypoxia-inducible, and their regio-selectivities favor increased 11,12-EET over the other regioisomers. Therefore, we performed *in vitro* experiments to establish the effects of 11,12-EET to stimulate human retinal microvascular endothelial cell (HRMEC) proliferation and tubulogenesis. Furthermore, we assessed the effect of a general CYP inhibitor on induction of VEGF in human retinal glial cells and VEGF-induced angiogenic behaviors in HRMEC. We measured the expression of the human CYP2C homologs in primary human retinal cells exposed to hypoxia and determined the expression profile of CYP2C11 and CYP2C23

in OIR rats. Lastly, we tested the efficacy of the CYP inhibitor against pre-retinal NV *in vivo*, and whether its efficacy correlated with retinal VEGF levels in OIR rats.

Results

CYP2C23, but Not CYP2C11, is Increased in OIR Retinas

In rat OIR, retinal VEGF peaks around two days post-oxygen exposure (14(2)).[84] Therefore we chose to investigate retinal CYP expression at this time because VEGF has previously been shown to crosstalk with the CYP pathway.[149,160] Retinas collected on 14(2) from OIR showed a 2.4-fold ($p<0.0001$) increase in *CYP2C23* mRNA relative to room air controls. Conversely, OIR had no effect on *CYP2C11* expression (**Figure 23**).

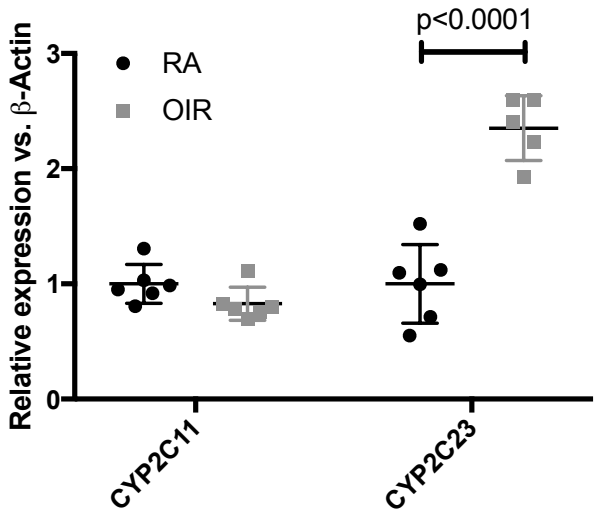

Figure 23. *CYP2C11* and *CYP2C23* mRNA expression in rat OIR. Two days after removal from oxygen exposure (14(2)), *CYP2C23* expression is significantly increased, while *CYP2C11* is unaffected in OIR compared to RA control (P16). Data are presented as mean ± SEM (n=6).

Hypoxia Induces CYP2C Expression in Human Retinal Astrocytes, but Not Human Müller Cells or HRMEC

Cytochrome P450s are expressed in retinal endothelial cells, Müller cells and brain astrocytes.[312-315] Therefore, we measured CYP expression in primary HRMEC, human Müller cells, and human retinal astrocytes (HRA). Exposure of HRA to hypoxia for 24 hours significantly induced human *CYP2C8* (2.5-fold; p=0.0004) and *CYP2C9* (3.1-fold; p=0.0154; **Figure 24C**). However, the same hypoxic conditions did not induce *CYP2C8* or *CYP2C9* in either human Müller cells or HRMEC (**Figure 24A and 24B**, respectively).

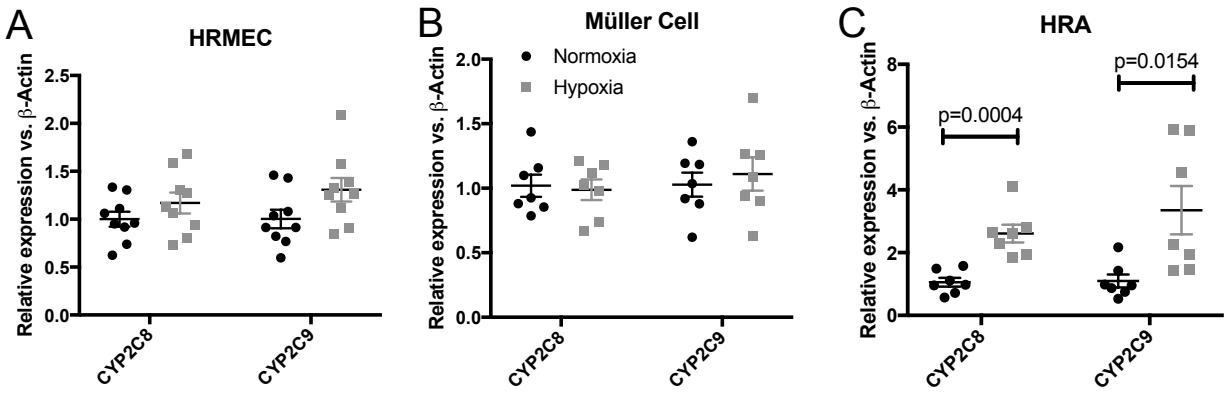

Figure 24. The effect of 24-hour hypoxic exposure of CYP-expressing retinal cell types on CYP2C8 and CYP2C9 expression. Hypoxia has not effect on CYP2C8 or CYP2C9 expression by (A) Müller cells or (B) HRMEC. However, hypoxia significantly elevates CYP2C8 and CYP2C9 expression by HRA. Data are presented as mean ± SEM (n=7-9).

SKF-525A Reduces VEGF Production by HRA, but Not Müller Cells

In response to hypoxia, Müller cells and retinal astrocytes have the greatest capacity to produce VEGF of all retinal cells.[97] Therefore, VEGF production in hypoxic Müller cells and HRA was measured after treatment with SKF-525A for 24 hours

(**Figure 25**). Müller cells produced 3.6-fold more VEGF than astrocytes when exposed to hypoxia. Hypoxia-induced VEGF production was 7.1-fold in Müller cells and 11.5-fold in HRA. SKF-525A had no effect on Müller cell production of VEGF, however, it reduced HRA VEGF production by 26.8% (p=0.0097).

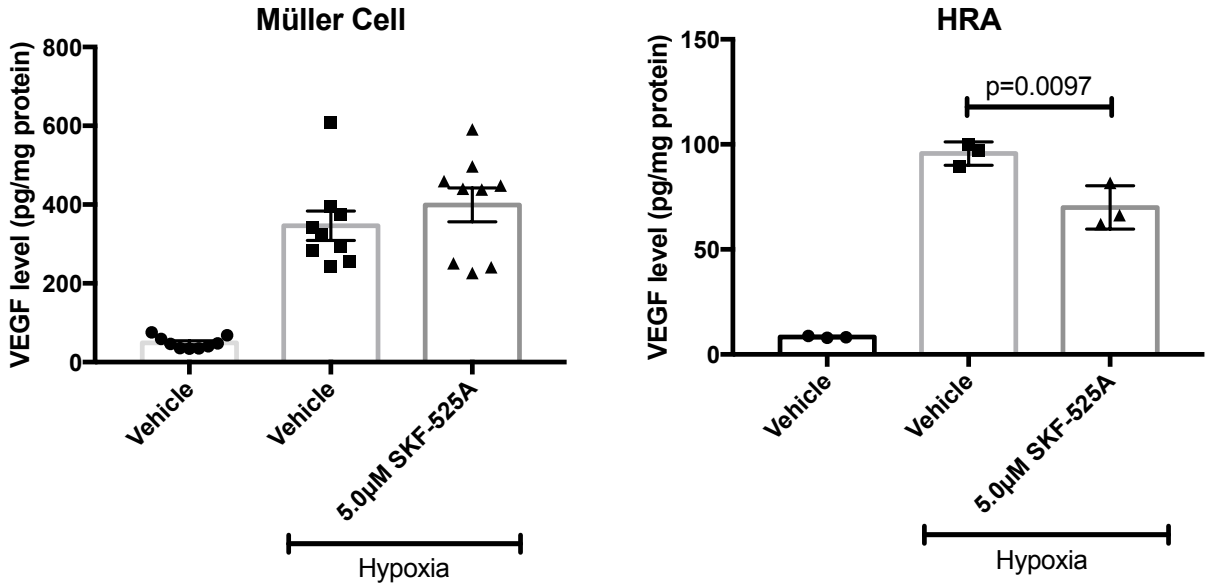

Figure 25. The effect of SKF-525A on hypoxia-induced VEGF production in retinal glial cells. Human Müller cells (A) and HRA (B) were exposed to either normoxia (20.9% O_2) or hypoxia (0.1% O_2) in the presence or absence of SKF-525A (5.0μM) for 24 hours. The VEGF levels were measured in the culture medium and normalized to total protein. SKF-525A significantly decreased VEGF levels in hypoxic cultures of HRA, but not in hypoxic cultures of Müller cells. Data are presented as mean ± SEM (n=3-9).

11,12-EET and SKF-525A Modulate HRMEC Proliferation

As shown in **Figure 26**, treatment of HRMEC with increasing concentrations of 11,12-EET stimulated proliferation in a dose-dependent manner. Proliferation was significantly increased by 1.5-fold (p=0.0051) and 1.6-fold (p=0.0004) at the 0.1μM and 0.5μM doses of 11,12-EET, respectively. General CYP inhibition using SKF-525A significantly reduced VEGF-induced proliferation by 46% (p<0.0001) at the highest concentration (5.0μM).

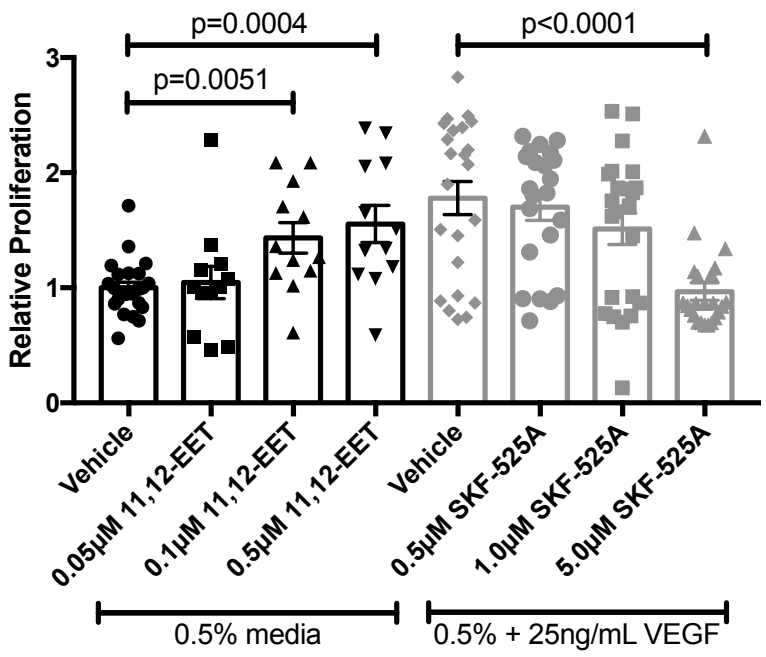

Figure 26. The effect of 11,12-EET or SKF-525A on VEGF-induced proliferation of HRMEC. Treatment of HRMEC with 11,12-EET led to a dose-dependent increase in proliferation. Treatment with SKF-525A inhibited VEGF-induced proliferation at the highest concentration (5.0μM). Data are presented as mean ± SEM (n=9).

Administration of Exogenous 11,12-EET, but Not SKF-525A, Affects HRMEC Tubulogenesis

HRMEC were grown on Matrigel® in the presence of vehicle, 11,12-EET, VEGF vehicle, or VEGF plus SKF-525A. Tube formation was significantly induced by all doses of 11,12-EET (p=0.0135 at 0.05μM; p=0.0009 at 0.1μM; and p=0.0078 at 0.5μM). CYP inhibition by SKF-525A did not significantly inhibit VEGF-induced tube formation (**Figure 27**).

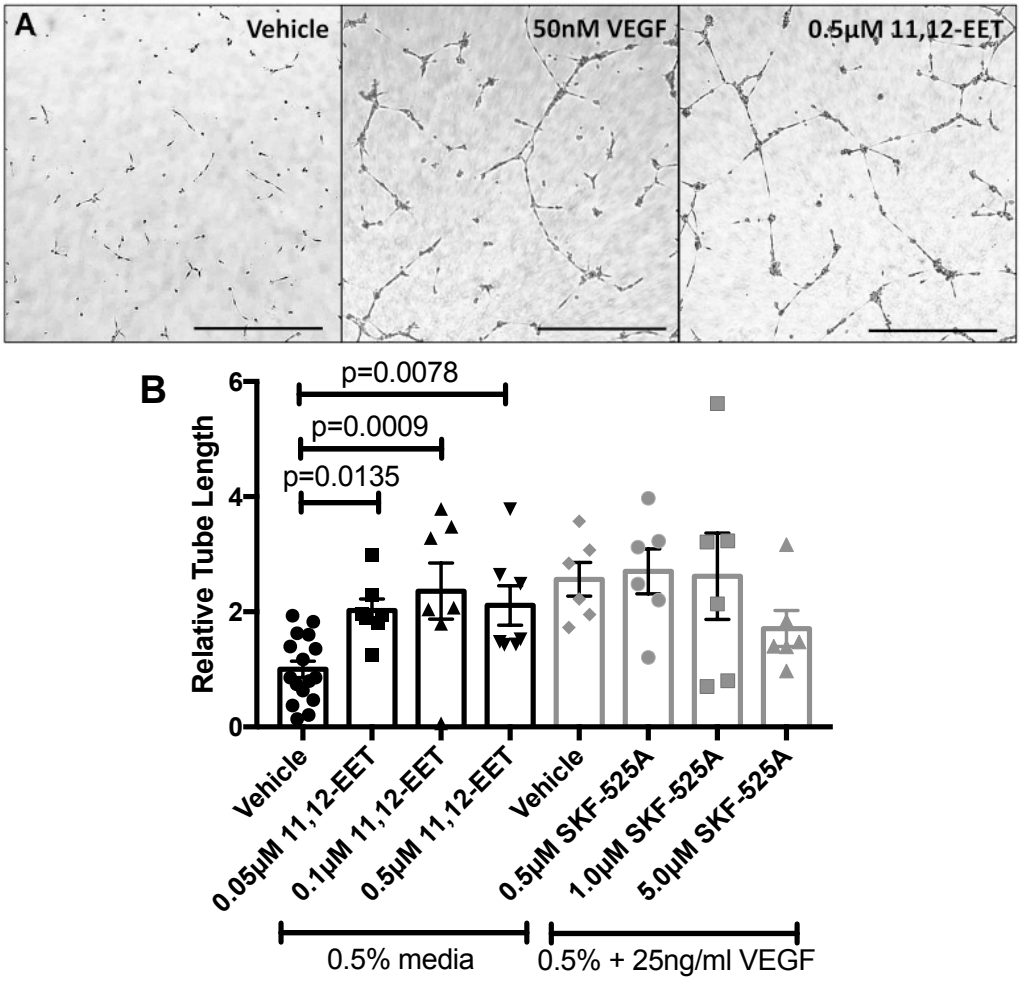

Figure 27. The effect of 11,12-EET or SKF-525A on VEGF-induced tube formation in HRMEC. (A) Representative images from vehicle, 50ng/ml VEGF or 11,12-EET (0.5µM). The bar on each image represents 500µm. (B) HRMEC treatment with 11,12-EET significantly induced tube formation at all doses used. SKF-525A did not significantly inhibit VEGF-induced tube formation. Data are presented as mean ± SEM (n=6-12).

SKF-525A Reduces Retinal NV in OIR

Retinal NV was assessed in the rat model of OIR following intravitreal injection of vehicle or increasing concentrations of SKF-525A. 5.0µM SKF-525A significantly inhibited NV formation by 48% (p=0.0239). Representative retinal quadrants and SKF-525A efficacy are shown in **Figure 28A and 28B**, respectively.

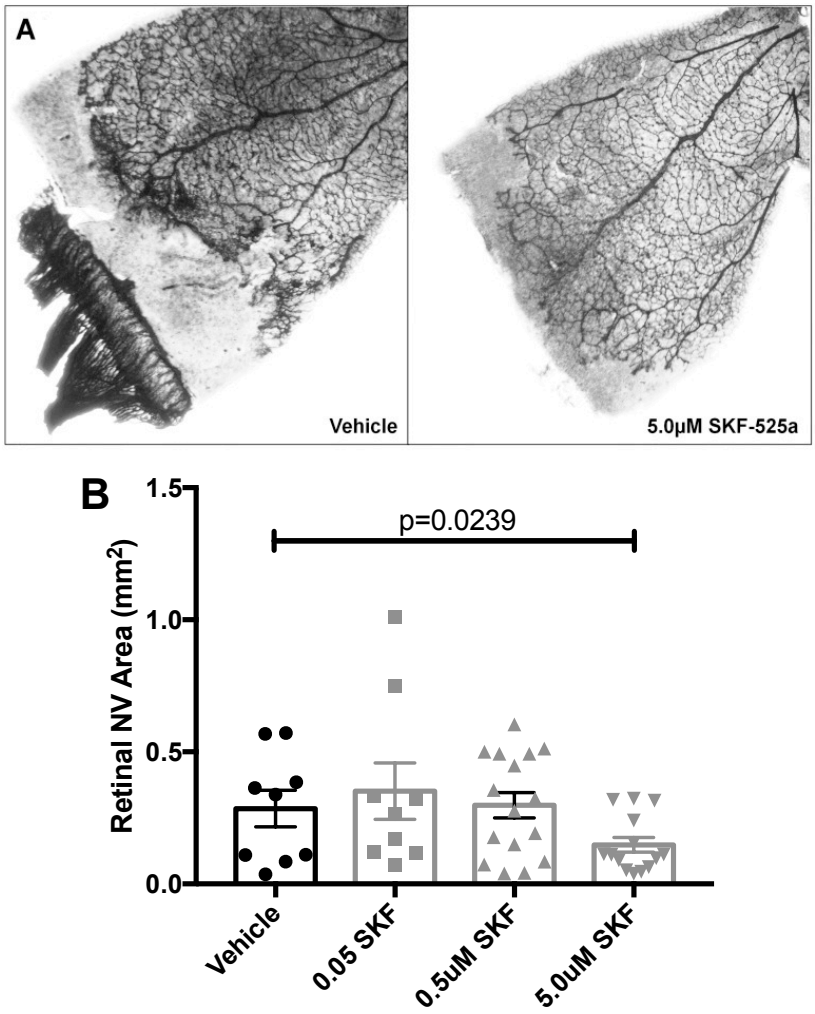

Figure 28. The effect of intravitreal injection of SKF-525A on OIR-induced pre-retinal NV. (A) Representative images from vehicle-treated and 5.0μM SKF-525A-treated OIR retinas. (B) Dose response of SKF-525A in OIR animals. Data are presented as mean ± SEM (n=8-12).

SKF-525A Attenuates Retinal VEGF Production in OIR

Animals were injected on 14(1) with vehicle or SKF-525A, and collected on 14(2), when retinal VEGF is known to peak in this model.[84] Soluble VEGF protein was up-regulated 5.6-fold in OIR retinas compared to room air controls. SKF-525A (5.0μM) significantly reduced VEGF induction in the OIR model by 34% (p=0.0229), as shown in **Figure 29**.

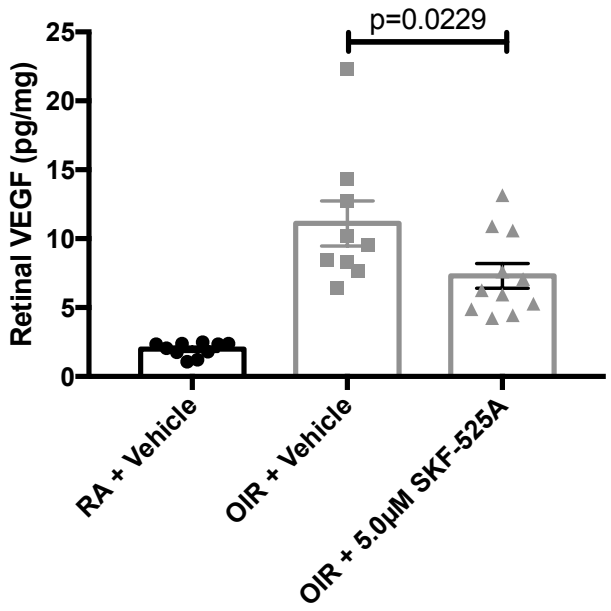

Figure 29. The effect of intravitreal injection of SKF-525A on VEGF production in rat OIR. Injection of 5.0μM SKF-525A significantly reduced retinal VEGF protein level at 14(2) compared to vehicle injection in rat OIR. Data are presented as mean ± SEM (n=18).

Conclusions

Hypoxia is a known inducer of CYP2C expression in bovine RMEC (BRMEC), and subsequently causes increased EET levels.[159,312] Additionally, EETs are downstream effectors in the VEGF signaling pathway, promoting endothelial cell proliferation, tube formation, and migration.[160,316] Therefore, EET production is likely to facilitate an enhanced retinal neovascular response. However, to our knowledge, reduction of EETs by CYP epoxygenase inhibition has never been tested as a therapeutic modality against retinal NV.

In BRMEC, 11,12-EET is the only EET product significantly increased when cells are stimulated by hypoxia.[312] In the present study, we showed that *CYP2C23* is the primary OIR-induced CYP epoxygenase in the rat retina (**Figure 23**). Because CYP2C23 preferentially produces the 11,12-EET regioisomer,[317] we chose to use

11,12-EET in our *in vitro* experiments. In this study, we show for the first time that 11,12-EET induces pro-angiogenic cell behaviors in HRMEC (**Figure 26** and **27**).

There are a number of possible cell types that produce cytochrome P450-derived EET products in the retina. Brain-derived astrocytes were the first source identified as hypoxia-stimulated producers of pro-angiogenic EETs.[314,315] Additionally, BRMEC demonstrated hypoxia-induction of *CYP2C* mRNA expression over 24hrs.[312] The retina also contains a large population of Müller glial cells that express CYP epoxygenases and the EET-metabolizing enzyme, soluble epoxide hydrolase, in a high abundance, yet their response to hypoxia has never been tested.[132,313] In the present study, using primary human retinal cell types, we demonstrate that astrocytes are likely the predominant cell type contributing to hypoxia-induced *CYP2C* expression in the retina (**Figures 23** and **24)**.

Currently, no EET-specific receptor has been identified. However, data suggest that EETs likely bind and activate G-coupled protein receptors and/or peroxisome proliferator-activated receptors.[143,157,318,319] The pro-angiogenic effects of EETs are mediated at least in part by activation of PI3K/Akt, ERK, and p38 MAPK.[148,160,320] Yang and colleagues demonstrated that CYP activation in mouse primary lung endothelial cells led to phosphorylation of ERK1/2 and Akt and knockdown of the primary mouse CYP epoxygenase, Cyp2c44, inhibited VEGF-induced ERK and Akt phosphorylation and subsequent tube formation.[160] Another study by Potente and colleagues showed that EET activates PI3K/Akt, inhibiting FOXO1 and FOXO3b and thereby downregulating p27Kip1, a cyclin-dependent kinase inhibitor. Subsequently Cyclin D1 increases, inducing proliferation by promoting cell cycle progression.[321] More recently,

GPR40, a medium/long chain fatty acid g-coupled protein receptor, was demonstrated as the mediator of EET-induced mitogenesis in kidney cell cultures.[142] GPR40 deletion in the retina attenuated retinal angiogenesis in the *Vldlr*$^{-/-}$ mice,[255] suggesting that perhaps EET pro-angiogenic activities occur through direct binding of this receptor.

The general CYP epoxygenase inhibitor, SKF-525A, inhibits neuronal nitric oxide synthase (IC_{50} = 90mM) and blocks the potassium channel Kir6.1 (IC_{50} = 4.4mM).[316,322] Previous studies in models of hypertension have shown that at 50μM, SKF-525A inhibits CYP metabolism of AA by 90%.[323] However at this concentration, we observed loss of cell viability in our experiments. We did not expect off-target effects of the drug because our experiments were performed using substantially lower doses. In our *in vitro* experiments, SKF-525A significantly inhibited VEGF-induced proliferation, however we did not observe any effect on VEGF-induced tube formation. Yet, in studies using HUVEC, the EET antagonist 14,15-epoxyeicosa-5(Z)-enoic acid (14,15-EEZE) inhibited VEGF-induced tube formation.[149] Additionally, Webler and colleagues demonstrated that VEGF stimulated CYP2C promoter activity and induced *CYP2C8* expression.[149] In the present study, we did not observe a VEGF-induced increase in *CYP2C8* expression (data not shown). Therefore, VEGF induction of tubulogenesis likely occurs by CYP-independent mechanisms in HRMEC.

To our knowledge, this is the first demonstration that CYP inhibition can reduce neovascularization in an *in vivo* model of retinopathy. It has recently been shown that retinal Cyp2c expression is increased in mice exposed to hyperoxia.[324] In addition, human *CYP2C8* overexpression in OIR-exposed mice fed ω-3-enriched diet promoted retinal angiogenesis.[324] Similarly, we show an up-regulation of *CYP2C23* expression in

rats during the post-oxygen exposure period in OIR rats. Moreover, we show that inhibition of CYP activity, and presumably the consequent decrease in EET levels, reduces retinal NV. In rat OIR, retinal VEGF normally peaks at 14(2).[84] In this study, OIR rats receiving intravitreal injections of SKF-525A showed reduced retinal VEGF levels at 14(2) (**Figure 29**), perhaps contributing to the inhibition of retinal NV observed at 14(6). Induction or exogenous addition of EETs has been shown to induce VEGF.[325] Inhibition of CYP2C9 by sulfaphenazole suppressed the hypoxia-induced transcriptional activity of the VEGF hypoxia response element in human umbilical arterial endothelial cells.[326] In human dermal microvascular endothelial cells, 14,15-EET induced VEGF via a Src-STAT-3-dependent mechanism.[325] However, in the retina, endothelial cells are not the major source of hypoxia-induced VEGF; Müller cells and astrocytes are the primary producers of VEGF of the retinal cell types.[97] We found that inhibition of CYP epoxygenases in hypoxia-induced primary human Müller cells had no effect on VEGF production, however it significantly reduced production of VEGF by astrocytes (**Figure 25**). This suggests that astrocytes are the primary cell type involved in SKF-525A inhibition of retinal VEGF, as shown in **Figure 29**.

A previous study from Scicli's group demonstrated the pro-angiogenic activity of the 20-HETE product derived from the CYP4A family.[327] In this study, inhibitors of CYP4A demonstrated potent anti-angiogenic capacity in VEGF-induced HUVEC proliferation and VEGF-induced corneal vasculature growth.[327] However, we believe that CYP epoxygenase inhibitors may provide better efficacy in retinal angiogenesis because they can inhibit both hypoxia-induced VEGF production by astrocytes and VEGF-induced angiogenic behaviors in retinal microvascular endothelial cells.

One limitation to the present study is that the focus was on AA-derived epoxides, and not DHA-derived epoxides. There is evidence that EDPs are angiostatic in cancer,[164] and thus the presumed reduction of their levels via the use of SKF-525A may be counterproductive for pathological angiogenesis in the OIR model. However, the effects of EDP are controversial in ocular angiogenesis, where it has been most commonly studied. Lois Smith's group has shown pro-angiogenic activity of 19,20-EDP in HRMEC, choroidal explants, and aortic ring assays,[166,328,329] while Kip Connor's group demonstrated an angiostatic effect of 19,20-EDP injections in the laser-induced choroidal neovascularization model.[165] Furthermore, Ingrid Fleming's group found that the diol product of 19,20-EDP, 19,20-DHDP, is involved in retinal angiogenesis during normal development, and not its epoxide substrate.[132] Further work must be performed to understand these discrepancies.

In this study, we have identified a novel contribution of CYP-derived epoxyeicosatrienoic acids to retinal angiogenesis. The CYP inhibitor SKF-525A reduced VEGF production by retinal astrocytes, VEGF-induced pro-angiogenic behavior in HRMEC, and NV area in the rat model of oxygen-induced retinopathy. Our findings suggest that EET-elevating therapies would likely promote the neovascularization in the late stages of DR. In fact, CYP-directed therapeutics may provide a promising target for inhibition of retinal NV, because it can partially inhibit both VEGF induction and downstream signaling of VEGF.

CHAPTER VI

CONCLUSIONS AND FUTURE DIRECTIONS

The work presented in this dissertation relates to the roles of CYP-derived epoxides in retinal vascular pathology secondary to diabetes. In **Chapter I**, I introduced the reader to pathology in diabetic retinopathy and the potential for elevating CYP-derived epoxides as a potential therapeutic strategy for DR. **Chapter II** described the methodology used to complete the aims of the project. In **Chapter III**, I established Müller cell culture models utilizing diabetes-relevant stimuli that recapitulate early aspects of disease progression. The work in **Chapter IV** demonstrated a comparable anti-inflammatory effect of 11,12-EET and 19,20-EDP in TNFα-induced retinal vascular inflammation. Lastly, in **Chapter V**, I demonstrated that 11,12-EET induced angiogenesis in retinal microvascular endothelial cells, and thus inhibition of CYP activity reduced neovascularization in oxygen-induced retinopathy.

Arguably the most significant finding from the study in **Chapter III** was that PA provides a more DR-relevant stimulus than D-glucose. Despite thorough investigation of high glucose as a diabetes-relevant stimulus, our studies in both **Chapter III** and **Appendix A** demonstrated that high glucose, which remains the gold standard for *in vitro* studies of DR, does not recapitulate diabetes-relevant endpoints, and instead fatty acid enriched culture conditions may be a better model to study the initiation of inflammation and angiogenesis by Müller cells. Notably, when cells were pretreated with D-glucose prior to stimulation with PA, expression of several targets of interest was

further amplified, suggesting that glucose predisposed the cells to greater sensitivity and/or responsivity. Müller cells were the focus of this work because fatty acid induction of pro-inflammatory and pro-angiogenic mediators appeared to be Müller cell-specific (**Appendix A**). Taken together, these data suggest that Müller cells may be more sensitive to systemic factors associated with diabetes. Being that Müller cell activation occurs early in animal models of diabetes,[96] it is possible that their early activation may be an initial step in the development of chronic inflammation in DR. Future studies should be directed at how fatty acids specifically activate Müller cell production of pro-inflammatory and pro-angiogenic mediators.

Furthermore, while IL-1β and TNFα were potent stimulators of Müller cell inflammation, the analysis of PA-treated Müller cells showed the greatest overlap with targets identified by whole transcriptome analysis of STZ-treated animals. Transcripts in several pathways, including angiogenesis (Vegfa, Vegfb and Angptl4), WNT signaling (Sfrp1, Cldn1, Bmp4, Wisp1, and Wnt2b), and inflammation (Ltbp1, Islr, and Bmp4), were elevated in both our PA-treated Müller cell cultures as well as retinas of STZ-treated animals.[330] Additionally, the levels of these transcripts were sensitive to treatment with a p38 MAPK inhibitor, PHA666859, in STZ animals.[330] MAPK signaling was identified as a significantly modulated pathway by both KEGG analysis (**Figure 8**) and Biocarta analysis (**Figure 9**) in our PA-treated Müller cell samples. Further evidence from retinal endothelium showed that ERK signaling contributes to retinal capillary dropout.[331] Additionally, JNK phosphorylation is associated with neuronal apoptosis in retinas collected from STZ-induced diabetic rats and patients with DR.[332,333] Thus, modulation of MAPK signaling may be particularly efficacious for DR. Thus, one

impact of our PA-Müller cell model is that it provides a novel platform for high-throughput analysis of therapeutic agents, before going to more expensive pre-clinical models.

Co-treatment of palmitic acid and D-glucose, without any D-glucose pretreatment, did not yield an amplified inflammatory response. Additionally, pre-treatment with D-glucose followed by treatment with D-glucose plus LA did not evoke the amplification observed following PA treatment (**Appendix H**). These data led us to hypothesize that glucose pre-treatment up-regulated components of PA-specific signaling pathways. One potential mechanism by which D-glucose could amplify PA-induced inflammatory transcription is via induction of toll like receptor 4 (TLR4). In retinal microvascular endothelial cells, glucose elevated expression levels of TLR4.[334] Additionally, PA, but not any other unsaturated fatty acid, is a known ligand for TLR4, and its activation of the receptor leads to NFκB-dependent transcription and subsequent induction of inflammation.[335,336] Our preliminary work did not show any effect of glucose on the expression of TLR4, however, this only demonstrates that levels remained unchanged and further work is necessary to determine whether: a) TLR4 receptors alter their localization for greater availability at the cell surface in response to glucose treatment or b) downstream signaling intermediates in the TLR4 pathway become increasingly elevated in response to combination treatments with glucose and PA. Another potential target for D-glucose amplification of PA responses is via increased HIF-1α stabilization and consequent transcription of angiogenic targets. As described in the study by Lois Smith's group, alteration of glucose and fatty acid metabolism can cause hypoxia-independent HIF-1α stabilization,[255] which could explain the increased

transcription of a variety of angiogenic factors in our whole transcriptome analysis. Identifying the mechanism by which D-glucose amplifies cells' response to PA should remain a priority, as this may lead to the identification of several potential drug targets for treatment of early DR.

Hyperlipidemia in the absence of diabetes does not yield DR-like pathology, so further understanding of metabolic and systemic interactions in the retina need to be pursued. Modeling a chronic, multifaceted disease like DR *in vitro* remains a challenge, but it is necessary to continue to develop better *in vitro* models for many reasons; a) PDR cannot be recapitulated in any known animal models. In rodent models, the disease pathology is mild and never progresses to late stages, so these models lack the potential to yield information about an important aspect of DR – the transition from NPDR to PDR; b) Use of human cells brings additional clinical relevance to *in vivo* findings. For example, IL-8 is one of the most elevated proteins found in the vitreous of diabetic patients, yet mice do not express IL-8. While rodents do express functional analogs, they might be regulated differently than IL-8. Therefore, human cells, which produce IL-8 may be important for understanding the mechanism of its induction as well its functional effects in DR pathogenesis; c) Cell culture models that recapitulate multiple disease processes allow for better mechanistic understanding of the disease. Use of human culture systems allows for assessment of efficacy for drugs targeting specific disease processes, as well as mechanistic steps in the pathologic cascade, which would allow for identification of novel therapeutic targets; and d) Cell culture models allow for high-throughput analysis in controlled treatment conditions. DR takes years to develop in humans, and months to develop in rodents. For these reasons, we

believe our culture model using human Müller cells and appropriate disease-relevant stimuli represents a useful tool for the DR research community.

While further work must be performed, particularly in the *in vivo* setting using disease-relevant models, the work presented in **Chapter III** constitutes an important step in understanding the initial causes of diabetic retinopathy. Our results, which demonstrate that glucose elevation has no effect on important retinal cell types, suggest that we should reconsider our interpretations of the conclusions drawn from seminal clinical trials. Tight control of hyperglycemia was found to slow the progression of DR in the DCCT trials,[13] and this has provided the basis for the mechanistic study of hyperglycemia-induced pathology. While it is likely that elevated circulating glucose can affect cellular signaling, studies in culture suggest that glucose is not a potent stimulus for a variety of endpoints observed in DR. Our lab and others have observed no effect of elevated glucose, outside of the effect caused by increased osmolarity of the growth medium, on cellular responses related to inflammation, basement membrane thickening, and angiogenesis in culture.[237,256] Thus, it is worth considering the entire metabolic implication of altering HbA1c and how that might be translated into cell culture systems. For example, tight glucose control is currently maintained by altering systemic insulin levels. Elevating insulin systemically may have a direct impact on retinal disease. The full effect of insulin has not been thoroughly studied, however Tom Gardner's group has demonstrated altered insulin receptor phosphorylation, and thus activation, in the retinas of both type 1 and type 2 models of diabetic complications.[337,338] Furthermore, both increasing insulin levels in the eye via subconjunctival injections or lowering systemic glucose levels in an insulin-independent manner via SGLT2 inhibition had

equivalent effects on preventing photoreceptor cell death in an STZ rodent model.[339] This demonstrates that other diabetes-relevant metabolic factors besides glucose are abnormal in the diabetic state and likely contribute to diabetes-induced retinal dysfunction. Elevated circulating lipid is just one of many insults associated with altered insulin signaling. The majority of metabolic alterations have yet to be assessed as stimulators of DR-related pathology. Thus, determining the effect of non-glucose, diabetes-relevant stimuli should remain a high priority for understanding the onset of the disease. Identifying the initiating factors of DR would likely yield more efficacious therapeutic strategies, because they could be administered before severe structural damage occurs.

Based on the results of our pathway analysis in **Chapter III**, I would expect epoxide-elevating therapies to be effective at inhibiting cytokine-induced inflammation. However, it remains unclear whether these epoxides could modulate PA- or DG/PA-stimulated behaviors. PA-induced cytokine expression in hepatocytes correlated with sEH up-regulation and was down-regulated by CYP2J2 overexpression or 14,15-EET treatment,[195,196,206] suggesting that PA-induced inflammation in Müller cells should also be susceptible to CYP-derived epoxide therapies. However, EETs have been shown to activate the MAPK pathway to exert pro-angiogenic activities,[340] while p38 MAPK inhibition in diabetic animals decreased retinal COX-2 and vascular leukostasis.[341] PA enriched MAPK signaling (**Figures 8** and **9**), suggesting that perhaps PA induction of the MAPK signaling pathway may be causally linked to expression of angiogenic factors, and EETs may exacerbate this effect. However, NFκB-dependent pathways were elevated as well, and this likely drives the inflammatory mediator expression

caused by PA. Thus, I would expect epoxides to be efficacious for inhibiting the induction of NFκB-regulated transcripts. As for cytokine auto-amplification, I would expect epoxides to reduce inflammatory mediator expression, because virtually all the enriched pathways (**Figures 14** and **15**) are regulated by CYP-derived epoxides. In preliminary studies (**Figure 30)**, I have demonstrated that 11,12-EET or 19,20-EDP may be viable inhibitors of IL-1β-induced *IL1β*, *IL6*, or *IL8* expression by human Müller cells. However, 11,12-EET and 19,20-EDP treatment significantly elevated *TNFα*. Further functional characterization of this response is required to understand the implications of these changes. For instance, Müller cells could be treated with IL-1β in the presence or absence of epoxide treatments, and the conditioned medium from these cells could be used to stimulate HRMEC outputs, such as leukocyte adhesion in the PPFC assay. As discussed in **Chapter III**, of all the stimuli analyzed by RNAseq, only TNFα significantly decreased the expression of a CYP epoxygenase enzyme. While my preliminary results suggest that EET and EDP can inhibit IL-1β-induced inflammatory mediator expression by Müller cells, I would expect an even greater efficacy of EET and EDP on TNFα induction of these targets (*TNFα*, *IL1β*, *IL6*, and *IL8*), because their exogenous addition would be overcoming an endogenous deficit.

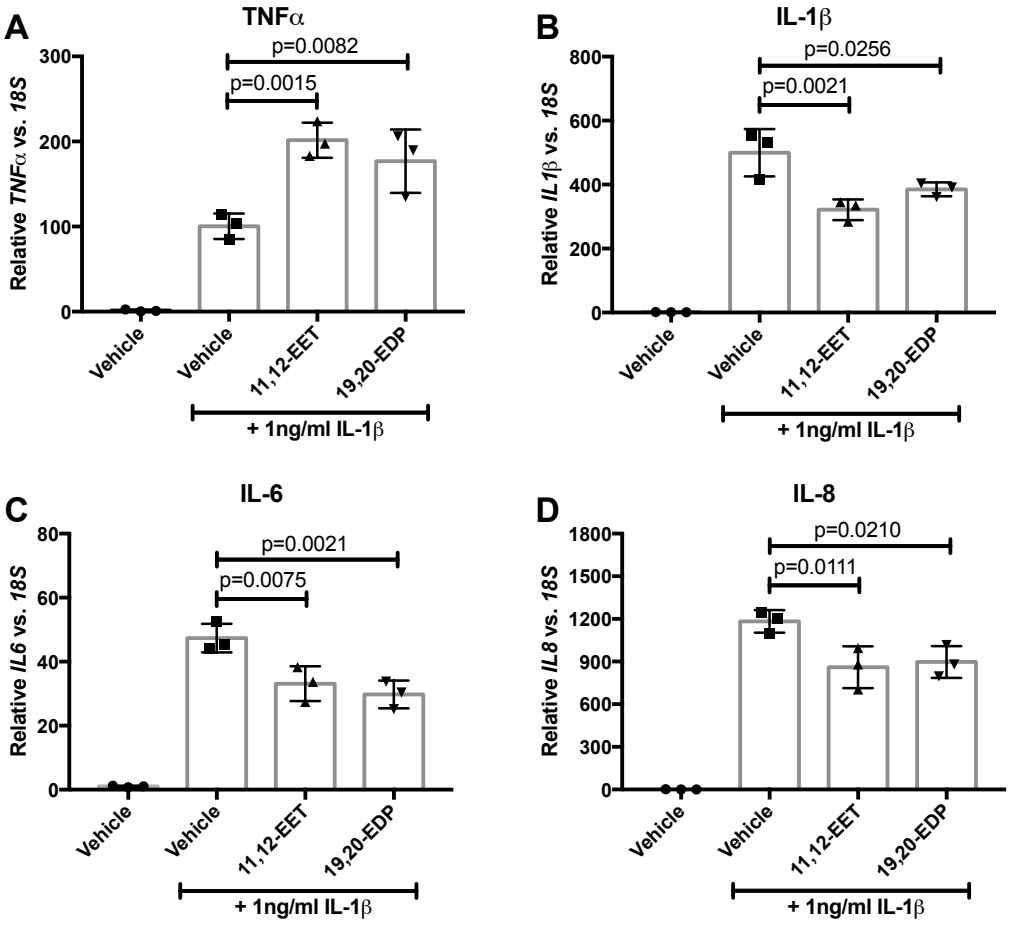

Figure 30. The effect of 11,12-EET and 19,20-EDP on IL-1β-induced inflammatory mediator expression by Müller cells. Human Müller cells were treated concomitantly with IL-1β (1ng/ml) and 11,12-EET (0.5μM) or 19,20-EDP (0.5μM). After 8 hours, RNA was isolated and expression was analyzed by qRT-PCR. (A) *TNFα* expression was significantly elevated while (B) *IL1β*, (C) *IL6*, and (D) *IL8* expression was significantly decreased by these epoxides in this preliminary experiment. Bars represent mean ± SD (n=3).

In **Chapter IV**, I demonstrated that EETs and EDPs are anti-inflammatory in cytokine-stimulated retinal microvasculature using both *in vitro* and *in vivo* models. Notably, this is the first study to compare EET and EDP head-to-head for their anti-inflammatory actions in endothelial cells. My work established that, in human retinal microvascular endothelial cells, TNFα reduced EET levels in conditioned medium. Furthermore, TNFα-induced cell adhesion molecule expression and leukocyte adhesion

to treated monolayers was decreased when cultured with 11,12-EET or 19,20-EDP plus the sEH inhibitor, AUDA. These data were then translated into an *in vivo* acute retinal inflammation model, where co-treatment of 11,12-EET or 19,20-EDP with AUDA inhibited TNFα-induced retinal leukostasis.

In addition to demonstrating that 11,12-EET and 19,20-EDP reduced vascular inflammation, I showed that treatment with the diol product of 19,20-EDP hydrolysis, 19,20-DHDP, was pro-inflammatory. This is particularly interesting considering the results reported by Ingrid Fleming's group in the retina, in which 19,20-DHDP, and not the parent substrate, drove physiologic angiogenesis.[132] No other functions of this diol have been reported outside of the retina. Additional studies of the 19,20-EDP demonstrated opposing results as to whether it possesses angiogenic or angiostatic activities in retinal and choroidal neovascularization.[165,166,328,329] Hence, determining whether 19,20-EDP is pro-angiogenic, or if this is in fact a characteristic of the diol product, remains particularly important for the development of epoxide-elevating therapies. 11,12-EET, while equally anti-inflammatory to 19,20-EDP, unequivocally exerts a pro-angiogenic effect in the retina, based on our studies in **Chapter V,** and this is supported from additional evidence in the retina.[166,283] Thus, if EDP is anti-angiogenic, promoting its levels would be the ideal therapeutic strategy for epoxide-directed therapies in DR, because unlike EET, its positive effects would not be contraindicated in late stages of the disease characterized by neovascularization. This could be accomplished by either administration of exogenous 19,20-EDP or increased ω-3 fatty acid consumption, either of which could be combined with a sEH inhibitor.

Another approach to harnessing the anti-inflammatory capacity of epoxides is to understand the downstream signaling mechanisms involved. I observed in **Chapter IV** that EET and EDP exerted similar anti-inflammatory effects on retinal microvascular endothelial cells, yet several studies have shown an opposite effect of EET and EDP in angiogenesis. This suggests that perhaps the two epoxide classes are working through separate pathways, and potentially different receptors, for their inflammatory and angiogenic behaviors. I began to query the GPR40 receptor as a potential target of epoxide signaling in retinal endothelial cells, because it was recently demonstrated to mediate the mitogenic effects of EET on kidney cells in culture.[142] GPR40 is a 7-transmembrane domain, medium/long chain fatty acid receptor that is highly expressed in pancreas and brain.[342] While only the mitogenic effect of EET activity has been attributed to GPR40 agonism, several studies show similar bioactivities between epoxides and GPR40 agonism. Most relevant to our studies, GPR40 agonism inhibited inflammatory mediator production by keratinocytes and beta cells.[343,344] AA and DHA, acting as ligands for GPR40, have shown opposing effects on mitogenesis; AA induced wound healing via GPR40 activation of mesenchymal stem cells,[345] while DHA and the GPR40 agonist, TAK-875, reduced melanoma size in a rodent subcutaneous xenograft model of human melanoma.[346] Notably, deletion of GPR40 (*Ffar1*) reduced retinal angiogenesis in the deep vascular plexus of $Vldlr^{-/-}$ mice.[255] These data suggest that perhaps GPR40-mediated epoxide signaling in HRMEC regulates inflammation and/or angiogenesis. I performed preliminary studies to characterize the potential role of GRP40 in retinal angiogenesis and HRMEC inflammation. While I did not observe an effect of GPR40 in the mouse OIR model (**Figure 31**), I did observe a potential role for

GPR40 in 11,12-EET's inhibition of TNFα-induced *VCAM1* expression (**Figure 32**), suggesting that the anti-inflammatory, but not pro-angiogenic activities of EET might be mediated via GPR40 activation. However, preliminary studies utilizing GPR40 agonists have not demonstrated any anti-inflammatory activities against TNFα-stimulated HRMEC cultures (**Appendix G**). Notably, GPR40 agonism was clinically tested for glycemic control in Japanese type 2 diabetics, and was found to be efficacious and well tolerated.[347] Taken together, these data suggest that future work should focus on understanding epoxide signaling in HRMEC, potentially through the GPR40 pathway, as a way to harness the positive attributes of the epoxide activities for DR.

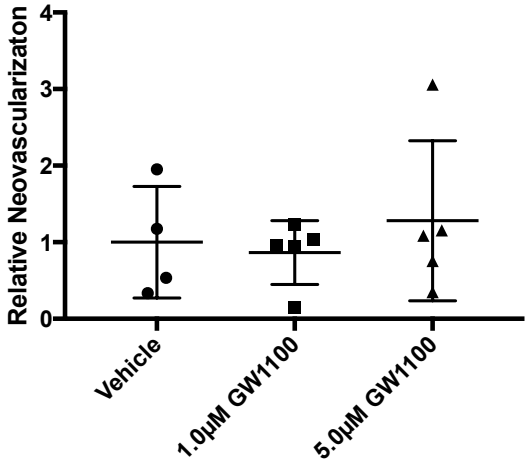

Figure 31. The effect of GPR40 antagonism on pre-retinal neovascularization in mouse OIR model. Mice received intravitreal injection of either vehicle (0.1% DMSO), or two doses of GW1100, a GPR40 inhibitor, upon removal from hyperoxic exposure. Neovascularization was measured in retinal flat-mounts 5 days post-removal from oxygen exposure. No effect of GPR40 inhibition was observed (n=4-5).

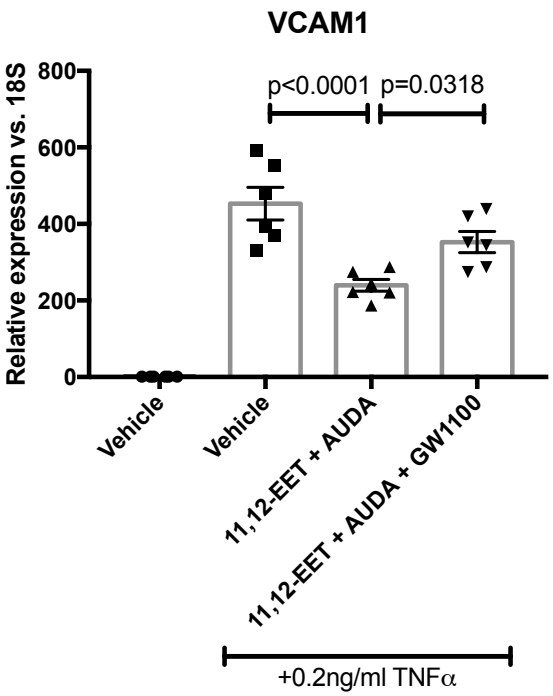

Figure 32. The effect of the GPR40 inhibitor, GW1100, on 11,12-EET + AUDA inhibition of TNFα-induced VCAM1 expression. HRMEC were treated with vehicle, TNF-α vehicle (50ng/ml), TNFα + 11,12-EET (0.5μM) + AUDA (10μM), or TNFα + 11,12-EET (0.5μM) + AUDA (10μM) + GW1100 (1.0μM) for 2hrs, and *VCAM1* expression was analyzed by qRT-PCR. As anticipated, 11,12-EET + AUDA inhibited TNFα-induced *VCAM1*, as shown in **Figure 18**. Addition of a GPR40 inhibitor, GW1100, partially attenuated this inhibition (n=6).

Currently, there are several anti-inflammatory options available for clinical use, including corticosteroids, NSAIDs, TNFα inhibitors, and anti-VEGF therapies. Like the epoxides, corticosteroids have a broad range of targets and are capable of reducing inflammation, vascular leakage and VEGF transcription, but they are short acting and yield unwanted complication including elevation of IOP and cataract.[348] While COX-2 inhibition via low oral doses of aspirin uses a more desirable route of administration and is widely known to be safe, clinical trials assessing its potential use for DR have not demonstrated any benefits.[125,126] Etanercept, which inhibits TNFα, is approved for the treatment of psoriasis, and due to TNFα's proven role in DR pathogenesis would be a likely candidate for anti-inflammatory treatment. However, in preliminary reports of its

use in patients with DME, no statistically significant improvements were observed.[349] This may be due, in part, to the large number of inflammatory cytokines elevated during DR, with some functional redundancy to TNFα, such as IL-1β. Thus, there remains a need to develop novel anti-inflammatory agents that are safe, efficacious, and more easily delivered.

Based on the data from **Chapter IV** and the preliminary data in **Figure 30**, epoxide-elevating therapies may be superior anti-inflammatory agents compared to the current strategies considered for clinical use. First, epoxide levels were decreased in retinal endothelial cells stimulated with TNFα (**Figure 16**), and while total retinal epoxide levels were unaffected, the ratio of diols to epoxides was decreased in response to acute inflammation (**Appendix F**). This is consistent with the observation of decreased epoxides in the vitreous of patients with diabetic retinopathy.[89] These data suggest that enzymes controlling epoxide levels are dysregulated in DR. Thus, epoxide elevation strategies would be tolerated because treatments would be designed to return epoxides to endogenous levels. Additionally, epoxide therapies appear to exert their activities against both upstream production of inflammatory mediators and downstream response to these inflammatory mediators. Hence, epoxide therapy could exert influence at multiple steps along the DR pathogenic cascade, potentially providing greater overall efficacy. Lastly, epoxides regulate multiple inflammatory targets, which provide an advantage over mono-therapy strategies.

An important and logical next step for this project is to demonstrate whether diabetes alters the levels of CYP-derived epoxides in the retina. A goal of the present work was to identify the effects of various diabetes-relevant stimuli on the levels of

epoxides, because, as reviewed in **Chapter I**, several studies have shown down-regulation of CYP enzymes or up-regulation of sEH in response to diabetes-relevant conditions in other cell types or tissues. We began to characterize these changes in our models (**Figures 16**, **23**, **24**, and **Appendix C** and **F**). However, more appropriate models need to be utilized to assess whether the CYP/sEH enzymes are impaired in the diabetic retina. Future studies should use a complement of models to understand the role of systemic diabetes on retinal epoxide levels, since several factors are known to modulate these enzymes and the metabolic profile will likely vary between models. I recommend comparing studies of CYP-derived epoxides from vitreous or aqueous samples of diabetic retinopathy patients to a variety of animal models, including STZ-induced diabetes models, diet-induced obesity or other genetic type 2 models, and OIR models. Retinal epoxide levels should be measured instead of CYP enzyme levels in these studies, because the full complement of CYP epoxygenase enzymes is unknown. Furthermore, CYPs possessing epoxygenase activity continue to be identified. While members of the CYP2C and CYP2J family are the most thoroughly studied, several other CYP enzymes exhibit epoxygenase activity.[129] In fact, in Müller cell whole transcriptome analysis, the only epoxygenase that was significantly altered by any stimulus was CYP2S1, which until recently was considered an orphan P450.[129] Thus, before analyzing expression of specific CYP enzymes, a systematic study of all CYP epoxygenases in the human retina needs to be performed.

Ultimately, our results demonstrate proof of concept for retinal anti-inflammatory activity of CYP-derived epoxides. Therefore, the next studies in the lab should focus on long-term treatment with EET and EDP analogs or sEH inhibitor in systemic diabetes

models. Water-soluble epoxide analogs have been developed and utilized *in vivo* for systemic treatment of hypertension and nephrotoxicity.[350,351] Furthermore, the sEH inhibitor, GSK2256294, which has been used in early phase clinical trials, shows favorable pharmacokinetics profiles when delivered to rodents by oral administration.[352,353] Thus, the ability to systemically administer these therapeutics is particularly advantageous, because current DR treatment strategies utilize a more invasive route of administration, intravitreal delivery. Furthermore, in rodents, the globe does not tolerate repeat injections, thereby posing problems for dosing and pharmacokinetic optimization in preclinical, long-term disease models. I hypothesize that epoxide-directed therapies would be efficacious against early non-proliferative DR. I expect that these therapies will have several beneficial effects related to their direct anti-inflammatory activities, indirect effects mediated by the resulting inhibition of cytokine production and leukostasis (i.e. reduced vascular permeability), and additional biological activities (i.e. vaso-dilation). However, any beneficial effects should be interpreted with caution because no experimental diabetes models have been shown to progress to PDR. Hence, it is unlikely that the pro-angiogenic capacity of epoxide elevation can be analyzed in diabetic animals, and this is important to gauge whether epoxides promote transition to PDR. Furthermore, this potential negative impact of epoxide elevation in the retina should be a consideration for the development of sEH inhibitors in the clinic. For instance, clinical trials have been performed in pre-diabetic patients to assess the effect of systemic sEH inhibition on hypertension (Arete Therapeutics; NLM identifier: NCT00847899), and this treatment would presumably elevate intraocular epoxide levels. This patient population may be susceptible to DR and subsequent

neovascularization, and therefore retinal outcomes should be considered when designing these clinical trials.

In summary, I have defined novel disease-relevant Müller cell culture conditions, demonstrated the comparative anti-inflammatory capacity of EET and EDP in the retina, and confirmed the pro-angiogenic activity of EET in retinal neovascularization. Taken together, this work comprises an important step in our understanding of DR pathogenesis and the potential development of CYP epoxide-elevating therapeutic strategies for early, but not late, DR.

Appendix A

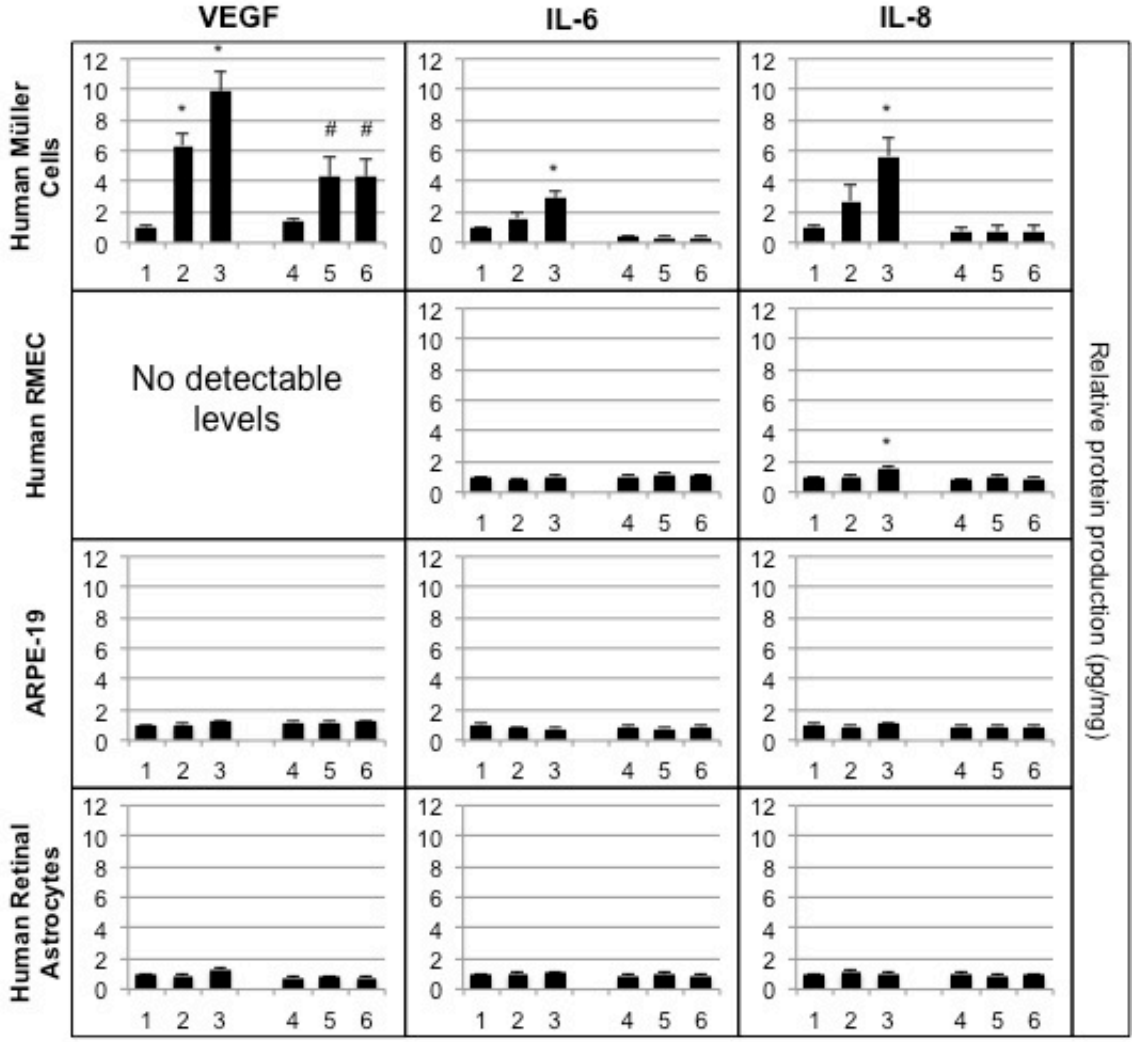

The effect of oleic acid, linoleic acid, and elevated glucose on the production of VEGF, IL-6, and IL-8 by human retinal glial cells and blood-retina barrier cells. Human Müller cells, retinal microvascular endothelial cells, ARPE-19, and retinal astrocytes were treated with 1) BSA control (100µg/ml), 2) BSA-bound oleic acid (60µM), 3) BSA-bound linoleic acid (60µM), 4) Normal glucose (5.5mM), 5) L-glucose (5.5mM D-Glucose + 20mM L-glucose); osmotic control, and 6) D-glucose (25.5mM) for 36 hours. Secreted VEGF, IL-6, and IL-8 was assayed in the culture medium by ELISA. *$p<0.05$ compared to BSA control, #$p<0.05$ compared to normal glucose control. Bars represent average ± SEM (n=9).

Appendix B

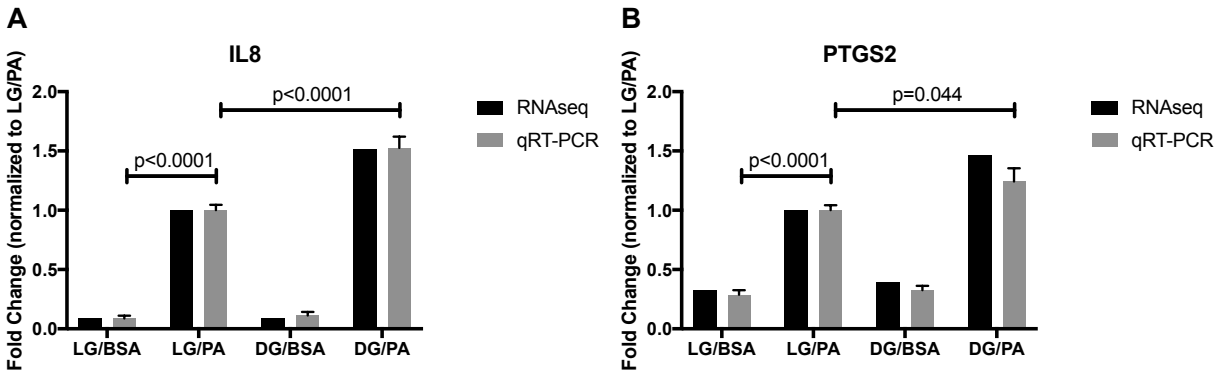

Comparison of RNAseq differences to PCR validation expression assays for (A) *IL8* and (B) *PTGS2* expression. Using human Müller cells derived from 3 individual donors, we recapitulated the differential expression observed by RNAseq. The treatment groups are as follows: LG/BSA, 24 hours L-glucose, 24 hours L-glucose + BSA; LG/PA, 24 hours L-glucose, 24 hours L-glucose + PA; DG/BSA, 24 hours D-glucose, 24 hours D-glucose + BSA; DG/PA, 24 hours D-glucose, 24 hours D-glucose + PA. RNAseq bars represent mean value of log2fold change from RNAseq (n=2); qRT-PCR bars represent mean ± SEM (n=9).

Appendix C

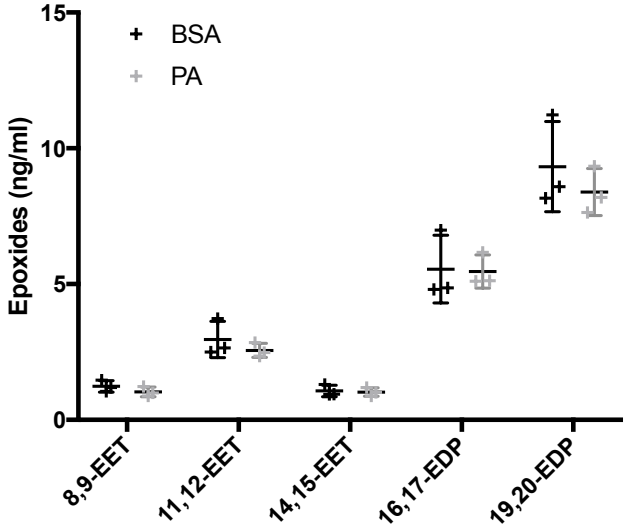

The effect of PA on EET/EDP levels in Müller cell cultured medium. Müller cells were treated with either BSA (vehicle; 100mg/ml) or BSA-conjugated PA (250μM) for 24 hours. AA (10μM) or DHA (10μM) was added for the last 3 hours of treatment. PA had no effect on epoxide levels in this preliminary experiment (n=3).

Appendix D

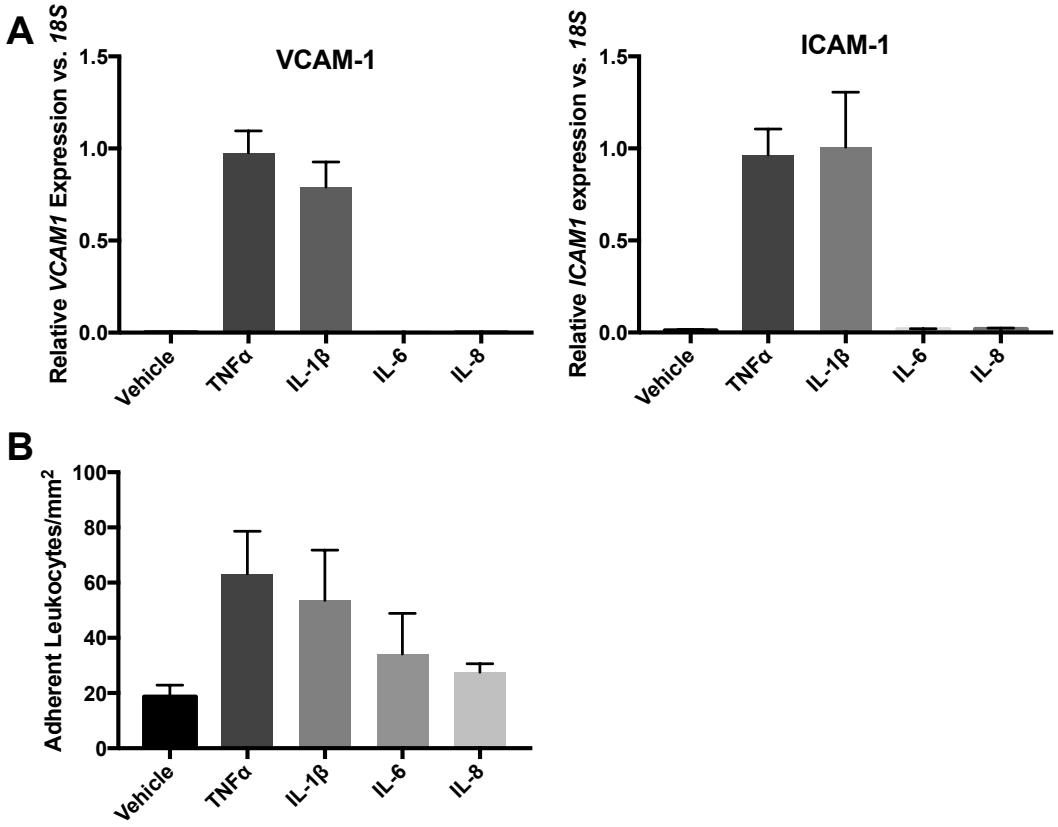

The effect of inflammatory mediators on leukocyte adhesion behaviors in HRMEC. (A) HRMEC were treated with 1ng/ml of TNFα, IL-1β, IL-6, or IL-8 for 2 hours and cell adhesion molecule expression was assessed by qRT-PCR. VCAM-1 and ICAM-1 were elevated by TNFα and IL-1β, but not IL-6 or IL-8. (B) HRMEC monolayers were treated with 1ng/ml of TNFα, IL-1β, IL-6, or IL-8 for 4 hours, PBMC were flowed over the monolayers in a parallel plate flow chamber, and leukocyte adhesion was counted. TNFα was the only mediator that significantly induced leukocyte adhesion to treated monolayers. Bars represent mean ± SEM (A: n=9; B: n=4-6).

Appendix E

A

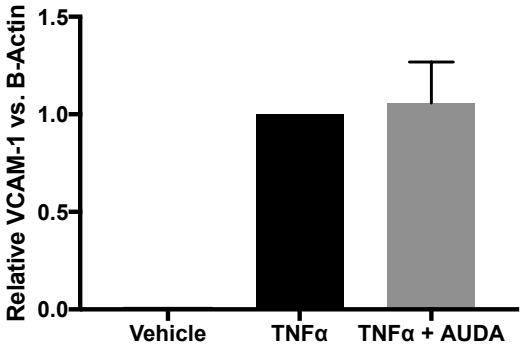

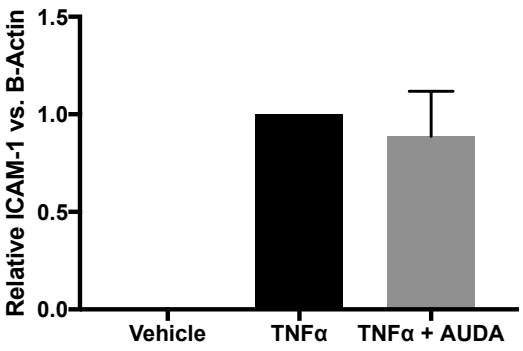

B

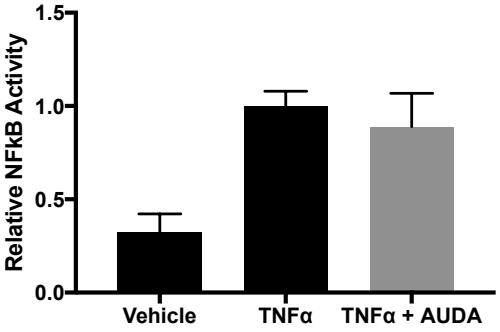

C

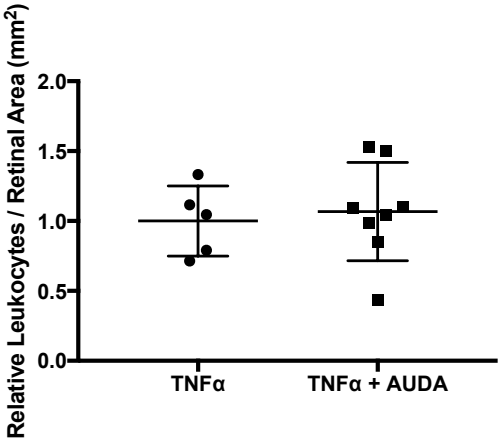

The effect of AUDA alone on TNFα-induced inflammation. (A) Cells were treated as described for **Figure 18**, but in the absence of exogenous epoxides. sEH inhibition with AUDA (10μM) has no effect on TNFα-induced VCAM-1 and ICAM-1 protein levels in HRMEC. Bars represent mean ± SD (n=4). (B) Cells were treated as described for **Figure 21**, but in the absence of exogenous epoxides. sEH inhibition with AUDA (10μM) had no effect on TNFα-induced NFκB activity in HRMEC. Bar represent mean ± SEM (n=8). (C) Animals were treated as described for **Figure 22**, but in the absence of exogenous epoxides. sEH inhibition with AUDA (10μM) had no effect on TNFα-induced retinal leukostasis (TNFα: n=5; AUDA: n=8).

Appendix F

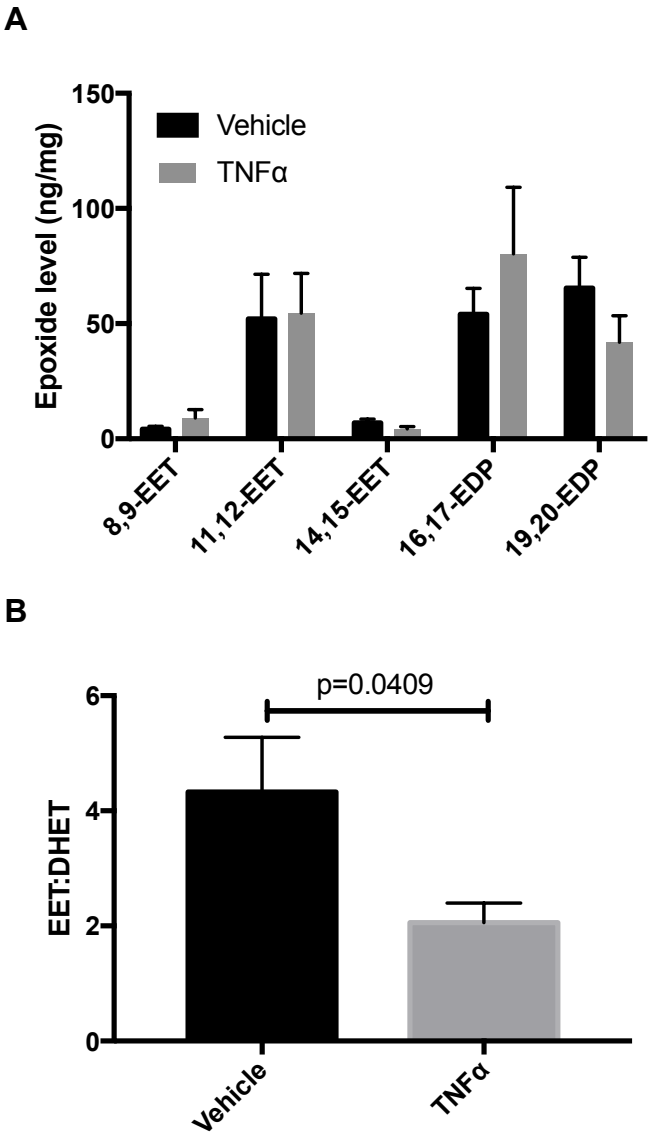

The effect of TNFα intravitreal injection on (A) retinal epoxide levels and (B) EET:DHET ratio. (A) Animals received intravitreal injection of TNFα (50ng/ml) and retinas were collected 6hrs post-injection. Four retinas were pooled for each measurement. None of the CYP epoxide products were significantly altered in the retina. Bars represent mean ± SEM (n=6-9). (B) Retinas were treated as described for (A). Retinal DHETs were only detectable from 3 of the samples. For these samples, the totals EETs were compared to the total amount of their diol products. TNFα treatment significantly decreased EET:DHET, suggesting an increased activity of sEH. Bars represent mean ± SD (n=3).

Appendix G

A

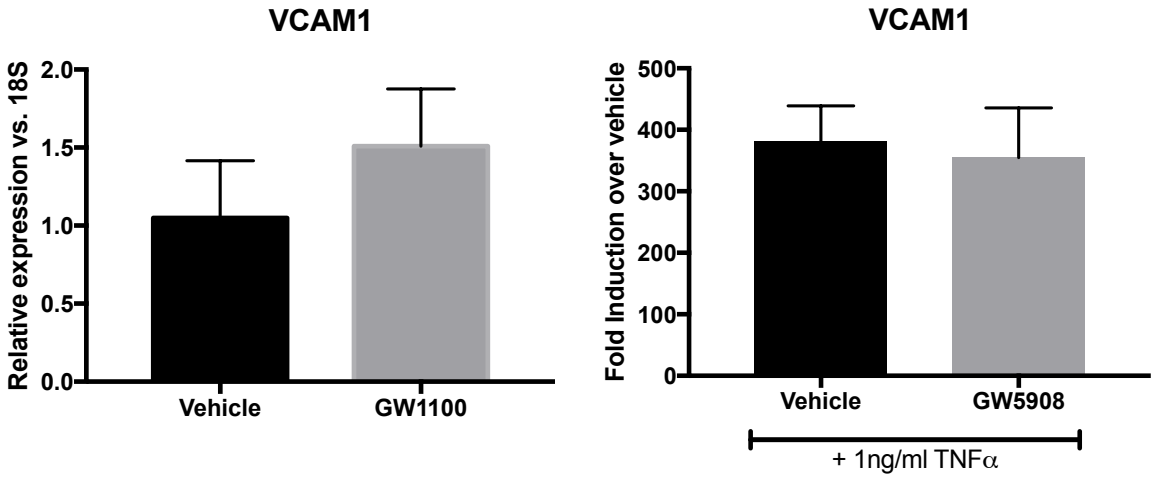

B

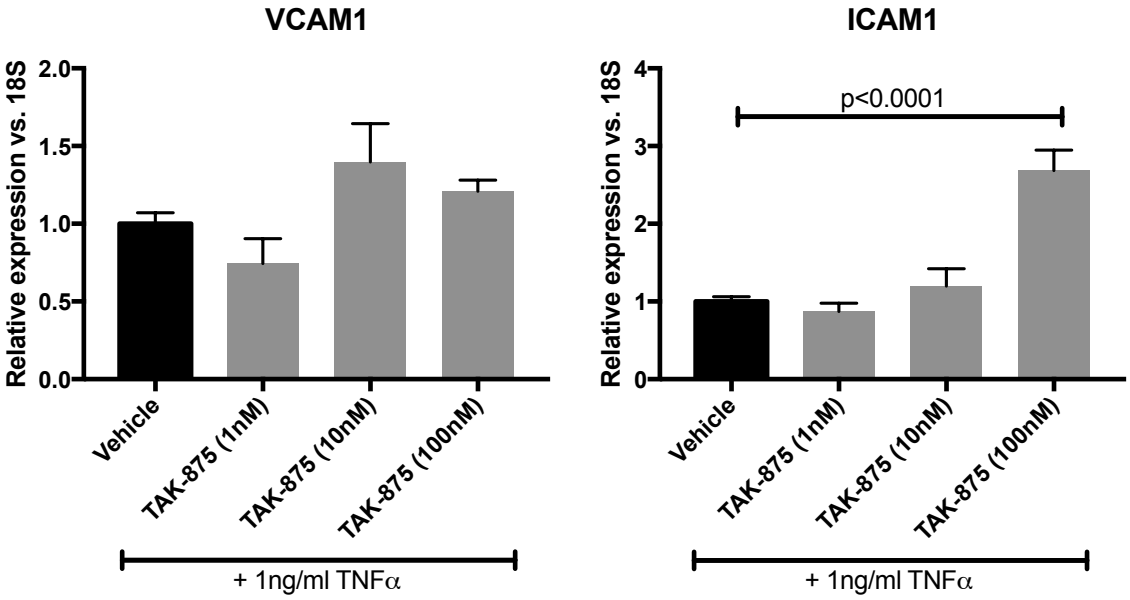

The effect of GPR40 on HRMEC cell adhesion molecule expression. HRMEC were treated with either a GPR40 inhibitor, GW1100, TNFα, or TNFα plus one of two GPR40 agonists; GW9508 or TAK-875. (A) GPR40 antagonism had no effect on basal *VCAM1* expression and GPR40 agonism did not inhibit TNFα-induced *VCAM1* expression. (B) A dose response of GPR40 agonism with TAK-875 did not inhibit TNFα-induced VCAM1 expression. However, TAK-875 at the highest dose (100nM) stimulated *ICAM1* expression. Bars represent mean ± SD (n=3).

Appendix H

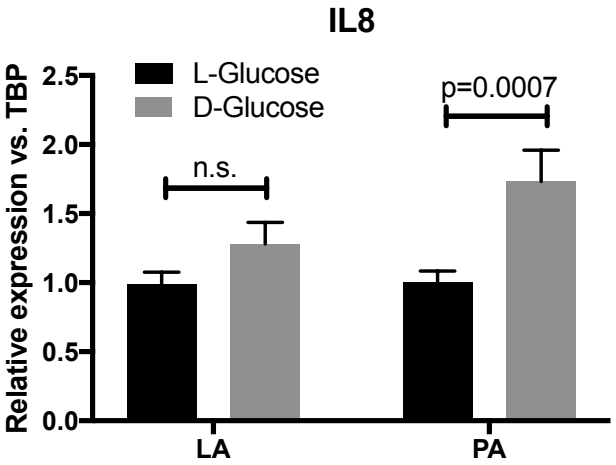

The effect of D-glucose pre-treatment on LA and PA-stimulated IL8 expression in human Müller cells. Müller cells were pre-treated with either L-glucose or D-glucose as described for the studies in **Chapter III**. Cells were then treated with the same stimulus (L-glucose or D-glucose) plus either LA (60μM) or PA (250μM). These different doses were identified to be optimal stimulators of Müller cell inflammation for each fatty acid. PA, but not LA, further stimulated IL8 expression when pre-treated with D-glucose. Bars represent mean ± SD (n=3).

REFERENCES

1 *Statistics About Diabetes*, 2016).

2 Cheung, N., Mitchell, P. & Wong, T. Y. Diabetic retinopathy. *Lancet* **376**, 124-136, doi:10.1016/S0140-6736(09)62124-3 (2010).

3 Lee, R., Wong, T. Y. & Sabanayagam, C. Epidemiology of diabetic retinopathy, diabetic macular edema and related vision loss. *Eye Vis (Lond)* **2**, 17, doi:10.1186/s40662-015-0026-2 (2015).

4 Romero-Aroca, P. Managing diabetic macular edema: The leading cause of diabetes blindness. *World J Diabetes* **2**, 98-104, doi:10.4239/wjd.v2.i6.98 (2011).

5 Fong, D. S. *et al.* Retinopathy in diabetes. *Diabetes Care* **27 Suppl 1**, S84-87 (2004).

6 Klein, R., Klein, B. E., Moss, S. E., Davis, M. D. & DeMets, D. L. The Wisconsin epidemiologic study of diabetic retinopathy. II. Prevalence and risk of diabetic retinopathy when age at diagnosis is less than 30 years. *Arch Ophthalmol* **102**, 520-526 (1984).

7 Yau, J. W. *et al.* Global prevalence and major risk factors of diabetic retinopathy. *Diabetes Care* **35**, 556-564, doi:10.2337/dc11-1909 (2012).

8 Zhang, X. *et al.* Prevalence of diabetic retinopathy in the United States, 2005-2008. *JAMA* **304**, 649-656, doi:10.1001/jama.2010.1111 (2010).

9 Wong, T. Y. *et al.* Prevalence and risk factors for diabetic retinopathy: the Singapore Malay Eye Study. *Ophthalmology* **115**, 1869-1875, doi:10.1016/j.ophtha.2008.05.014 (2008).

10 Tapp, R. J. *et al.* The prevalence of and factors associated with diabetic retinopathy in the Australian population. *Diabetes Care* **26**, 1731-1737 (2003).

11 Hu, F. B., Satija, A. & Manson, J. E. Curbing the Diabetes Pandemic: The Need for Global Policy Solutions. *JAMA* **313**, 2319-2320, doi:10.1001/jama.2015.5287 (2015).

12 Matthews, D. R. *et al.* Risks of progression of retinopathy and vision loss related to tight blood pressure control in type 2 diabetes mellitus: UKPDS 69. *Arch Ophthalmol* **122**, 1631-1640, doi:10.1001/archopht.122.11.1631 (2004).

13 The effect of intensive treatment of diabetes on the development and progression of long-term complications in insulin-dependent diabetes mellitus. The Diabetes Control and Complications Trial Research Group. *The New England journal of medicine* **329**, 977-986, doi:10.1056/NEJM199309303291401 (1993).

14 Cryer, P. E. The barrier of hypoglycemia in diabetes. *Diabetes* **57**, 3169-3176, doi:10.2337/db08-1084 (2008).

15 Chew, E. Y. *et al.* Association of elevated serum lipid levels with retinal hard exudate in diabetic retinopathy. Early Treatment Diabetic Retinopathy Study (ETDRS) Report 22. *Arch Ophthalmol* **114**, 1079-1084 (1996).

16 Wright, A. D. & Dodson, P. M. Medical management of diabetic retinopathy: fenofibrate and ACCORD Eye studies. *Eye (Lond)* **25**, 843-849, doi:10.1038/eye.2011.62 (2011).

17 Keech, A. C. *et al.* Effect of fenofibrate on the need for laser treatment for diabetic retinopathy (FIELD study): a randomised controlled trial. *Lancet* **370**, 1687-1697, doi:10.1016/S0140-6736(07)61607-9 (2007).

18 Photocoagulation for diabetic macular edema. Early Treatment Diabetic Retinopathy Study report number 1. Early Treatment Diabetic Retinopathy Study research group. *Arch Ophthalmol* **103**, 1796-1806 (1985).

19 Paulus, Y. & M.S., B. *Panretinal Photocoagulation for Treatment of Proliferative Diabetic Retinopathy*, 2013).

20 Fong, D. S., Girach, A. & Boney, A. Visual side effects of successful scatter laser photocoagulation surgery for proliferative diabetic retinopathy: a literature review. *Retina* **27**, 816-824, doi:10.1097/IAE.0b013e318042d32c (2007).

21 Praidou, A. *et al.* Vitreous and serum levels of vascular endothelial growth factor and platelet-derived growth factor and their correlation in patients with non-proliferative diabetic retinopathy and clinically significant macula oedema. *Acta Ophthalmol* **89**, 248-254, doi:10.1111/j.1755-3768.2009.01661.x (2011).

22 McAuley, A. K. *et al.* Vitreous biomarkers in diabetic retinopathy: a systematic review and meta-analysis. *J Diabetes Complications* **28**, 419-425, doi:10.1016/j.jdiacomp.2013.09.010 (2014).

23 Arevalo, J. F. & Garcia-Amaris, R. A. Intravitreal bevacizumab for diabetic retinopathy. *Curr Diabetes Rev* **5**, 39-46 (2009).

24 Haddock, L. J., Ramsey, D. J. & Young, L. H. Complications of Subspecialty Ophthalmic Care: Endophthalmitis after Intravitreal Injections of Anti-Vascular Endothelial Growth Factor Medications. *Seminars in Ophthalmology* **29**, 257-262, doi:10.3109/08820538.2014.959616 (2014).

25 El-Mollayess, G. M., Saadeh, J. S. & Salti, H. I. Exogenous endophthalmitis in diabetic patients: a systemic review. *ISRN Ophthalmol* **2012**, 456209, doi:10.5402/2012/456209 (2012).

26 Fintak, D. R. *et al.* Incidence of endophthalmitis related to intravitreal injection of bevacizumab and ranibizumab. *Retina* **28**, 1395-1399, doi:10.1097/IAE.0b013e3181884fd2 (2008).

27 Saint-Geniez, M. *et al.* Endogenous VEGF is required for visual function: evidence for a survival role on muller cells and photoreceptors. *PloS one* **3**, e3554, doi:10.1371/journal.pone.0003554 (2008).

28 Hombrebueno, J. R., Ali, I. H., Xu, H. & Chen, M. Sustained intraocular VEGF neutralization results in retinal neurodegeneration in the Ins2(Akita) diabetic mouse. *Sci Rep* **5**, 18316, doi:10.1038/srep18316 (2015).

29 Nishijima, K. *et al.* Vascular endothelial growth factor-A is a survival factor for retinal neurons and a critical neuroprotectant during the adaptive response to ischemic injury. *Am J Pathol* **171**, 53-67, doi:10.2353/ajpath.2007.061237 (2007).

30 Das, A., Stroud, S., Mehta, A. & Rangasamy, S. New treatments for diabetic retinopathy. *Diabetes Obes Metab* **17**, 219-230, doi:10.1111/dom.12384 (2015).

31 Antonetti, D. A., Klein, R. & Gardner, T. W. Diabetic retinopathy. *The New England journal of medicine* **366**, 1227-1239, doi:10.1056/NEJMra1005073 (2012).

32 Wong-Riley, M. T. Energy metabolism of the visual system. *Eye Brain* **2**, 99-116, doi:10.2147/EB.S9078 (2010).

33 Barber, A. J. A new view of diabetic retinopathy: a neurodegenerative disease of the eye. *Prog Neuropsychopharmacol Biol Psychiatry* **27**, 283-290, doi:10.1016/S0278-5846(03)00023-X (2003).

34 Bresnick, G. H. Diabetic retinopathy viewed as a neurosensory disorder. *Arch Ophthalmol* **104**, 989-990 (1986).

35 Barber, A. J. *et al.* Neural apoptosis in the retina during experimental and human diabetes. Early onset and effect of insulin. *J Clin Invest* **102**, 783-791, doi:10.1172/JCI2425 (1998).

36 Bloodworth, J. M., Jr. Diabetic retinopathy. *Diabetes* **11**, 1-22 (1962).

37 Wolter, J. R. Diabetic retinopathy. *Am J Ophthalmol* **51**, 1123-1141 (1961).

38 Antonetti, D. A. *et al.* Diabetic retinopathy: seeing beyond glucose-induced microvascular disease. *Diabetes* **55**, 2401-2411, doi:10.2337/db05-1635 (2006).

39 Frost-Larsen, K., Larsen, H. W. & Simonsen, S. E. Oscillatory potential and nyctometry in insulin-dependent diabetics. *Acta Ophthalmol (Copenh)* **58**, 879-888 (1980).

40 Simonsen, S. E. The value of the oscillatory potential in selecting juvenile diabetics at risk of developing proliferative retinopathy. *Acta Ophthalmol (Copenh)* **58**, 865-878 (1980).

41 Bearse, M. A., Jr. *et al.* Local multifocal oscillatory potential abnormalities in diabetes and early diabetic retinopathy. *Investigative ophthalmology & visual science* **45**, 3259-3265, doi:10.1167/iovs.04-0308 (2004).

42 Parisi, V. & Uccioli, L. Visual electrophysiological responses in persons with type 1 diabetes. *Diabetes Metab Res Rev* **17**, 12-18 (2001).

43 Della Sala, S., Bertoni, G., Somazzi, L., Stubbe, F. & Wilkins, A. J. Impaired contrast sensitivity in diabetic patients with and without retinopathy: a new technique for rapid assessment. *Br J Ophthalmol* **69**, 136-142 (1985).

44 Dosso, A. A. *et al.* Contrast sensitivity in obese dyslipidemic patients with insulin resistance. *Arch Ophthalmol* **116**, 1316-1320 (1998).

45 Han, Y. *et al.* Multifocal electroretinogram delays predict sites of subsequent diabetic retinopathy. *Investigative ophthalmology & visual science* **45**, 948-954 (2004).

46 Realini, T., Lai, M. Q. & Barber, L. Impact of diabetes on glaucoma screening using frequency-doubling perimetry. *Ophthalmology* **111**, 2133-2136, doi:10.1016/j.ophtha.2004.05.024 (2004).

47 Mizutani, M., Gerhardinger, C. & Lorenzi, M. Muller cell changes in human diabetic retinopathy. *Diabetes* **47**, 445-449 (1998).

48 Gerhardinger, C. *et al.* Expression of acute-phase response proteins in retinal Muller cells in diabetes. *Investigative ophthalmology & visual science* **46**, 349-357, doi:10.1167/iovs.04-0860 (2005).

49 Iandiev, I., Pannicke, T., Reichenbach, A., Wiedemann, P. & Bringmann, A. Diabetes alters the localization of glial aquaporins in rat retina. *Neurosci Lett* **421**, 132-136, doi:10.1016/j.neulet.2007.04.076 (2007).

50 Fukuda, M. *et al.* Altered expression of aquaporins 1 and 4 coincides with neurodegenerative events in retinas of spontaneously diabetic Torii rats. *Exp Eye Res* **90**, 17-25, doi:10.1016/j.exer.2009.09.003 (2010).

51 Bringmann, A., Grosche, A., Pannicke, T. & Reichenbach, A. GABA and Glutamate Uptake and Metabolism in Retinal Glial (Muller) Cells. *Front Endocrinol (Lausanne)* **4**, 48, doi:10.3389/fendo.2013.00048 (2013).

52 Lieth, E. *et al.* Glial reactivity and impaired glutamate metabolism in short-term experimental diabetic retinopathy. Penn State Retina Research Group. *Diabetes* **47**, 815-820 (1998).

53 Puro, D. G. Diabetes-induced dysfunction of retinal Muller cells. *Trans Am Ophthalmol Soc* **100**, 339-352 (2002).

54 Klaassen, I., Van Noorden, C. J. & Schlingemann, R. O. Molecular basis of the inner blood-retinal barrier and its breakdown in diabetic macular edema and other pathological conditions. *Prog Retin Eye Res* **34**, 19-48, doi:10.1016/j.preteyeres.2013.02.001 (2013).

55 Antonetti, D. A., Lieth, E., Barber, A. J. & Gardner, T. W. Molecular mechanisms of vascular permeability in diabetic retinopathy. *Semin Ophthalmol* **14**, 240-248, doi:10.3109/08820539909069543 (1999).

56 Aveleira, C. A., Lin, C. M., Abcouwer, S. F., Ambrosio, A. F. & Antonetti, D. A. TNF-alpha signals through PKCzeta/NF-kappaB to alter the tight junction complex and increase retinal endothelial cell permeability. *Diabetes* **59**, 2872-2882, doi:10.2337/db09-1606 (2010).

57 Desai, T. R., Leeper, N. J., Hynes, K. L. & Gewertz, B. L. Interleukin-6 causes endothelial barrier dysfunction via the protein kinase C pathway. *J Surg Res* **104**, 118-123, doi:10.1006/jsre.2002.6415 (2002).

58 Harhaj, N. S. *et al.* VEGF activation of protein kinase C stimulates occludin phosphorylation and contributes to endothelial permeability. *Investigative ophthalmology & visual science* **47**, 5106-5115, doi:10.1167/iovs.06-0322 (2006).

59 Leto, G. *et al.* Increased retinal endothelial cell monolayer permeability induced by the diabetic milieu: role of advanced non-enzymatic glycation and polyol pathway activation. *Diabetes Metab Res Rev* **17**, 448-458 (2001).

60 Armulik, A., Genove, G. & Betsholtz, C. Pericytes: developmental, physiological, and pathological perspectives, problems, and promises. *Dev Cell* **21**, 193-215, doi:10.1016/j.devcel.2011.07.001 (2011).

61 Enge, M. *et al.* Endothelium-specific platelet-derived growth factor-B ablation mimics diabetic retinopathy. *EMBO J* **21**, 4307-4316 (2002).

62 Cacicedo, J. M., Benjachareowong, S., Chou, E., Ruderman, N. B. & Ido, Y. Palmitate-induced apoptosis in cultured bovine retinal pericytes: roles of NAD(P)H oxidase, oxidant stress, and ceramide. *Diabetes* **54**, 1838-1845 (2005).

63 Suarez, S., McCollum, G. W., Jayagopal, A. & Penn, J. S. High Glucose-induced Retinal Pericyte Apoptosis Depends on Association of GAPDH and Siah1. *The Journal of biological chemistry* **290**, 28311-28320, doi:10.1074/jbc.M115.682385 (2015).

64 Beltramo, E. & Porta, M. Pericyte loss in diabetic retinopathy: mechanisms and consequences. *Curr Med Chem* **20**, 3218-3225 (2013).

65 Li, W., Yanoff, M., Liu, X. & Ye, X. Retinal capillary pericyte apoptosis in early human diabetic retinopathy. *Chin Med J (Engl)* **110**, 659-663 (1997).

66 Wang, Z. & Gleichmann, H. GLUT2 in pancreatic islets: crucial target molecule in diabetes induced with multiple low doses of streptozotocin in mice. *Diabetes* **47**, 50-56 (1998).

67 Kern, T. S., Du, Y., Miller, C. M., Hatala, D. A. & Levin, L. A. Overexpression of Bcl-2 in vascular endothelium inhibits the microvascular lesions of diabetic retinopathy. *Am J Pathol* **176**, 2550-2558, doi:10.2353/ajpath.2010.091062 (2010).

68 Li, G., Tang, J., Du, Y., Lee, C. A. & Kern, T. S. Beneficial effects of a novel RAGE inhibitor on early diabetic retinopathy and tactile allodynia. *Mol Vis* **17**, 3156-3165 (2011).

69 Wang, J., Xu, X., Elliott, M. H., Zhu, M. & Le, Y. Z. Muller cell-derived VEGF is essential for diabetes-induced retinal inflammation and vascular leakage. *Diabetes* **59**, 2297-2305, doi:10.2337/db09-1420 (2010).

70 Feit-Leichman, R. A. *et al.* Vascular damage in a mouse model of diabetic retinopathy: relation to neuronal and glial changes. *Investigative ophthalmology & visual science* **46**, 4281-4287, doi:10.1167/iovs.04-1361 (2005).

71 Martin, P. M., Roon, P., Van Ells, T. K., Ganapathy, V. & Smith, S. B. Death of retinal neurons in streptozotocin-induced diabetic mice. *Investigative ophthalmology & visual science* **45**, 3330-3336, doi:10.1167/iovs.04-0247 (2004).

72 Robinson, R., Barathi, V. A., Chaurasia, S. S., Wong, T. Y. & Kern, T. S. Update on animal models of diabetic retinopathy: from molecular approaches to mice and higher mammals. *Dis Model Mech* **5**, 444-456, doi:10.1242/dmm.009597 (2012).

73 Yang, Q. *et al.* Retinal Neurodegeneration in db/db Mice at the Early Period of Diabetes. *Journal of ophthalmology* **2015**, 757412, doi:10.1155/2015/757412 (2015).

74 Rajagopal, R. *et al.* Functional Deficits Precede Structural Lesions in Mice With High-Fat Diet-Induced Diabetic Retinopathy. *Diabetes* **65**, 1072-1084, doi:10.2337/db15-1255 (2016).

75 Zheng, L., Gong, B., Hatala, D. A. & Kern, T. S. Retinal ischemia and reperfusion causes capillary degeneration: similarities to diabetes. *Investigative ophthalmology & visual science* **48**, 361-367, doi:10.1167/iovs.06-0510 (2007).

76 Bretz, C. A., Savage, S. R., Capozzi, M. E., Suarez, S. & Penn, J. S. NFAT isoforms play distinct roles in TNFalpha-induced retinal leukostasis. *Sci Rep* **5**, 14963, doi:10.1038/srep14963 (2015).

77 Murakami, T., Frey, T., Lin, C. & Antonetti, D. A. Protein kinase cbeta phosphorylates occludin regulating tight junction trafficking in vascular endothelial growth factor-induced permeability in vivo. *Diabetes* **61**, 1573-1583, doi:10.2337/db11-1367 (2012).

78 Smith, L. E. *et al.* Oxygen-induced retinopathy in the mouse. *Investigative ophthalmology & visual science* **35**, 101-111 (1994).

79 Scott, A. & Fruttiger, M. Oxygen-induced retinopathy: a model for vascular pathology in the retina. *Eye (Lond)* **24**, 416-421, doi:10.1038/eye.2009.306 (2010).

80 Quinn, G. E. Retinopathy of prematurity blindness worldwide: phenotypes in the third epidemic. *Eye and Brain* **8**, 6 (2016).

81 Penn, J. S., Tolman, B. L. & Henry, M. M. Oxygen-induced retinopathy in the rat: relationship of retinal nonperfusion to subsequent neovascularization. *Investigative ophthalmology & visual science* **35**, 3429-3435 (1994).

82 Hartnett, M. E. Pathophysiology and mechanisms of severe retinopathy of prematurity. *Ophthalmology* **122**, 200-210, doi:10.1016/j.ophtha.2014.07.050 (2015).

83 Purcaro, V. *et al.* Fluorescein angiography and retinal vascular development in premature infants. *J Matern Fetal Neonatal Med* **25 Suppl 3**, 53-56, doi:10.3109/14767058.2012.712313 (2012).

84 Werdich, X. Q., McCollum, G. W., Rajaratnam, V. S. & Penn, J. S. Variable oxygen and retinal VEGF levels: correlation with incidence and severity of pathology in a rat model of oxygen-induced retinopathy. *Exp Eye Res* **79**, 623-630, doi:10.1016/j.exer.2004.07.006 (2004).

85 Cai, M., Zhang, X., Li, Y. & Xu, H. Toll-like receptor 3 activation drives the inflammatory response in oxygen-induced retinopathy in rats. *Br J Ophthalmol* **99**, 125-132, doi:10.1136/bjophthalmol-2014-305690 (2015).

86 Doganay, S. *et al.* Comparison of serum NO, TNF-alpha, IL-1beta, sIL-2R, IL-6 and IL-8 levels with grades of retinopathy in patients with diabetes mellitus. *Eye (Lond)* **16**, 163-170, doi:10.1038/sj/EYE/6700095 (2002).

87 Kern, T. S. Contributions of inflammatory processes to the development of the early stages of diabetic retinopathy. *Exp Diabetes Res* **2007**, 95103, doi:10.1155/2007/95103 (2007).

88 Zhang, W., Liu, H., Al-Shabrawey, M., Caldwell, R. W. & Caldwell, R. B. Inflammation and diabetic retinal microvascular complications. *Journal of cardiovascular disease research* **2**, 96-103, doi:10.4103/0975-3583.83035 (2011).

89 Schwartzman, M. L. *et al.* Profile of lipid and protein autacoids in diabetic vitreous correlates with the progression of diabetic retinopathy. *Diabetes* **59**, 1780-1788, doi:10.2337/db10-0110 (2010).

90 Suzuki, Y., Nakazawa, M., Suzuki, K., Yamazaki, H. & Miyagawa, Y. Expression profiles of cytokines and chemokines in vitreous fluid in diabetic retinopathy and central retinal vein occlusion. *Japanese journal of ophthalmology* **55**, 256-263, doi:10.1007/s10384-011-0004-8 (2011).

91 Rangasamy, S., McGuire, P. G. & Das, A. Diabetic retinopathy and inflammation: novel therapeutic targets. *Middle East Afr J Ophthalmol* **19**, 52-59, doi:10.4103/0974-9233.92116 (2012).

92 Mohammad, G., Mairaj Siddiquei, M., Imtiaz Nawaz, M. & Abu El-Asrar, A. M. The ERK1/2 Inhibitor U0126 Attenuates Diabetes-Induced Upregulation of MMP-9 and Biomarkers of Inflammation in the Retina. *J Diabetes Res* **2013**, 658548, doi:10.1155/2013/658548 (2013).

93 Liu, Y., Biarnes Costa, M. & Gerhardinger, C. IL-1beta is upregulated in the diabetic retina and retinal vessels: cell-specific effect of high glucose and IL-1beta autostimulation. *PloS one* **7**, e36949, doi:10.1371/journal.pone.0036949 (2012).

94 Jiang, Y., Pagadala, J., Miller, D. & Steinle, J. J. Reduced insulin receptor signaling in retinal Muller cells cultured in high glucose. *Mol Vis* **19**, 804-811 (2013).

95 Mohamed, I. N. *et al.* Thioredoxin-interacting protein is required for endothelial NLRP3 inflammasome activation and cell death in a rat model of high-fat diet. *Diabetologia* **57**, 413-423, doi:10.1007/s00125-013-3101-z (2014).

96 Barber, A. J., Antonetti, D. A. & Gardner, T. W. Altered expression of retinal occludin and glial fibrillary acidic protein in experimental diabetes. The Penn State Retina Research Group. *Investigative ophthalmology & visual science* **41**, 3561-3568 (2000).

97 Watkins, W. M. *et al.* Hypoxia-induced expression of VEGF splice variants and protein in four retinal cell types. *Exp Eye Res* **116**, 240-246, doi:10.1016/j.exer.2013.09.014 (2013).

98 Bai, Y. *et al.* Muller cell-derived VEGF is a significant contributor to retinal neovascularization. *J Pathol* **219**, 446-454, doi:10.1002/path.2611 (2009).

99 Liu, X. *et al.* IL-1beta Upregulates IL-8 Production in Human Muller Cells Through Activation of the p38 MAPK and ERK1/2 Signaling Pathways. *Inflammation* **37**, 1486-1495, doi:10.1007/s10753-014-9874-5 (2014).

100 Yoshida, S., Sotozono, C., Ikeda, T. & Kinoshita, S. Interleukin-6 (IL-6) production by cytokine-stimulated human Muller cells. *Curr Eye Res* **22**, 341-347 (2001).

101 Zhang, W., Liu, H., Rojas, M., Caldwell, R. W. & Caldwell, R. B. Anti-inflammatory therapy for diabetic retinopathy. *Immunotherapy* **3**, 609-628, doi:10.2217/imt.11.24 (2011).

102 Chen, W., Jump, D. B., Grant, M. B., Esselman, W. J. & Busik, J. V. Dyslipidemia, but not hyperglycemia, induces inflammatory adhesion molecules in human retinal vascular endothelial cells. *Investigative ophthalmology & visual science* **44**, 5016-5022 (2003).

103 Falck, J. R. *et al.* 11,12-epoxyeicosatrienoic acid (11,12-EET): structural determinants for inhibition of TNF-alpha-induced VCAM-1 expression. *Bioorg Med Chem Lett* **13**, 4011-4014 (2003).

104 Chen, W., Esselman, W. J., Jump, D. B. & Busik, J. V. Anti-inflammatory effect of docosahexaenoic acid on cytokine-induced adhesion molecule expression in human retinal vascular endothelial cells. *Investigative ophthalmology & visual science* **46**, 4342-4347, doi:10.1167/iovs.05-0601 (2005).

105 Wiese, G., Barthel, S. R. & Dimitroff, C. J. Analysis of physiologic E-selectin-mediated leukocyte rolling on microvascular endothelium. *Journal of visualized experiments : JoVE*, doi:10.3791/1009 (2009).

106 Wyble, C. W. *et al.* TNF-alpha and IL-1 upregulate membrane-bound and soluble E-selectin through a common pathway. *The Journal of surgical research* **73**, 107-112, doi:10.1006/jsre.1997.5207 (1997).

107 Barreiro, O., Martin, P., Gonzalez-Amaro, R. & Sanchez-Madrid, F. Molecular cues guiding inflammatory responses. *Cardiovascular research* **86**, 174-182, doi:10.1093/cvr/cvq001 (2010).

108 Noda, K., Nakao, S., Ishida, S. & Ishibashi, T. Leukocyte adhesion molecules in diabetic retinopathy. *Journal of ophthalmology* **2012**, 279037, doi:10.1155/2012/279037 (2012).

109 Noda, K., Nakao, S., Ishida, S. & Ishibashi, T. Leukocyte adhesion molecules in diabetic retinopathy. *Journal of ophthalmology* **2012**, 279037, doi:10.1155/2012/279037 (2012).

110 Cantero, M., Parra, T. & Conejo, J. R. Increased hydrogen peroxide formation in polymorphonuclear leukocytes of IDDM patients. *Diabetes Care* **21**, 326-327 (1998).

111 Freedman, S. F. & Hatchell, D. L. Enhanced superoxide radical production by stimulated polymorphonuclear leukocytes in a cat model of diabetes. *Exp Eye Res* **55**, 767-773 (1992).

112 Karima, M. *et al.* Enhanced superoxide release and elevated protein kinase C activity in neutrophils from diabetic patients: association with periodontitis. *J Leukoc Biol* **78**, 862-870, doi:10.1189/jlb.1004583 (2005).

113 Joussen, A. M. *et al.* Leukocyte-mediated endothelial cell injury and death in the diabetic retina. *Am J Pathol* **158**, 147-152, doi:10.1016/S0002-9440(10)63952-1 (2001).

114 Chibber, R., Ben-Mahmud, B. M., Chibber, S. & Kohner, E. M. Leukocytes in diabetic retinopathy. *Curr Diabetes Rev* **3**, 3-14 (2007).

115 Kim, S. Y. *et al.* Neutrophils are associated with capillary closure in spontaneously diabetic monkey retinas. *Diabetes* **54**, 1534-1542 (2005).

116 Schroder, S., Palinski, W. & Schmid-Schonbein, G. W. Activated monocytes and granulocytes, capillary nonperfusion, and neovascularization in diabetic retinopathy. *Am J Pathol* **139**, 81-100 (1991).

117 Miyamoto, K. *et al.* Prevention of leukostasis and vascular leakage in streptozotocin-induced diabetic retinopathy via intercellular adhesion molecule-1 inhibition. *Proceedings of the National Academy of Sciences of the United States of America* **96**, 10836-10841 (1999).

118 Joussen, A. M. *et al.* Nonsteroidal anti-inflammatory drugs prevent early diabetic retinopathy via TNF-alpha suppression. *FASEB journal : official publication of the Federation of American Societies for Experimental Biology* **16**, 438-440, doi:10.1096/fj.01-0707fje (2002).

119 Joussen, A. M. *et al.* TNF-alpha mediated apoptosis plays an important role in the development of early diabetic retinopathy and long-term histopathological alterations. *Mol Vis* **15**, 1418-1428 (2009).

120 Miyamoto, K. *et al.* Vascular endothelial growth factor (VEGF)-induced retinal vascular permeability is mediated by intercellular adhesion molecule-1 (ICAM-1). *Am J Pathol* **156**, 1733-1739, doi:10.1016/S0002-9440(10)65044-4 (2000).

121 Joussen, A. M. *et al.* A central role for inflammation in the pathogenesis of diabetic retinopathy. *FASEB journal : official publication of the Federation of American Societies for Experimental Biology* **18**, 1450-1452, doi:10.1096/fj.03-1476fje (2004).

122 Du, Y., Sarthy, V. P. & Kern, T. S. Interaction between NO and COX pathways in retinal cells exposed to elevated glucose and retina of diabetic rats. *American*

journal of physiology. Regulatory, integrative and comparative physiology **287**, R735-741, doi:10.1152/ajpregu.00080.2003 (2004).

123 Ayalasomayajula, S. P. & Kompella, U. B. Celecoxib, a selective cyclooxygenase-2 inhibitor, inhibits retinal vascular endothelial growth factor expression and vascular leakage in a streptozotocin-induced diabetic rat model. *Eur J Pharmacol* **458**, 283-289 (2003).

124 Sun, W., Gerhardinger, C., Dagher, Z., Hoehn, T. & Lorenzi, M. Aspirin at low-intermediate concentrations protects retinal vessels in experimental diabetic retinopathy through non-platelet-mediated effects. *Diabetes* **54**, 3418-3426 (2005).

125 Effects of aspirin treatment on diabetic retinopathy. ETDRS report number 8. Early Treatment Diabetic Retinopathy Study Research Group. *Ophthalmology* **98**, 757-765 (1991).

126 Effect of aspirin alone and aspirin plus dipyridamole in early diabetic retinopathy. A multicenter randomized controlled clinical trial. The DAMAD Study Group. *Diabetes* **38**, 491-498 (1989).

127 Tamura, H. *et al.* Intravitreal injection of corticosteroid attenuates leukostasis and vascular leakage in experimental diabetic retina. *Investigative ophthalmology & visual science* **46**, 1440-1444, doi:10.1167/iovs.04-0905 (2005).

128 Sim, S. C. & Ingelman-Sundberg, M. The Human Cytochrome P450 (CYP) Allele Nomenclature website: a peer-reviewed database of CYP variants and their associated effects. *Hum Genomics* **4**, 278-281 (2010).

129 Nebert, D. W., Wikvall, K. & Miller, W. L. Human cytochromes P450 in health and disease. *Philos Trans R Soc Lond B Biol Sci* **368**, 20120431, doi:10.1098/rstb.2012.0431 (2013).

130 Spector, A. A. & Kim, H. Y. Cytochrome P450 epoxygenase pathway of polyunsaturated fatty acid metabolism. *Biochim Biophys Acta* **1851**, 356-365, doi:10.1016/j.bbalip.2014.07.020 (2015).

131 Lecomte, M., Paget, C., Ruggiero, D., Wiernsperger, N. & Lagarde, M. Docosahexaenoic acid is a major n-3 polyunsaturated fatty acid in bovine retinal microvessels. *Journal of neurochemistry* **66**, 2160-2167 (1996).

132 Hu, J. *et al.* Muller glia cells regulate Notch signaling and retinal angiogenesis via the generation of 19,20-dihydroxydocosapentaenoic acid. *The Journal of experimental medicine* **211**, 281-295, doi:10.1084/jem.20131494 (2014).

133 Norwood, S., Liao, J., Hammock, B. D. & Yang, G. Y. Epoxyeicosatrienoic acids and soluble epoxide hydrolase: potential therapeutic targets for inflammation and its induced carcinogenesis. *Am J Transl Res* **2**, 447-457 (2010).

134 Spector, A. A., Fang, X., Snyder, G. D. & Weintraub, N. L. Epoxyeicosatrienoic acids (EETs): metabolism and biochemical function. *Prog Lipid Res* **43**, 55-90 (2004).

135 Spector, A. A. & Norris, A. W. Action of epoxyeicosatrienoic acids on cellular function. *Am J Physiol Cell Physiol* **292**, C996-1012, doi:10.1152/ajpcell.00402.2006 (2007).

136 Newman, J. W., Morisseau, C., Harris, T. R. & Hammock, B. D. The soluble epoxide hydrolase encoded by EPXH2 is a bifunctional enzyme with novel lipid phosphate phosphatase activity. *Proceedings of the National Academy of Sciences of the United States of America* **100**, 1558-1563, doi:10.1073/pnas.0437724100 (2003).

137 Morisseau, C. & Hammock, B. D. Impact of soluble epoxide hydrolase and epoxyeicosanoids on human health. *Annu Rev Pharmacol Toxicol* **53**, 37-58, doi:10.1146/annurev-pharmtox-011112-140244 (2013).

138 Morisseau, C. *et al.* Naturally occurring monoepoxides of eicosapentaenoic acid and docosahexaenoic acid are bioactive antihyperalgesic lipids. *J Lipid Res* **51**, 3481-3490, doi:10.1194/jlr.M006007 (2010).

139 Li, P. L. & Campbell, W. B. Epoxyeicosatrienoic acids activate K+ channels in coronary smooth muscle through a guanine nucleotide binding protein. *Circulation research* **80**, 877-884 (1997).

140 Node, K. *et al.* Activation of Galpha s mediates induction of tissue-type plasminogen activator gene transcription by epoxyeicosatrienoic acids. *The Journal of biological chemistry* **276**, 15983-15989, doi:10.1074/jbc.M100439200 (2001).

141 Liu, X. *et al.* Functional screening for G protein-coupled receptor targets of 14,15-epoxyeicosatrienoic acid. *Prostaglandins & other lipid mediators*, doi:10.1016/j.prostaglandins.2016.09.002 (2016).

142 Ma, S. K. *et al.* Overexpression of G-protein-coupled receptor 40 enhances the mitogenic response to epoxyeicosatrienoic acids. *PloS one* **10**, e0113130, doi:10.1371/journal.pone.0113130 (2015).

143 Liu, Y. *et al.* The antiinflammatory effect of laminar flow: the role of PPARgamma, epoxyeicosatrienoic acids, and soluble epoxide hydrolase. *Proceedings of the National Academy of Sciences of the United States of America* **102**, 16747-16752, doi:10.1073/pnas.0508081102 (2005).

144 Wray, J. & Bishop-Bailey, D. Epoxygenases and peroxisome proliferator-activated receptors in mammalian vascular biology. *Exp Physiol* **93**, 148-154, doi:10.1113/expphysiol.2007.038612 (2008).

145 Ng, V. Y. *et al.* Cytochrome P450 eicosanoids are activators of peroxisome proliferator-activated receptor alpha. *Drug Metab Dispos* **35**, 1126-1134, doi:10.1124/dmd.106.013839 (2007).

146 Node, K. *et al.* Anti-inflammatory properties of cytochrome P450 epoxygenase-derived eicosanoids. *Science* **285**, 1276-1279 (1999).

147 Potente, M., Michaelis, U. R., Fisslthaler, B., Busse, R. & Fleming, I. Cytochrome P450 2C9-induced endothelial cell proliferation involves induction of mitogen-activated protein (MAP) kinase phosphatase-1, inhibition of the c-Jun N-terminal kinase, and up-regulation of cyclin D1. *The Journal of biological chemistry* **277**, 15671-15676, doi:10.1074/jbc.M110806200 (2002).

148 Wang, Y. *et al.* Arachidonic acid epoxygenase metabolites stimulate endothelial cell growth and angiogenesis via mitogen-activated protein kinase and phosphatidylinositol 3-kinase/Akt signaling pathways. *The Journal of pharmacology and experimental therapeutics* **314**, 522-532, doi:10.1124/jpet.105.083477 (2005).

149 Webler, A. C. *et al.* Epoxyeicosatrienoic acids are part of the VEGF-activated signaling cascade leading to angiogenesis. *Am J Physiol Cell Physiol* **295**, C1292-1301, doi:10.1152/ajpcell.00230.2008 (2008).

150 Campbell, W. B., Gebremedhin, D., Pratt, P. F. & Harder, D. R. Identification of epoxyeicosatrienoic acids as endothelium-derived hyperpolarizing factors. *Circulation research* **78**, 415-423 (1996).

151 Fleming, I. The factor in EDHF: Cytochrome P450 derived lipid mediators and vascular signaling. *Vascul Pharmacol*, doi:10.1016/j.vph.2016.03.001 (2016).

152 Ye, D. *et al.* Cytochrome p-450 epoxygenase metabolites of docosahexaenoate potently dilate coronary arterioles by activating large-conductance calcium-activated potassium channels. *The Journal of pharmacology and experimental therapeutics* **303**, 768-776 (2002).

153 Zhang, G., Kodani, S. & Hammock, B. D. Stabilized epoxygenated fatty acids regulate inflammation, pain, angiogenesis and cancer. *Prog Lipid Res* **53**, 108-123, doi:10.1016/j.plipres.2013.11.003 (2014).

154 Chen, D. *et al.* Pharmacokinetics and pharmacodynamics of AR9281, an inhibitor of soluble epoxide hydrolase, in single- and multiple-dose studies in healthy human subjects. *J Clin Pharmacol* **52**, 319-328, doi:10.1177/0091270010397049 (2012).

155 Panigrahy, D., Greene, E. R., Pozzi, A., Wang, D. W. & Zeldin, D. C. EET signaling in cancer. *Cancer Metastasis Rev* **30**, 525-540, doi:10.1007/s10555-011-9315-y (2011).

156 Fleming, I. Epoxyeicosatrienoic acids, cell signaling and angiogenesis. *Prostaglandins & other lipid mediators* **82**, 60-67, doi:10.1016/j.prostaglandins.2006.05.003 (2007).

157 Michaelis, U. R. & Fleming, I. From endothelium-derived hyperpolarizing factor (EDHF) to angiogenesis: Epoxyeicosatrienoic acids (EETs) and cell signaling. *Pharmacology & therapeutics* **111**, 584-595, doi:10.1016/j.pharmthera.2005.11.003 (2006).

158 Marden, N. Y., Fiala-Beer, E., Xiang, S. H. & Murray, M. Role of activator protein-1 in the down-regulation of the human CYP2J2 gene in hypoxia. *The Biochemical journal* **373**, 669-680, doi:10.1042/BJ20021903 (2003).

159 Michaelis, U. R. *et al.* Cytochrome P450 epoxygenases 2C8 and 2C9 are implicated in hypoxia-induced endothelial cell migration and angiogenesis. *Journal of cell science* **118**, 5489-5498, doi:10.1242/jcs.02674 (2005).

160 Yang, S., Wei, S., Pozzi, A. & Capdevila, J. H. The arachidonic acid epoxygenase is a component of the signaling mechanisms responsible for VEGF-stimulated angiogenesis. *Archives of biochemistry and biophysics* **489**, 82-91, doi:10.1016/j.abb.2009.05.006 (2009).

161 Fleming, I. Cytochrome p450 and vascular homeostasis. *Circulation research* **89**, 753-762 (2001).

162 Medhora, M. *et al.* Epoxygenase-driven angiogenesis in human lung microvascular endothelial cells. *American journal of physiology. Heart and circulatory physiology* **284**, H215-224, doi:10.1152/ajpheart.01118.2001 (2003).

163 Panigrahy, D. *et al.* Epoxyeicosanoids stimulate multiorgan metastasis and tumor dormancy escape in mice. *The Journal of clinical investigation* **122**, 178-191, doi:10.1172/JCI58128 (2012).

164 Zhang, G. *et al.* Epoxy metabolites of docosahexaenoic acid (DHA) inhibit angiogenesis, tumor growth, and metastasis. *Proceedings of the National Academy of Sciences of the United States of America* **110**, 6530-6535, doi:10.1073/pnas.1304321110 (2013).

165 Yanai, R. *et al.* Cytochrome P450-generated metabolites derived from omega-3 fatty acids attenuate neovascularization. *Proceedings of the National Academy of Sciences of the United States of America* **111**, 9603-9608, doi:10.1073/pnas.1401191111 (2014).

166 Shao, Z. *et al.* Cytochrome P450 2C8 omega3-long-chain polyunsaturated fatty acid metabolites increase mouse retinal pathologic neovascularization--brief report. *Arteriosclerosis, thrombosis, and vascular biology* **34**, 581-586, doi:10.1161/ATVBAHA.113.302927 (2014).

167 Zhang, T. *et al.* Drug transporter and cytochrome P450 mRNA expression in human ocular barriers: implications for ocular drug disposition. *Drug metabolism and disposition: the biological fate of chemicals* **36**, 1300-1307, doi:10.1124/dmd.108.021121 (2008).

168 Hu, J., Popp, R., Fleming, I. in *Joint Meeting of the Scandinavian and German Physiological Societies.* (Acta Physiologica).

169 Hu, J. *et al.* Muller glia cells regulate Notch signaling and retinal angiogenesis via the generation of 19,20-dihydroxydocosapentaenoic acid. *The Journal of experimental medicine* **211**, 281-295, doi:10.1084/jem.20131494 (2014).

170 Kozak, W., Aronoff, D. M., Boutaud, O. & Kozak, A. 11,12-epoxyeicosatrienoic acid attenuates synthesis of prostaglandin E2 in rat monocytes stimulated with lipopolysaccharide. *Exp Biol Med (Maywood)* **228**, 786-794 (2003).

171 Bystrom, J. *et al.* Endogenous epoxygenases are modulators of monocyte/macrophage activity. *PloS one* **6**, e26591, doi:10.1371/journal.pone.0026591 (2011).

172 Liu, W., Wang, B., Ding, H., Wang, D. W. & Zeng, H. A potential therapeutic effect of CYP2C8 overexpression on anti-TNF-alpha activity. *Int J Mol Med* **34**, 725-732, doi:10.3892/ijmm.2014.1844 (2014).

173 Moshal, K. S. *et al.* Cytochrome P450 (CYP) 2J2 gene transfection attenuates MMP-9 via inhibition of NF-kappabeta in hyperhomocysteinemia. *J Cell Physiol* **215**, 771-781, doi:10.1002/jcp.21356 (2008).

174 Dong, L. *et al.* Soluble Epoxide Hydrolase Inhibitor Suppresses the Expression of Triggering Receptor Expressed on Myeloid Cells-1 by Inhibiting NF-kB Activation in Murine Macrophage. *Inflammation*, doi:10.1007/s10753-016-0448-6 (2016).

175 Samokhvalov, V. *et al.* PPARgamma signaling is required for mediating EETs protective effects in neonatal cardiomyocytes exposed to LPS. *Front Pharmacol* **5**, 242, doi:10.3389/fphar.2014.00242 (2014).

176 Deng, Y. *et al.* Endothelial CYP epoxygenase overexpression and soluble epoxide hydrolase disruption attenuate acute vascular inflammatory responses in mice. *FASEB journal : official publication of the Federation of American Societies for Experimental Biology* **25**, 703-713, doi:10.1096/fj.10-171488 (2011).

177 Zhao, G. *et al.* Epoxyeicosatrienoic acids protect rat hearts against tumor necrosis factor-alpha-induced injury. *Journal of lipid research* **53**, 456-466, doi:10.1194/jlr.M017319 (2012).

178 Jia, J. *et al.* Sex- and isoform-specific mechanism of neuroprotection by transgenic expression of P450 epoxygenase in vascular endothelium. *Exp Neurol* **279**, 75-85, doi:10.1016/j.expneurol.2016.02.016 (2016).

179 Gilroy, D. W. *et al.* CYP450-derived oxylipins mediate inflammatory resolution. *Proceedings of the National Academy of Sciences of the United States of America* **113**, E3240-3249, doi:10.1073/pnas.1521453113 (2016).

180 Schmelzer, K. R. *et al.* Soluble epoxide hydrolase is a therapeutic target for acute inflammation. *Proc Natl Acad Sci U S A* **102**, 9772-9777, doi:10.1073/pnas.0503279102 (2005).

181 Lopez-Vicario, C. *et al.* Inhibition of soluble epoxide hydrolase modulates inflammation and autophagy in obese adipose tissue and liver: role for omega-3 epoxides. *Proceedings of the National Academy of Sciences of the United States of America* **112**, 536-541, doi:10.1073/pnas.1422590112 (2015).

182 Liu, Y. *et al.* Attenuation of cisplatin-induced renal injury by inhibition of soluble epoxide hydrolase involves nuclear factor kappaB signaling. *The Journal of pharmacology and experimental therapeutics* **341**, 725-734, doi:10.1124/jpet.111.191247 (2012).

183 Deng, Y. *et al.* Endothelial CYP epoxygenase overexpression and soluble epoxide hydrolase disruption attenuate acute vascular inflammatory responses in mice. *FASEB journal : official publication of the Federation of American Societies for Experimental Biology* **25**, 703-713, doi:10.1096/fj.10-171488 (2011).

184 Koerner, I. P. *et al.* Soluble epoxide hydrolase: regulation by estrogen and role in the inflammatory response to cerebral ischemia. *Front Biosci* **13**, 2833-2841 (2008).

185 Ma, W. J. *et al.* Epoxyeicosatrienoic acids attenuate cigarette smoke extract-induced interleukin-8 production in bronchial epithelial cells. *Prostaglandins Leukot Essent Fatty Acids* **94**, 13-19, doi:10.1016/j.plefa.2014.10.006 (2015).

186 Theken, K. N. *et al.* Activation of the acute inflammatory response alters cytochrome P450 expression and eicosanoid metabolism. *Drug Metab Dispos* **39**, 22-29, doi:10.1124/dmd.110.035287 (2011).

187 Aitken, A. E. & Morgan, E. T. Gene-specific effects of inflammatory cytokines on cytochrome P450 2C, 2B6 and 3A4 mRNA levels in human hepatocytes. *Drug Metab Dispos* **35**, 1687-1693, doi:10.1124/dmd.107.015511 (2007).

188 Rodriguez, M. & Clare-Salzler, M. Eicosanoid imbalance in the NOD mouse is related to a dysregulation in soluble epoxide hydrolase and 15-PGDH expression. *Ann N Y Acad Sci* **1079**, 130-134, doi:10.1196/annals.1375.019 (2006).

189 Sanders, W. G., Morisseau, C., Hammock, B. D., Cheung, A. K. & Terry, C. M. Soluble epoxide hydrolase expression in a porcine model of arteriovenous graft stenosis and anti-inflammatory effects of a soluble epoxide hydrolase inhibitor.

Am J Physiol Cell Physiol **303**, C278-290, doi:10.1152/ajpcell.00386.2011 (2012).

190 Brazionis, L., Rowley, K., Sr., Itsiopoulos, C., Harper, C. A. & O'Dea, K. Homocysteine and diabetic retinopathy. *Diabetes Care* **31**, 50-56, doi:10.2337/dc07-0632 (2008).

191 Guthikonda, S. & Haynes, W. G. Homocysteine: role and implications in atherosclerosis. *Curr Atheroscler Rep* **8**, 100-106 (2006).

192 Chorvathova, V. & Ondreicka, R. The fatty acid composition of the tissues of streptozotocin-diabetic rats. *Physiol Bohemoslov* **32**, 466-475 (1983).

193 Tikhonenko, M. *et al.* Remodeling of retinal Fatty acids in an animal model of diabetes: a decrease in long-chain polyunsaturated fatty acids is associated with a decrease in fatty acid elongases Elovl2 and Elovl4. *Diabetes* **59**, 219-227, doi:10.2337/db09-0728 (2010).

194 Korani, M. *et al.* Distribution of fatty acids in adipose tissue of patients with type 2 diabetes. *Clin Lab* **58**, 457-464 (2012).

195 Chen, G. *et al.* CYP2J2 overexpression attenuates nonalcoholic fatty liver disease induced by high-fat diet in mice. *Am J Physiol Endocrinol Metab* **308**, E97-E110, doi:10.1152/ajpendo.00366.2014 (2015).

196 Li, R. *et al.* CYP2J2 attenuates metabolic dysfunction in diabetic mice by reducing hepatic inflammation via the PPARgamma. *Am J Physiol Endocrinol Metab* **308**, E270-282, doi:10.1152/ajpendo.00118.2014 (2015).

197 Li, D. *et al.* Inhibition of soluble epoxide hydrolase alleviated atherosclerosis by reducing monocyte infiltration in Ldlr(-/-) mice. *J Mol Cell Cardiol* **98**, 128-137, doi:10.1016/j.yjmcc.2016.08.001 (2016).

198 Jouihan, S. A. *et al.* Role of soluble epoxide hydrolase in exacerbation of stroke by streptozotocin-induced type 1 diabetes mellitus. *Journal of cerebral blood flow and metabolism : official journal of the International Society of Cerebral Blood Flow and Metabolism*, doi:10.1038/jcbfm.2013.130 (2013).

199 Zhang, L. N. *et al.* Inhibition of soluble epoxide hydrolase attenuated atherosclerosis, abdominal aortic aneurysm formation, and dyslipidemia. *Arteriosclerosis, thrombosis, and vascular biology* **29**, 1265-1270, doi:10.1161/ATVBAHA.109.186064 (2009).

200 Elmarakby, A. A. *et al.* Deletion of soluble epoxide hydrolase gene improves renal endothelial function and reduces renal inflammation and injury in streptozotocin-induced type 1 diabetes. *American journal of physiology. Regulatory, integrative and comparative physiology* **301**, R1307-1317, doi:10.1152/ajpregu.00759.2010 (2011).

201 Dey, A. *et al.* Altered kidney CYP2C and cyclooxygenase-2 levels are associated with obesity-related albuminuria. *Obesity research* **12**, 1278-1289, doi:10.1038/oby.2004.162 (2004).

202 Jouihan, S. A. *et al.* Role of soluble epoxide hydrolase in exacerbation of stroke by streptozotocin-induced type 1 diabetes mellitus. *Journal of cerebral blood flow and metabolism : official journal of the International Society of Cerebral Blood Flow and Metabolism* **33**, 1650-1656, doi:10.1038/jcbfm.2013.130 (2013).

203 Thum, T. & Borlak, J. Mechanistic role of cytochrome P450 monooxygenases in oxidized low-density lipoprotein-induced vascular injury: therapy through LOX-1 receptor antagonism? *Circulation research* **94**, e1-13, doi:10.1161/01.RES.0000110081.03480.E9 (2004).

204 Tsai, S. H., Hein, T. W., Kuo, L. & Yang, V. C. High glucose impairs EDHF-mediated dilation of coronary arterioles via reduced cytochrome P450 activity. *Microvascular research* **82**, 356-363, doi:10.1016/j.mvr.2011.09.008 (2011).

205 Zhao, X. *et al.* Decreased epoxygenase and increased epoxide hydrolase expression in the mesenteric artery of obese Zucker rats. *American journal of physiology. Regulatory, integrative and comparative physiology* **288**, R188-196, doi:10.1152/ajpregu.00018.2004 (2005).

206 Bettaieb, A. *et al.* Soluble epoxide hydrolase deficiency or inhibition attenuates diet-induced endoplasmic reticulum stress in liver and adipose tissue. *The Journal of biological chemistry* **288**, 14189-14199, doi:10.1074/jbc.M113.458414 (2013).

207 Zhang, D. *et al.* Homocysteine upregulates soluble epoxide hydrolase in vascular endothelium in vitro and in vivo. *Circulation research* **110**, 808-817, doi:10.1161/CIRCRESAHA.111.259325 (2012).

208 Wang, M. H. *et al.* Downregulation of renal CYP-derived eicosanoid synthesis in rats with diet-induced hypertension. *Hypertension* **42**, 594-599, doi:10.1161/01.HYP.0000090123.55365.BA (2003).

209 Dey, A. *et al.* Rofecoxib decreases renal injury in obese Zucker rats. *Clinical science* **107**, 561-570, doi:10.1042/CS20040125 (2004).

210 Dey, A. *et al.* Altered kidney CYP2C and cyclooxygenase-2 levels are associated with obesity-related albuminuria. *Obesity research* **12**, 1278-1289, doi:10.1038/oby.2004.162 (2004).

211 Imig, J. D. Eicosanoids and renal vascular function in diseases. *Clinical science* **111**, 21-34, doi:10.1042/CS20050251 (2006).

212 Sindhu, R. K. *et al.* Differential regulation of hepatic cytochrome P450 monooxygenases in streptozotocin-induced diabetic rats. *Free radical research* **40**, 921-928, doi:10.1080/10715760600801272 (2006).

213 Luria, A. *et al.* Soluble epoxide hydrolase deficiency alters pancreatic islet size and improves glucose homeostasis in a model of insulin resistance. *Proceedings of the National Academy of Sciences of the United States of America* **108**, 9038-9043, doi:10.1073/pnas.1103482108 (2011).

214 Chen, G. *et al.* Genetic disruption of soluble epoxide hydrolase is protective against streptozotocin-induced diabetic nephropathy. *American journal of physiology. Endocrinology and metabolism* **303**, E563-575, doi:10.1152/ajpendo.00591.2011 (2012).

215 Xu, X. *et al.* Increased CYP2J3 expression reduces insulin resistance in fructose-treated rats and db/db mice. *Diabetes* **59**, 997-1005, doi:10.2337/db09-1241 (2010).

216 Elmarakby, A., Katary, M., Mohamed, I. & El-Remessy, A. in *American Heart Association.* AP238.

217 Chadderdon, S. M. *et al.* Vasoconstrictor eicosanoids and impaired microvascular function in inactive and insulin-resistant primates. *Int J Obes (Lond)* **40**, 1600-1603, doi:10.1038/ijo.2016.117 (2016).

218 Schafer, A. *et al.* The Epoxyeicosatrienoic Acid Pathway Enhances Hepatic Insulin Signaling and is Repressed in Insulin-Resistant Mouse Liver. *Mol Cell Proteomics* **14**, 2764-2774, doi:10.1074/mcp.M115.049064 (2015).

219 Ramirez, C. E. *et al.* Arg287Gln variant of EPHX2 and epoxyeicosatrienoic acids are associated with insulin sensitivity in humans. *Prostaglandins & other lipid mediators* **113-115**, 38-44, doi:10.1016/j.prostaglandins.2014.08.001 (2014).

220 Wang, C. P. *et al.* Genetic variation in the G-50T polymorphism of the cytochrome P450 epoxygenase CYP2J2 gene and the risk of younger onset type 2 diabetes among Chinese population: potential interaction with body mass index and family history. *Exp Clin Endocrinol Diabetes* **118**, 346-352, doi:10.1055/s-0029-1243604 (2010).

221 Ohtoshi, K. *et al.* Association of soluble epoxide hydrolase gene polymorphism with insulin resistance in type 2 diabetic patients. *Biochem Biophys Res Commun* **331**, 347-350, doi:10.1016/j.bbrc.2005.03.171 (2005).

222 Arete, T. (2009).

223 GlaxoSmithKline. (2014).

224 Lazaar, A. L. *et al.* Pharmacokinetics, pharmacodynamics and adverse event profile of GSK2256294, a novel soluble epoxide hydrolase inhibitor. *British journal of clinical pharmacology*, doi:10.1111/bcp.12855 (2015).

225 Chen, D. *et al.* Pharmacokinetics and pharmacodynamics of AR9281, an inhibitor of soluble epoxide hydrolase, in single- and multiple-dose studies in healthy human subjects. *J Clin Pharmacol* **52**, 319-328, doi:10.1177/0091270010397049 (2012).

226 Shen, H. C. & Hammock, B. D. Discovery of inhibitors of soluble epoxide hydrolase: a target with multiple potential therapeutic indications. *J Med Chem* **55**, 1789-1808, doi:10.1021/jm201468j (2012).

227 Hicks, D. & Courtois, Y. The growth and behaviour of rat retinal Muller cells in vitro. 1. An improved method for isolation and culture. *Experimental eye research* **51**, 119-129 (1990).

228 Guo, Y. *et al.* Multi-perspective quality control of Illumina exome sequencing data using QC3. *Genomics* **103**, 323-328, doi:10.1016/j.ygeno.2014.03.006 (2014).

229 Guo, Y., Zhao, S., Ye, F., Sheng, Q. & Shyr, Y. MultiRankSeq: multiperspective approach for RNAseq differential expression analysis and quality control. *Biomed Res Int* **2014**, 248090, doi:10.1155/2014/248090 (2014).

230 Chan, J. Y., Cole, E. & Hanna, A. K. Diabetic nephropathy and proliferative retinopathy with normal glucose tolerance. *Diabetes Care* **8**, 385-390 (1985).

231 Harrower, A. D. & Clarke, B. F. Diabetic retinopathy with normal glucose tolerance. *Br J Ophthalmol* **60**, 459-463 (1976).

232 Hutton, W. L., Snyder, W. B., Vaiser, A. & Siperstein, M. D. Retinal microangiopathy without associated glucose intolerance. *Trans Am Acad Ophthalmol Otolaryngol* **76**, 968-980 (1972).

233 Amin, A. M. *et al.* The impact of bariatric surgery on retinopathy in patients with type 2 diabetes: a retrospective cohort study. *Surg Obes Relat Dis* **12**, 606-612, doi:10.1016/j.soard.2015.08.508 (2016).

234 Boden, G. Fatty acid-induced inflammation and insulin resistance in skeletal muscle and liver. *Current diabetes reports* **6**, 177-181 (2006).

235 Decsi, T. *et al.* Low contribution of n-3 polyunsaturated fatty acids to plasma and erythrocyte membrane lipids in diabetic young adults. *Prostaglandins, leukotrienes, and essential fatty acids* **76**, 159-164, doi:10.1016/j.plefa.2006.12.003 (2007).

236 Hegde, K. R. & Varma, S. D. Electron impact mass spectroscopic studies on mouse retinal fatty acids: effect of diabetes. *Ophthalmic research* **42**, 9-14, doi:10.1159/000219679 (2009).

237 Chen, W., Jump, D. B., Grant, M. B., Esselman, W. J. & Busik, J. V. Dyslipidemia, but not hyperglycemia, induces inflammatory adhesion molecules in human retinal vascular endothelial cells. *Investigative ophthalmology & visual science* **44**, 5016-5022 (2003).

238 Konkel, A. & Schunck, W. H. Role of cytochrome P450 enzymes in the bioactivation of polyunsaturated fatty acids. *Biochim Biophys Acta* **1814**, 210-222, doi:10.1016/j.bbapap.2010.09.009 (2011).

239 Veenstra, M. & Ransohoff, R. M. Chemokine receptor CXCR2: physiology regulator and neuroinflammation controller? *J Neuroimmunol* **246**, 1-9, doi:10.1016/j.jneuroim.2012.02.016 (2012).

240 Petrovic, M. G., Korosec, P., Kosnik, M. & Hawlina, M. Vitreous levels of interleukin-8 in patients with proliferative diabetic retinopathy. *Am J Ophthalmol* **143**, 175-176, doi:10.1016/j.ajo.2006.07.032 (2007).

241 Koskela, U. E., Kuusisto, S. M., Nissinen, A. E., Savolainen, M. J. & Liinamaa, M. J. High vitreous concentration of IL-6 and IL-8, but not of adhesion molecules in relation to plasma concentrations in proliferative diabetic retinopathy. *Ophthalmic research* **49**, 108-114, doi:10.1159/000342977 (2013).

242 Bromberg-White, J. L. *et al.* Identification of VEGF-independent cytokines in proliferative diabetic retinopathy vitreous. *Investigative ophthalmology & visual science* **54**, 6472-6480, doi:10.1167/iovs.13-12518 (2013).

243 Suarez, S. *et al.* Modulation of VEGF-Induced Retinal Vascular Permeability by Peroxisome Proliferator-Activated Receptor-beta/delta. *Investigative ophthalmology & visual science* **55**, 8232-8240, doi:10.1167/iovs.14-14217 (2014).

244 Capozzi, M. E., McCollum, G. W., Savage, S. R. & Penn, J. S. Peroxisome Proliferator-Activated Receptor-beta/delta Regulates Angiogenic Cell Behaviors and Oxygen-Induced Retinopathy. *Investigative ophthalmology & visual science* **54**, 4197-4207, doi:10.1167/iovs.13-11608 (2013).

245 Babapoor-Farrokhran, S. *et al.* Angiopoietin-like 4 is a potent angiogenic factor and a novel therapeutic target for patients with proliferative diabetic retinopathy. *Proceedings of the National Academy of Sciences of the United States of America* **112**, E3030-E3039, doi:10.1073/pnas.1423765112 (2015).

246 Jee, K. J., Puchner, B., Hassan, S. J., Dent, M. & Sodhi, A. Correlation of Serum Levels of Angiopoietin-like 4 with Diabetic Retinopathy. *Investigative ophthalmology & visual science* **56** (2015).

247 Mysona, B. A. *et al.* Imbalance of the nerve growth factor and its precursor as a potential biomarker for diabetic retinopathy. *Biomed Res Int* **2015**, 571456, doi:10.1155/2015/571456 (2015).

248 Mysona, B. A., Shanab, A. Y., Elshaer, S. L. & El-Remessy, A. B. Nerve growth factor in diabetic retinopathy: beyond neurons. *Expert Rev Ophthalmol* **9**, 99-107, doi:10.1586/17469899.2014.903157 (2014).

249 Park, K. S. *et al.* Serum and tear levels of nerve growth factor in diabetic retinopathy patients. *Am J Ophthalmol* **145**, 432-437, doi:10.1016/j.ajo.2007.11.011 (2008).

250 Matragoon, S. *et al.* Electroporation-mediated gene delivery of cleavage-resistant pro-nerve growth factor causes retinal neuro- and vascular degeneration. *Mol Vis* **18**, 2993-3003 (2012).

251 Sennlaub, F. *et al.* Cyclooxygenase-2 in human and experimental ischemic proliferative retinopathy. *Circulation* **108**, 198-204, doi:10.1161/01.CIR.0000080735.93327.00 (2003).

252 Yanni, S. E., Clark, M. L., Yang, R., Bingaman, D. P. & Penn, J. S. The effects of nepafenac and amfenac on retinal angiogenesis. *Brain Res Bull* **81**, 310-319, doi:10.1016/j.brainresbull.2009.10.018 (2010).

253 Schoenberger, S. D. *et al.* Increased prostaglandin E2 (PGE2) levels in proliferative diabetic retinopathy, and correlation with VEGF and inflammatory cytokines. *Investigative ophthalmology & visual science* **53**, 5906-5911, doi:10.1167/iovs.12-10410 (2012).

254 Yanni, S. E., Barnett, J. M., Clark, M. L. & Penn, J. S. The role of PGE2 receptor EP4 in pathologic ocular angiogenesis. *Investigative ophthalmology & visual science* **50**, 5479-5486, doi:10.1167/iovs.09-3652 (2009).

255 Joyal, J. S. *et al.* Retinal lipid and glucose metabolism dictates angiogenesis through the lipid sensor Ffar1 (vol 22, pg 439, 2016). *Nat Med* **22**, 692-692, doi:10.1038/nm0616-692a (2016).

256 Madonna, R. *et al.* High glucose-induced hyperosmolarity contributes to COX-2 expression and angiogenesis: implications for diabetic retinopathy. *Cardiovasc Diabetol* **15**, 18, doi:10.1186/s12933-016-0342-4 (2016).

257 Devi, T. S. *et al.* TXNIP links innate host defense mechanisms to oxidative stress and inflammation in retinal Muller glia under chronic hyperglycemia: implications for diabetic retinopathy. *Exp Diabetes Res* **2012**, 438238, doi:10.1155/2012/438238 (2012).

258 Li, J. *et al.* Calcium mediates high glucose-induced HIF-1alpha and VEGF expression in cultured rat retinal Muller cells through CaMKII-CREB pathway. *Acta Pharmacol Sin* **33**, 1030-1036, doi:10.1038/aps.2012.61 (2012).

259 Mu, H., Zhang, X. M., Liu, J. J., Dong, L. & Feng, Z. L. Effect of high glucose concentration on VEGF and PEDF expression in cultured retinal Muller cells. *Mol Biol Rep* **36**, 2147-2151, doi:10.1007/s11033-008-9428-8 (2009).

260 Vellanki, S., Ferrigno, A., Alanis, Y., Betts-Obregon, B. S. & Tsin, A. T. High Glucose and Glucose Deprivation Modulate Muller Cell Viability and VEGF Secretion. *Int J Ophthalmol Eye Sci* **4**, 178-183 (2016).

261 Zhong, Y. *et al.* Activation of endoplasmic reticulum stress by hyperglycemia is essential for Muller cell-derived inflammatory cytokine production in diabetes. *Diabetes* **61**, 492-504, doi:10.2337/db11-0315 (2012).

262 Zong, H. *et al.* Hyperglycaemia-induced pro-inflammatory responses by retinal Muller glia are regulated by the receptor for advanced glycation end-products (RAGE). *Diabetologia* **53**, 2656-2666, doi:10.1007/s00125-010-1900-z (2010).

263 He, J. *et al.* Blockade of vascular endothelial growth factor receptor 1 prevents inflammation and vascular leakage in diabetic retinopathy. *Journal of ophthalmology* **2015**, 605946, doi:10.1155/2015/605946 (2015).

264 Goczalik, I. *et al.* Expression of CXCL8, CXCR1, and CXCR2 in neurons and glial cells of the human and rabbit retina. *Investigative ophthalmology & visual science* **49**, 4578-4589, doi:10.1167/iovs.08-1887 (2008).

265 Koleva-Georgieva, D. N., Sivkova, N. P. & Terzieva, D. Serum inflammatory cytokines IL-1beta, IL-6, TNF-alpha and VEGF have influence on the development of diabetic retinopathy. *Folia Med (Plovdiv)* **53**, 44-50 (2011).

266 Huang, H. *et al.* TNFalpha is required for late BRB breakdown in diabetic retinopathy, and its inhibition prevents leukostasis and protects vessels and neurons from apoptosis. *Investigative ophthalmology & visual science* **52**, 1336-1344, doi:10.1167/iovs.10-5768 (2011).

267 Li, J., Wang, J. J. & Zhang, S. X. Preconditioning with endoplasmic reticulum stress mitigates retinal endothelial inflammation via activation of X-box binding protein 1. *J Biol Chem* **286**, 4912-4921, doi:10.1074/jbc.M110.199729 (2011).

268 Abu El-Asrar, A. M., Soliman, R. T., Al-Amro, S. A. & Al-Shammary, F. J. Serum factor from diabetic patients with or without retinopathy stimulates superoxide anion production by normal polymorphonuclear leukocytes. *Doc Ophthalmol* **91**, 1-8 (1995).

269 El-Asrar, A. M. Role of inflammation in the pathogenesis of diabetic retinopathy. *Middle East Afr J Ophthalmol* **19**, 70-74, doi:10.4103/0974-9233.92118 (2012).

270 Adamis, A. P. & Berman, A. J. Immunological mechanisms in the pathogenesis of diabetic retinopathy. *Semin Immunopathol* **30**, 65-84, doi:10.1007/s00281-008-0111-x (2008).

271 Naveh-Floman, N., Weissman, C. & Belkin, M. Arachidonic acid metabolism by retinas of rats with streptozotocin-induced diabetes. *Current eye research* **3**, 1135-1139 (1984).

272 Johnson, E. I., Dunlop, M. E. & Larkins, R. G. Increased vasodilatory prostaglandin production in the diabetic rat retinal vasculature. *Current eye research* **18**, 79-82 (1999).

273 Zheng, L., Howell, S. J., Hatala, D. A., Huang, K. & Kern, T. S. Salicylate-based anti-inflammatory drugs inhibit the early lesion of diabetic retinopathy. *Diabetes* **56**, 337-345, doi:10.2337/db06-0789 (2007).

274 Talahalli, R., Zarini, S., Sheibani, N., Murphy, R. C. & Gubitosi-Klug, R. A. Increased synthesis of leukotrienes in the mouse model of diabetic retinopathy. *Investigative ophthalmology & visual science* **51**, 1699-1708, doi:10.1167/iovs.09-3557 (2010).

275 Al-Shabrawey, M. *et al.* Increased expression and activity of 12-lipoxygenase in oxygen-induced ischemic retinopathy and proliferative diabetic retinopathy: implications in retinal neovascularization. *Diabetes* **60**, 614-624, doi:10.2337/db10-0008 (2011).

276 Othman, A. *et al.* 12/15-Lipoxygenase-derived lipid metabolites induce retinal endothelial cell barrier dysfunction: contribution of NADPH oxidase. *PLoS One* **8**, e57254, doi:10.1371/journal.pone.0057254 (2013).

277 Ibrahim, A. S. *et al.* A lipidomic screen of hyperglycemia-treated HRECs links 12/15-Lipoxygenase to microvascular dysfunction during diabetic retinopathy via NADPH oxidase. *J Lipid Res* **56**, 599-611, doi:10.1194/jlr.M056069 (2015).

278 Jiang, J. X. *et al.* EETs Attenuate Ox-LDL-Induced LTB4 Production and Activity by Inhibiting p38 MAPK Phosphorylation and 5-LO/BLT1 Receptor Expression in Rat Pulmonary Arterial Endothelial Cells. *PLoS One* **10**, e0128278, doi:10.1371/journal.pone.0128278 (2015).

279 Elmarakby, A. A., Quigley, J. E., Pollock, D. M. & Imig, J. D. Tumor necrosis factor alpha blockade increases renal Cyp2c23 expression and slows the progression of renal damage in salt-sensitive hypertension. *Hypertension* **47**, 557-562, doi:10.1161/01.HYP.0000198545.01860.90 (2006).

280 Askari, A. A. *et al.* Basal and inducible anti-inflammatory epoxygenase activity in endothelial cells. *Biochemical and biophysical research communications* **446**, 633-637, doi:10.1016/j.bbrc.2014.03.020 (2014).

281 Liu, Y. *et al.* Epoxyeicosanoid Signaling Provides Multi-target Protective Effects on Neurovascular Unit in Rats After Focal Ischemia. *J Mol Neurosci* **58**, 254-265, doi:10.1007/s12031-015-0670-y (2016).

282 Olearczyk, J. J. *et al.* Substituted adamantyl-urea inhibitors of the soluble epoxide hydrolase dilate mesenteric resistance vessels. *J Pharmacol Exp Ther* **318**, 1307-1314, doi:10.1124/jpet.106.103556 (2006).

283 Capozzi, M. E., McCollum, G. W. & Penn, J. S. The role of cytochrome P450 epoxygenases in retinal angiogenesis. *Investigative ophthalmology & visual science* **55**, 4253-4260, doi:10.1167/iovs.14-14216 (2014).

284 Chen, W., Jump, D. B., Esselman, W. J. & Busik, J. V. Inhibition of cytokine signaling in human retinal endothelial cells through modification of caveolae/lipid rafts by docosahexaenoic acid. *Invest Ophthalmol Vis Sci* **48**, 18-26, doi:10.1167/iovs.06-0619 (2007).

285 Opreanu, M. *et al.* Inhibition of cytokine signaling in human retinal endothelial cells through downregulation of sphingomyelinases by docosahexaenoic acid. *Invest Ophthalmol Vis Sci* **51**, 3253-3263, doi:10.1167/iovs.09-4731 (2010).

286 Capdevila, J. H., Falck, J. R. & Harris, R. C. Cytochrome P450 and arachidonic acid bioactivation. Molecular and functional properties of the arachidonate monooxygenase. *J Lipid Res* **41**, 163-181 (2000).

287 Fang, X. *et al.* Pathways of epoxyeicosatrienoic acid metabolism in endothelial cells. Implications for the vascular effects of soluble epoxide hydrolase inhibition. *J Biol Chem* **276**, 14867-14874, doi:10.1074/jbc.M011761200 (2001).

288 Simpkins, A. N. *et al.* Soluble epoxide hydrolase inhibition modulates vascular remodeling. *Am J Physiol Heart Circ Physiol* **298**, H795-806, doi:10.1152/ajpheart.00543.2009 (2010).

289 Ai, D. *et al.* Angiotensin II up-regulates soluble epoxide hydrolase in vascular endothelium in vitro and in vivo. *Proc Natl Acad Sci U S A* **104**, 9018-9023, doi:10.1073/pnas.0703229104 (2007).

290 Enayetallah, A. E., French, R. A., Thibodeau, M. S. & Grant, D. F. Distribution of soluble epoxide hydrolase and of cytochrome P450 2C8, 2C9, and 2J2 in human tissues. *J Histochem Cytochem* **52**, 447-454 (2004).

291 De Taeye, B. M. *et al.* Expression and regulation of soluble epoxide hydrolase in adipose tissue. *Obesity (Silver Spring)* **18**, 489-498, doi:10.1038/oby.2009.227 (2010).

292 Tanaka, H. *et al.* Transcriptional regulation of the human soluble epoxide hydrolase gene EPHX2. *Biochim Biophys Acta* **1779**, 17-27, doi:10.1016/j.bbagrm.2007.11.005 (2008).

293 Ahmad, M., Theofanidis, P. & Medford, R. M. Role of activating protein-1 in the regulation of the vascular cell adhesion molecule-1 gene expression by tumor necrosis factor-alpha. *J Biol Chem* **273**, 4616-4621 (1998).

294 Fang, X. *et al.* Activation of peroxisome proliferator-activated receptor alpha by substituted urea-derived soluble epoxide hydrolase inhibitors. *J Pharmacol Exp Ther* **314**, 260-270, doi:10.1124/jpet.105.085605 (2005).

295 Marx, N., Sukhova, G. K., Collins, T., Libby, P. & Plutzky, J. PPARalpha activators inhibit cytokine-induced vascular cell adhesion molecule-1 expression in human endothelial cells. *Circulation* **99**, 3125-3131 (1999).

296 Demircan, N., Safran, B. G., Soylu, M., Ozcan, A. A. & Sizmaz, S. Determination of vitreous interleukin-1 (IL-1) and tumour necrosis factor (TNF) levels in proliferative diabetic retinopathy. *Eye (Lond)* **20**, 1366-1369, doi:10.1038/sj.eye.6702138 (2006).

297 Abiko, T. *et al.* Characterization of retinal leukostasis and hemodynamics in insulin resistance and diabetes: role of oxidants and protein kinase-C activation. *Diabetes* **52**, 829-837 (2003).

298 Barouch, F. C. *et al.* Integrin-mediated neutrophil adhesion and retinal leukostasis in diabetes. *Invest Ophthalmol Vis Sci* **41**, 1153-1158 (2000).

299 Patel, K. D. Mechanisms of selective leukocyte recruitment from whole blood on cytokine-activated endothelial cells under flow conditions. *J Immunol* **162**, 6209-6216 (1999).

300 Gustavsson, C. *et al.* Vascular cellular adhesion molecule-1 (VCAM-1) expression in mice retinal vessels is affected by both hyperglycemia and hyperlipidemia. *PLoS One* **5**, e12699, doi:10.1371/journal.pone.0012699 (2010).

301 Dai, M. *et al.* Epoxyeicosatrienoic acids regulate macrophage polarization and prevent LPS-induced cardiac dysfunction. *J Cell Physiol* **230**, 2108-2119, doi:10.1002/jcp.24939 (2015).

302 Fleming, I. DiscrEET regulators of homeostasis: epoxyeicosatrienoic acids, cytochrome P450 epoxygenases and vascular inflammation. *Trends Pharmacol Sci* **28**, 448-452, doi:10.1016/j.tips.2007.08.002 (2007).

303 Morisseau, C. *et al.* Structural refinement of inhibitors of urea-based soluble epoxide hydrolases. *Biochem Pharmacol* **63**, 1599-1608 (2002).

304 Wray, J. A. *et al.* The epoxygenases CYP2J2 activates the nuclear receptor PPARalpha in vitro and in vivo. *PLoS One* **4**, e7421, doi:10.1371/journal.pone.0007421 (2009).

305 Ding, Y. *et al.* The biological actions of 11,12-epoxyeicosatrienoic acid in endothelial cells are specific to the R/S-enantiomer and require the G(s) protein. *J Pharmacol Exp Ther* **350**, 14-21, doi:10.1124/jpet.114.214254 (2014).

306 Steinkuller, P. G. *et al.* Childhood blindness. *Journal of AAPOS : the official publication of the American Association for Pediatric Ophthalmology and Strabismus / American Association for Pediatric Ophthalmology and Strabismus* **3**, 26-32 (1999).

307 American Diabetes, A. Standards of medical care in diabetes--2012. *Diabetes care* **35 Suppl 1**, S11-63, doi:10.2337/dc12-s011 (2012).

308 Rahmani, B. *et al.* The cause-specific prevalence of visual impairment in an urban population. The Baltimore Eye Survey. *Ophthalmology* **103**, 1721-1726 (1996).

309 Penn, J. S. *et al.* Vascular endothelial growth factor in eye disease. *Progress in retinal and eye research* **27**, 331-371, doi:10.1016/j.preteyeres.2008.05.001 (2008).

310 Wilkinson-Berka, J. L., Alousis, N. S., Kelly, D. J. & Gilbert, R. E. COX-2 inhibition and retinal angiogenesis in a mouse model of retinopathy of prematurity. *Investigative ophthalmology & visual science* **44**, 974-979 (2003).

311 Beauchamp, M. H. *et al.* Role of thromboxane in retinal microvascular degeneration in oxygen-induced retinopathy. *Journal of applied physiology* **90**, 2279-2288 (2001).

312 Michaelis, U. R., Xia, N., Barbosa-Sicard, E., Falck, J. R. & Fleming, I. Role of cytochrome P450 2C epoxygenases in hypoxia-induced cell migration and angiogenesis in retinal endothelial cells. *Investigative ophthalmology & visual science* **49**, 1242-1247, doi:10.1167/iovs.07-1087 (2008).

313 Hu, J. *et al.* Muller glia cells regulate Notch signaling and retinal angiogenesis via the generation of 19,20-dihydroxydocosapentaenoic acid. *The Journal of experimental medicine*, doi:10.1084/jem.20131494 (2014).

314 Munzenmaier, D. H. & Harder, D. R. Cerebral microvascular endothelial cell tube formation: role of astrocytic epoxyeicosatrienoic acid release. *American journal of physiology. Heart and circulatory physiology* **278**, H1163-1167 (2000).

315 Zhang, C. & Harder, D. R. Cerebral capillary endothelial cell mitogenesis and morphogenesis induced by astrocytic epoxyeicosatrienoic Acid. *Stroke; a journal of cerebral circulation* **33**, 2957-2964 (2002).

316 Sakuta, H. & Yoneda, I. Inhibition by SKF 525A and quinacrine of endogenous glibenclamide-sensitive K+ channels in follicle-enclosed Xenopus oocytes. *European journal of pharmacology* **252**, 117-121 (1994).

317 Holla, V. R., Makita, K., Zaphiropoulos, P. G. & Capdevila, J. H. The kidney cytochrome P-450 2C23 arachidonic acid epoxygenase is upregulated during dietary salt loading. *The Journal of clinical investigation* **104**, 751-760, doi:10.1172/JCI7013 (1999).

318 Wong, P. Y., Lai, P. S. & Falck, J. R. Mechanism and signal transduction of 14 (R), 15 (S)-epoxyeicosatrienoic acid (14,15-EET) binding in guinea pig monocytes. *Prostaglandins & other lipid mediators* **62**, 321-333 (2000).

319 Imig, J. D., Inscho, E. W., Deichmann, P. C., Reddy, K. M. & Falck, J. R. Afferent arteriolar vasodilation to the sulfonimide analog of 11, 12-epoxyeicosatrienoic acid involves protein kinase A. *Hypertension* **33**, 408-413 (1999).

320 Michaelis, U. R. *et al.* Cytochrome P450 2C9-derived epoxyeicosatrienoic acids induce angiogenesis via cross-talk with the epidermal growth factor receptor (EGFR). *FASEB journal : official publication of the Federation of American Societies for Experimental Biology* **17**, 770-772, doi:10.1096/fj.02-0640fje (2003).

321 Potente, M., Fisslthaler, B., Busse, R. & Fleming, I. 11,12-Epoxyeicosatrienoic acid-induced inhibition of FOXO factors promotes endothelial proliferation by down-regulating p27Kip1. *The Journal of biological chemistry* **278**, 29619-29625, doi:10.1074/jbc.M305385200 (2003).

322 Hecker, M., Mulsch, A., Bassenge, E., Forstermann, U. & Busse, R. Subcellular localization and characterization of nitric oxide synthase(s) in endothelial cells: physiological implications. *The Biochemical journal* **299 (Pt 1)**, 247-252 (1994).

323 Carroll, M. A., Schwartzman, M., Abraham, N. G., Pinto, A. & McGiff, J. C. Cytochrome P450-dependent arachidonate metabolism in renomedullary cells: formation of Na+K+-ATPase inhibitor. *Journal of hypertension. Supplement : official journal of the International Society of Hypertension* **4**, S33-42 (1986).

324 Shao, Z. *et al.* Cytochrome P450 2C8 omega3-Long-Chain Polyunsaturated Fatty Acid Metabolites Increase Mouse Retinal Pathologic Neovascularization--Brief Report. *Arteriosclerosis, thrombosis, and vascular biology*, doi:10.1161/ATVBAHA.113.302927 (2014).

325 Cheranov, S. Y. *et al.* An essential role for SRC-activated STAT-3 in 14,15-EET-induced VEGF expression and angiogenesis. *Blood* **111**, 5581-5591, doi:10.1182/blood-2007-11-126680 (2008).

326 Suzuki, S., Oguro, A., Osada-Oka, M., Funae, Y. & Imaoka, S. Epoxyeicosatrienoic acids and/or their metabolites promote hypoxic response of cells. *Journal of pharmacological sciences* **108**, 79-88 (2008).

327 Chen, P. *et al.* Inhibitors of cytochrome P450 4A suppress angiogenic responses. *The American journal of pathology* **166**, 615-624, doi:10.1016/S0002-9440(10)62282-1 (2005).

328 Gong, Y. *et al.* Cytochrome P450 Oxidase 2C Inhibition Adds to omega-3 Long-Chain Polyunsaturated Fatty Acids Protection Against Retinal and Choroidal Neovascularization. *Arteriosclerosis, thrombosis, and vascular biology* **36**, 1919-1927, doi:10.1161/ATVBAHA.116.307558 (2016).

329 Gong, Y. *et al.* Fenofibrate Inhibits Cytochrome P450 Epoxygenase 2C Activity to Suppress Pathological Ocular Angiogenesis. *EBioMedicine*, doi:10.1016/j.ebiom.2016.09.025 (2016).

330 Kandpal, R. P. *et al.* Transcriptome analysis using next generation sequencing reveals molecular signatures of diabetic retinopathy and efficacy of candidate drugs. *Mol Vis* **18**, 1123-1146 (2012).

331 Mohammad, G. & Kowluru, R. A. Diabetic retinopathy and signaling mechanism for activation of matrix metalloproteinase-9. *J Cell Physiol* **227**, 1052-1061, doi:10.1002/jcp.22822 (2012).

332 Oshitari, T., Bikbova, G. & Yamamoto, S. Increased expression of phosphorylated c-Jun and phosphorylated c-Jun N-terminal kinase associated with neuronal cell death in diabetic and high glucose exposed rat retinas. *Brain Res Bull* **101**, 18-25, doi:10.1016/j.brainresbull.2013.12.002 (2014).

333 Oshitari, T., Yamamoto, S. & Roy, S. Increased expression of c-Fos, c-Jun and c-Jun N-terminal kinase associated with neuronal cell death in retinas of diabetic patients. *Curr Eye Res* **39**, 527-531, doi:10.3109/02713683.2013.833248 (2014).

334 Wang, L. *et al.* High glucose induces and activates Toll-like receptor 4 in endothelial cells of diabetic retinopathy. *Diabetol Metab Syndr* **7**, 89, doi:10.1186/s13098-015-0086-4 (2015).

335 Gupta, S., Knight, A. G., Gupta, S., Keller, J. N. & Bruce-Keller, A. J. Saturated long-chain fatty acids activate inflammatory signaling in astrocytes. *Journal of neurochemistry* **120**, 1060-1071, doi:10.1111/j.1471-4159.2012.07660.x (2012).

336 Shi, H. *et al.* TLR4 links innate immunity and fatty acid-induced insulin resistance. *J Clin Invest* **116**, 3015-3025, doi:10.1172/JCI28898 (2006).

337 Reiter, C. E. & Gardner, T. W. Functions of insulin and insulin receptor signaling in retina: possible implications for diabetic retinopathy. *Prog Retin Eye Res* **22**, 545-562 (2003).

338 Reiter, C. E. *et al.* Diabetes reduces basal retinal insulin receptor signaling: reversal with systemic and local insulin. *Diabetes* **55**, 1148-1156 (2006).

339 Fort, P. E. *et al.* Differential roles of hyperglycemia and hypoinsulinemia in diabetes induced retinal cell death: evidence for retinal insulin resistance. *PloS one* **6**, e26498, doi:10.1371/journal.pone.0026498 (2011).

340 Pozzi, A. *et al.* Characterization of 5,6- and 8,9-epoxyeicosatrienoic acids (5,6- and 8,9-EET) as potent in vivo angiogenic lipids. *The Journal of biological chemistry* **280**, 27138-27146, doi:10.1074/jbc.M501730200 (2005).

341 Du, Y. *et al.* Effects of p38 MAPK inhibition on early stages of diabetic retinopathy and sensory nerve function. *Investigative ophthalmology & visual science* **51**, 2158-2164, doi:10.1167/iovs.09-3674 (2010).

342 Briscoe, C. P. *et al.* The orphan G protein-coupled receptor GPR40 is activated by medium and long chain fatty acids. *The Journal of biological chemistry* **278**, 11303-11311, doi:10.1074/jbc.M211495200 (2003).

343 Fujita, T. *et al.* A GPR40 agonist GW9508 suppresses CCL5, CCL17, and CXCL10 induction in keratinocytes and attenuates cutaneous immune inflammation. *J Invest Dermatol* **131**, 1660-1667, doi:10.1038/jid.2011.123 (2011).

344 Verma, M. K. *et al.* Activation of GPR40 attenuates chronic inflammation induced impact on pancreatic beta-cells health and function. *BMC Cell Biol* **15**, 24, doi:10.1186/1471-2121-15-24 (2014).

345 Oh, S. Y., Lee, S. J., Jung, Y. H., Lee, H. J. & Han, H. J. Arachidonic acid promotes skin wound healing through induction of human MSC migration by MT3-MMP-mediated fibronectin degradation. *Cell Death Dis* **6**, e1750, doi:10.1038/cddis.2015.114 (2015).

346 Nehra, D. *et al.* Docosahexaenoic acid, G protein-coupled receptors, and melanoma: is G protein-coupled receptor 40 a potential therapeutic target? *J Surg Res* **188**, 451-458, doi:10.1016/j.jss.2014.01.037 (2014).

347 Kaku, K., Enya, K., Nakaya, R., Ohira, T. & Matsuno, R. Long-term safety and efficacy of fasiglifam (TAK-875), a G-protein-coupled receptor 40 agonist, as monotherapy and combination therapy in Japanese patients with type 2 diabetes: a 52-week open-label phase III study. *Diabetes Obes Metab* **18**, 925-929, doi:10.1111/dom.12693 (2016).

348 Jonas, J. B. Intravitreal triamcinolone acetonide for diabetic retinopathy. *Dev Ophthalmol* **39**, 96-110, doi:10.1159/000098502 (2007).

349 Tsilimbaris, M. K. *et al.* The use of intravitreal etanercept in diabetic macular oedema. *Semin Ophthalmol* **22**, 75-79, doi:10.1080/08820530701418243 (2007).

350 Khan, A. H., Falck, J. R., Manthati, V. L., Campbell, W. B. & Imig, J. D. Epoxyeicosatrienoic acid analog attenuates angiotensin II hypertension and kidney injury. *Front Pharmacol* **5**, 216, doi:10.3389/fphar.2014.00216 (2014).

351 Khan, M. A. *et al.* Novel orally active epoxyeicosatrienoic acid (EET) analogs attenuate cisplatin nephrotoxicity. *FASEB journal : official publication of the*

Federation of American Societies for Experimental Biology **27**, 2946-2956, doi:10.1096/fj.12-218040 (2013).

352 Lazaar, A. L. *et al.* Pharmacokinetics, pharmacodynamics and adverse event profile of GSK2256294, a novel soluble epoxide hydrolase inhibitor. *Br J Clin Pharmacol* **81**, 971-979, doi:10.1111/bcp.12855 (2016).

353 Podolin, P. L. *et al.* In vitro and in vivo characterization of a novel soluble epoxide hydrolase inhibitor. *Prostaglandins & other lipid mediators* **104-105**, 25-31, doi:10.1016/j.prostaglandins.2013.02.001 (2013).